②

NAVAL POSTGRADUATE SCHOOL
Monterey, California

AD-A186 929

DTIC
S ELECTE D
DEC 1 4 1987
D

THESIS

INDIRECT MEASUREMENT OF LOCAL CONDENSING
HEAT-TRANSFER COEFFICIENT AROUND
HORIZONTAL FINNED TUBES

by

Donald J. Lester, Jr.

September 1987

Thesis Advisor   P. J. Marto
Co-Advisor   A. S. Wanniarachchi

Approved for public; distribution is unlimited

REPORT DOCUMENTATION PAGE

1a REPORT SECURITY CLASSIFICATION UNCLASSIFIED	1b RESTRICTIVE MARKINGS
2a SECURITY CLASSIFICATION AUTHORITY	3 DISTRIBUTION / AVAILABILITY OF REPORT
2b DECLASSIFICATION / DOWNGRADING SCHEDULE	Approved for public release; distribution is unlimited.

4 PERFORMING ORGANIZATION REPORT NUMBER(S)	5 MONITORING ORGANIZATION REPORT NUMBER(S)

6a NAME OF PERFORMING ORGANIZATION Naval Postgraduate School	6b OFFICE SYMBOL (If applicable) 69	7a NAME OF MONITORING ORGANIZATION Naval Postgraduate School
6c ADDRESS (City, State, and ZIP Code) Monterey, California 93943-5000		7b ADDRESS (City, State, and ZIP Code) Monterey, California 93943-5000

8a NAME OF FUNDING / SPONSORING ORGANIZATION National Science Foundation	8b OFFICE SYMBOL (If applicable)	9 PROCUREMENT INSTRUMENT IDENTIFICATION NUMBER
8c ADDRESS (City, State and ZIP Code) Washington, DC 20550		10 SOURCE OF FUNDING NUMBERS

PROGRAM ELEMENT NO	PROJECT NO	TASK NO	WORK UNIT ACCESSION NO

11 TITLE (Include Security Classification)

INDIRECT MEASUREMENT OF LOCAL CONDENSING HEAT-TRANSFER COEFFICIENT AROUND HORIZONTAL FINNED TUBES

12 PERSONAL AUTHOR(S)

Lester, Jr, Donald J.

13a TYPE OF REPORT Master's Thesis	13b TIME COVERED FROM ___ TO ___	14 DATE OF REPORT (Year, Month, Day) 1987 September	15 PAGE COUNT 127

16 SUPPLEMENTARY NOTATION

17 COSATI CODES			18 SUBJECT TERMS (Continue on reverse if necessary and identify by block number)
FIELD	GROUP	SUB-GROUP	Steam, Condensation, Filmwise, Condensate Retention, Heat Transfer Coefficient, Finned Tubes

19 ABSTRACT (Continue on reverse if necessary and identify by block number)

Heat-transfer measurements were made for condensation of steam on three finned tubes with rectangular-section fins. These tubes have a fin thickness and fin height of 1.0 mm and fin spacings of 0.5, 1.0 and 1.5 mm. Data were taken by insulating both the inner and outer surfaces over up to 5 or 6 angular portions, including 0, 30, 60, 90, 150, 210 degrees, of the top portion of each tube. The measured average heat-transfer coefficients for the unblanked portion of the tube were processed to yield both the local and average heat-transfer performance as a function of the angle measured from

20 DISTRIBUTION / AVAILABILITY OF ABSTRACT ☒ UNCLASSIFIED/UNLIMITED ☐ SAME AS RPT ☐ DTIC USERS	21 ABSTRACT SECURITY CLASSIFICATION UNCLASSIFIED	
22a NAME OF RESPONSIBLE INDIVIDUAL P. J. Marto	22b TELEPHONE (Include Area Code) 408-646-2586	22c OFFICE SYMBOL 69Mx

DD FORM 1473, 84 MAR   83 APR edition may be used until exhausted   All other editions are obsolete

19 Abstract (Continued)

the top of the tube using a third-order polynomial.

The results show that the average enhancement for the fin spacings of 0.5, 1.0 and 1.5 mm were 2.5, 3.0 and 3.1, respectively, for the atmospheric-pressure condition. And they were 1.8, 2.3 and 2.4 for the low-pressure condition. The local enhancements at the top of tubes were 5.2 and 3.8 for s = 0.5 mm, 6.6 and 4.8 for s = 1.0 mm, and 6.6 and 5.5 for s = 1.5 mm at atmospheric and low pressures, respectively.

DTIC
COPY
INSPECTED

Accession For	
NTIS CRA&I	✓
DTIC TAB	☐
Unannounced	☐
Justification	
By	
Distribution /	
Availability Codes	
Dist	Avail and / or Special
A-1	

Indirect Measurement of Local Condensing Heat-Transfer
Coefficient Around Horizontal Finned Tubes

by

Donald J. Lester, Jr.
Lieutenant, United States Navy
B.S.Nuc.E., University of Oklahoma, 1980

Submitted in partial fulfillment of the
requirements for the degree of
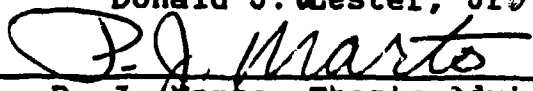

MASTER OF SCIENCE IN MECHANICAL ENGINEERING

from the

NAVAL POSTGRADUATE SCHOOL
September 1987

Author: _____
Donald J. Lester, Jr.

Approved by: _____
P. J. Marto, Thesis Advisor

_____
A. S. Wanniarachchi, Co-Advisor

_____
A. J. Healey, Chairman,
Department of Mechanical Engineering

_____
G. E. Schacher,
Dean of Science and Engineering

3

ABSTRACT

Heat-transfer measurements were made for condensation of steam on three finned tubes with rectangular-section fins. These tubes have a fin thickness and fin height of 1.0 mm and fin spacings of 0.5, 1.0 and 1.5 mm. Data were taken by insulating both the inner and outer surfaces over up to 5 or 6 angular portions, including 0, 30, 60, 90, 150, 210 degrees, of the top portion of each tube. The measured average heat-transfer coefficients for the unblanked portion of the tube were processed to yield both the local and average heat-transfer performance as a function of the angle measured from the top of the tube using a third-order polynomial.

The results show that the average enhancement for the fin spacings of 0.5, 1.0 and 1.5 mm were 2.5, 3.0 and 3.1, respectively, for the atmospheric-pressure condition. And they were 1.8, 2.3 and 2.4 for the low-pressure condition. The local enhancements at the top of tubes were 5.2 and 3.8 for s = 0.5 mm, 6.6 and 4.8 for s = 1.0 mm, and 6.6 and 5.5 for s = 1.5 mm at atmospheric and low pressures, respectively.

TABLE OF CONTENTS

5

6

LIST OF FIGURES

NOMENCLATURE

a_0 Local enhancement coefficient eqn. (4.4)

a_1 Local enhancement coefficient eqn. (4.4)

a_2 Local enhancement coefficient eqn. (4.4)

a_3 Local enhancement coefficient eqn. (4.4)

A Heat-transfer surface area (m^2)

A_{ef} Effective outside area of finned tube (m^2)

A_f Actual area of finned tube (m^2)

A_p Profile area of fin (m^2)

a Coefficient for eqn. (5.1)

a_f Coefficient used for finned tube in eqn. (5.4)

a_s Coefficient used for smooth tube in eqn. (5.4)

b_0 Average enhancement coefficient defined in Appendix C

b_1 Average enhancement coefficient defined in Appendix C

b_2 Average enhancement coefficient defined in Appendix C

b_3 Average enhancement coefficient defined in Appendix C

B Average enhancement value for a specific tube

C_i Sieder-Tate-type coefficient in eqn. (4.2)

C_{im} Modified Sieder-Tate-type coefficient in eqn. (5.2)

D Tube diameter (m)

D_{eq} Equivalent diameter of finned tube (m)

D_f Diameter of tube at tip of fins (m)

D_i Inside diameter of test tube (m)

D_r Root diameter of fin tubes of outside diameter of smooth tube (m)

e Fin height (mm or m)

g Acceleration due to gravity (m/s^2)

h Condensing heat-transfer coefficient (W/m^2K)

h_{BK} Condensing heat-transfer coefficient calculated using the Beatty & Katz method (W/m^2K)

h_f Condensing heat-transfer coefficient of a finned tube (W/m^2K)

h_i Inside condensing heat-transfer coefficient (W/m^2K)

h_o Outside Condensing heat-transfer coefficient (W/m^2K)

h_O Condensing heat-transfer coefficient calculated using the Owen method (W/m^2K)

h_t Condensing heat-transfer coefficient at the top of the tube (W/m^2K)

h_{RW} Condensing heat-transfer coefficient calculated using the Rudy & Webb method (W/m^2K)

h_s Condensing heat-transfer coefficient for smooth tube (W/m^2K)

h_W Condensing heat-transfer coefficient calculated using the Webb method (W/m^2K)

h_ϕ Condensing heat-transfer coefficient at some specified angle around the circumference of the tube (W/m^2K)

k_c Thermal conductivity of cooling water at T ($W/m\ K$)

k_m Thermal conductivity of tube metal ($W/m\ K$)

$\bar{L}$ Length of condenser test tube (m)

L_1 Length of tube portion (not exposed to vapor) inside nylon bushing at the inlet (m)

L_2 Length of tube portion (not exposed to vapor) inside nylon bushing at the outlet (m)

LMTD   Logarithmic-mean-temperature difference in eqn (1.1)

m Mass flow rate of cooling water (kg/s)

Nu_i Inside Nusselt number

p Fin pitch (m)

P	Wetted perimeter (m)
Pr	Prandtl number of cooling water
Q	Heat-transfer rate (W)
q	Heat flux (W/m^2)
q_f	Heat flux of finned tube based on A_o (W/m^2)
q_s	Heat flux of smooth tube based on A_o (W/m^2)
Re	Cooling water-side Reynolds number
R_w	Tube-wall thermal resistance eqn. (4.1)
s	Fin spacing (mm or m)
t	Fin thickness (m)
t_b	Fin thickness at base (m)
T_s	Saturation temperature of the steam (K)
$\overline{T}_{wo}$	Outside average wall temperature (K)
U	Overall heat-transfer coefficient (W/m^2K)
V_v	Velocity of the vapor (m/s)
V_w	Velocity of the water (m/s)

Greek Symbols

ΔT	Temperature difference (K)
ΔT_f	Temperature difference for the finned tube (K)
ΔT_s	Temperature difference for the smooth tube (K)
$\varepsilon_{\Delta T}$	Local enhancement based on a temperature difference
ε_q	Local enhancement based on a heat flux
ε_ϕ	Local enhancement at some angle around the circumference of the tube
$\overline{\varepsilon}_n$	Average enhancement of the uninsulated tube
$\overline{\varepsilon}_\phi$	Average enhancement at some angle around the circumference of the tube

$\bar{\varepsilon}_{n-\phi}$ Average enhancement of the top portion of the tube

β Fin tip half angle (rad)

η Fin efficiency

η_1 Fin efficiency of the portion of the tube L_1

η_2 Fin efficiency of the portion of the tube L_2

ρ_l Density of the water (Kg/m^3)

ϕ Insulated half angle (rad)

Ψ Condensate retention angle (angle measured from the bottom of the tube to the position at which the condensate first fills the interfin space) (rad)

θ Insulated angle (rad)

σ Surface tension of the water (N/m)

μ_c Dynamic viscosity of the cooling water $(N\ s/m^2)$

μ_w Dynamic viscosity of the cooling water at the inside wall temperature $(N\ s/m^2)$

ACKNOWLEDGEMENTS

The author would like to express his appreciation to Professor P. J. Marto and Professor A. S. Wanniarachchi for their guidance and support in completing this work. In addition, a special thanks to Professor John W. Rose for his contributions during the testing and review of this thesis.

The author would also like to thank Mr. Tom McCord and his machine shop crew for their support.

I. INTRODUCTION

A. BACKGROUND

In this highly technological society, the requirements to remove large quantities of heat efficiently has sparked numerous studies to collect information to assist in the improvement of the heat-removal process. Considering the basic equation which governs heat transfer for fluid systems, allows one to realize in which areas improvements are possible:

$$Q = UA(LMTD).$$

The equation involves the logarithmic-mean-temperature difference, which is normally defined by the application being considered and cannot be considered a variable quantity. Also, included in this relationship is the overall heat-transfer coefficient which is dependent on the construction, composition, and cleanliness of the condenser tube as well as the fluids being employed. Varying the above-mentioned parameters provides the designer with limited control over the efficiency of the system's condenser. That leaves the heat-transfer area which can be varied in order to increase the rate of heat transfer. There are only two possibilities when changing the heat-transfer area, which are: (a) increase the size or length of the tubes which increases the size and weight of the

14

condenser, or (b) replace smooth tubes with externally finned tubes, resulting in a smaller size and weight of the condenser.

In the application of steam to Naval vessels, both size and weight of major components have direct impact on the vessel's characteristics and ability to perform efficiently her mission requirements. Therefore, in order to increase the heat-transfer rate per unit weight, the addition of integral fins to the tubes of the condenser is the desired alternative under investigation.

Extended surfaces have been widely employed in refrigeration systems for many years. The presence of fins increases the effective heat-transfer area of the heat exchanger which enhances heat transfer. Further, when applied to condenser-type applications, the effect of the extended surfaces exceeds the expected increase in heat-transfer performance based on the increase in heat-transfer area alone [1,2]. The additional increase in heat-exchanger effectiveness is attributed to the smaller condensate travel distance (as discussed in Chapter II, $D_{eq} < D$) and the role played by the surface-tension forces which tend to thin the condensate film [2,3].

The enhancement of the condenser tube by the addition of fins can be accomplished either on the water or steam side of the tube. The addition of extended surfaces on the water side would increase frictional pressure drop, thus creating

15

additional pumping power. Most importantly, internal fins would raise serious questions as to increased fouling and difficulties associated with cleaning of such tubes. On the other hand, enhancement of the outside surface of the tube can be accomplished with greater economic advantage. Therefore, the addition of fins to the condenser tubes has been limited to the outside surface of the tubes.

Recent studies have considered both numerically and experimentally methods of predicting the effects on the outside heat-transfer coefficient due to the presence of fins [2,4,5,6,7,8,9]. Additionally, studies have considered a variety of fins of many different configurations and materials in order to determine the optimum characteristics when applied to specific applications [3,10].

The specific configuration of the fins on a condenser tube determine the steam-side heat-transfer performance. As it has been well established, some portion (i.e., lower portion) of a finned tube undergoing condensation is usually fully flooded by condensate. Owing to considerably large condensate film thickness, the heat-transfer performance of this flooded portion is generally poorer than the upper, unflooded portion of the tube. The extent of flooding is strongly dependent on the fin spacing and the surface tension to density ratio of the condensate. As discussed in Chapter II in detail, the extent of flooding is usually expressed by the condensate retention angle (i.e., the angle measured from

the bottom of the tube to the position at which the condensate just fills the interfin spacing, see Figure 1.1). The condensate retention angle has been studied thoroughly both theoretically and experimentally and agreement, in general, has been very good.

Wanniarachchi et al. [2] and Yau et al. [1] showed considerable heat-transfer enhancement for condensation of steam on finned tubes with a fin spacing of 0.5 mm even though these tubes were completely flooded by condensate (i.e., water). In fact, they reported enhancements (i.e., the ratio of finned tube condensing coefficient to the value for the corresponding smooth tube) at least as much as the area enhancement. These enhancements were higher than can be explained by one- or two-dimensional conduction through the composite of fins and condensate. Therefore, more complicated heat-transfer and fluid-flow mechanisms are believed to occur on finned tubes undergoing filmwise condensation.

Based on the above discussion, the major thrust of this thesis is to attempt experimentally to measure the "local" condensing heat-transfer coefficient of a finned tube undergoing filmwise condensation. As discussed in Chapter IV in detail, data have been taken on finned tubes by systematically insulating a measured angular portion (both on the inside and outside surfaces) of the finned tubes. A comprehensive pool of data for this situation has been

17
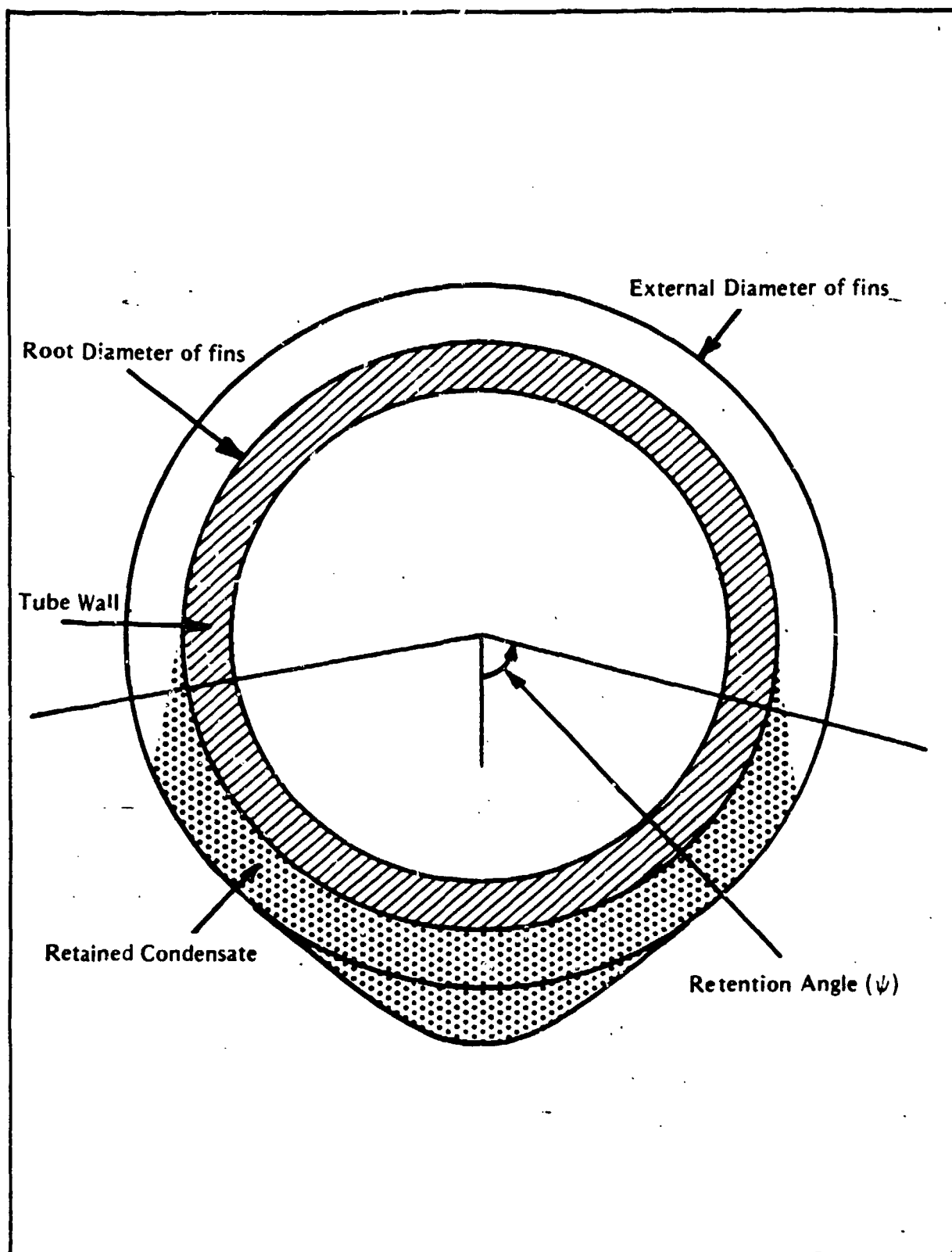
Figure 1.1   A Cross-Sectional View of a Finned Tube Showing
Condensate Retention.

gathered in order to reveal the relative heat-transfer performance of flooded and unflooded portions of finned tubes undergoing filmwise condensation.

This thesis effort is a continuation of research being conducted at the Naval Postgraduate School (NPS) under a grant from the National Science Foundation.

B. OBJECTIVES

The main objectives of this thesis are as follows:

1. Take data using three finned copper tubes with a fin thickness and height of 1.0 mm and fin spacings of 0.5 mm, 1.0 mm and 1.5 mm to demonstrate repeatability with the data collected on the present apparatus by previous investigators.

2. Take data using the above-mentioned tubes while systematically insulating upper portions of the tubes.

3. Determine the variation of the local outside heat-transfer coefficient in view of condensate retention angles.

4. Observe and study the mechanisms that occur in the flooded region of the tube.

19

II. PREVIOUS INVESTIGATIONS ON HORIZONTAL FINNED TUBES

A. GENERAL OBSERVATIONS

In a condenser, when vapor condenses in a filmwise mode on smooth horizontal tubes, a condensate film always exists around the tube. The latent heat of the vapor that is released during condensation will eventually be absorbed by the coolant flowing through the tube. The condensate film provides an additional resistance to the transfer of heat due to the low conductivity of the liquid. This resistance increases as the film thickness increases around the periphery of the tube starting from the top of the tube towards the bottom. Therefore, it becomes necessary to reduce the condensate film thickness in order to enhance the heat-transfer performance. For horizontal tubes, thinning of the condensate film can be achieved by employing finned surfaces.

On a finned tube, the flow of condensate between the fins is greatly affected by the ratio of surface tension forces to gravity forces. The surface tension effect on the behavior of the condensate is composed of two factors. One is the effect of reducing the condensate film thickness on the fin flanks in the unflooded region of the tube, which leads to enhanced heat transfer. In this region, the condensate on the fin surface is driven by combined gravity and surface tension forces into the fin root where it is drained by gravity. The other factor is the effect of retaining

20

condensate between the fins in the lower, flooded region of the tube, which leads to a decrease in effective surface area. The flooded portion of the tube is defined by the retention angle which was previously discussed in Chapter I. It is clear that for a given finned tube, the heat-transfer performance increases with decreasing retention angle. Therefore, any means of reducing the retention angle is beneficial.

B. EXPERIMENTAL AND THEORETICAL STUDIES

1. Condensate Retention

The first measurements of condensate retention were made by Katz et al. [11] in 1946. These measurements were made under static conditions (i.e., no condensation occurring) using water, aniline, acetone, and carbon tetrachloride on ten different tubes with fin densities from 276 to 984 fins/m, and fin heights from 1.2 to 5.7 mm. The retention measurements were performed both by visual observation and by weighing the amount of retained fluid. Theoretical treatment of the problem using the measurement of surface tension by a capillary tube and by the pendant drop method was made to develop a formula to predict condensate retention as a function of condensate properties and the dimensions of the tube. Their results for the condensate retention angle is given by the equation,

$$\frac{\psi}{\sin \psi} = \frac{\sigma}{\rho_l g}\left[\frac{4D_f - 2D_r - 2s}{\frac{\pi}{4}(D_f^2 - D_r^2)s}\left(\frac{180}{980}\right)\right] \qquad (2.1)$$

where

σ = surface tension,

ρ_l = density of condensate,

g = acceleration of gravity,

D_f = diameter of tube at fin tip,

D_o = outside diameter of tube, and

s = fin spacing.

It was shown that condensate retention depends mainly on the ratio of surface tension to liquid density and on the fin spacing.

In 1981, Rudy and Webb [4] measured condensate retention angles on three integral-fin tubes with three fin densities (748, 1024, and 1378 fins/m). They used three different fluids (water, R-11, and n-pentane) under both static and dynamic conditions. Their results showed that the retention angle increases as the surface tension to density ratio of the fluid increases. They also showed that the difference between static and dynamic retention angles was very small. For water, they reported that a significant portion of the tube surface was flooded.

In 1982, Rifert [13] developed equation (2.2) for the retention angle using a model of the capillary rise height of the fluid along a vertical plate,

$$\psi = \cos^{-1}\left[1 - \frac{2\sigma\,(P-p)}{\rho_l\,g\,D_f A_p}\right] \qquad (2.2)$$

where

  P = wetted perimeter,

  p = fin pitch, and

  A_p = profile area of the fin.

Later, in 1983, Rudy and Webb [6] developed an analytical model to predict condensate retention. They used two finned sections, one in tubular form and the other by splitting the tubular section and unrolling it into a vertical plate. They found that the vertical rise height of the condensate was the same for both these cases. Based on this observation, they modelled condensate retention on a flat plate to express the same on the finned tube. They made a simple force balance on the free body of condensate and developed an expression for the condensate retention angle as given by equation (2.3):

$$\psi = \cos^{-1}\left[1 - \frac{2\,\sigma\,(2e-t)}{\rho_l\,g\,e\,s\,D_f}\right] \qquad (2.3)$$

where

  e = fin height.

Both their analytical and test results showed that the retention angle increases with increasing surface tension-to-density ratio. Experimental results using water, R-11, R-12, ammonia, and n-pentane were predicted to within 10 percent.

Owen et al. [8] also recognized the necessity of including the effects of condensate retention in the heat-transfer models. They also assumed an analysis for the static case to be valid for the dynamic situation. A simple force balance between surface tension and gravitational forces resulted in an equation of the condensate retention angle as shown below:

$$\psi = \cos^{-1}\left[1 - \frac{4\sigma}{\rho_l \, g \, s \, D_f}\right]. \tag{2.4}$$

This equation is the same as equation (2.3), except that equation (2.4) is independent of fin thickness (t). A good agreement between this equation and the available data was reported by Rudy and Webb [4].

In 1983, Honda et al. [5] performed experiments on finned tubes with and without porous drainage plates employing methanol and R-113 as working fluids. They showed through a photographic study that the static and dynamic profiles of the retained condensate were approximately the same, and, by attaching a porous drainage plate, they demonstrated a significant reduction in the retention angle by reducing the amount of fluid retained between the fins. Performing a simple force balance which considered the effects of gravity and surface tension forces on the condensate, they developed a theoretical equation to be used to predict the condensate retention angle as follows;

$$\psi = \cos^{-1}\left[1 - \frac{4\sigma\cos\beta}{\rho_l \, g \, s D_f}\right] \qquad (2.5)$$

where β = fin tip half-angle.

They reported very good agreement between their theory, their own data and other available experimental data [4].

Yau et al. [1] measured the condensate retention angle using R-113, water, and ethylene glycol for finned tubes with and without drainage strips. They used an apparatus to simulate condensation on the tubes. They showed that a drainage strip attached edgewise along the bottom of the tube has a significant effect on removing the condensate reducing the amount of liquid retained between the tube fins. They modified the Honda et al. model (equation 2.5) in order to fit their experimental data, and developed the following empirical relationship:

$$\psi = \cos^{-1}\left[1 - \frac{1.66\sigma\cos\beta}{\rho_l \, g \, s D_f}\right]. \qquad (2.6)$$

Continuing with their investigation of condensate retention, Rudy and Webb [14], in 1985, modified their previous model [6] for predicting the condensate retention angle on horizontal tubes with fins of arbitrary shape. Experiments were made on four finned tubes possessing fin densities ranging from 748 to 1378 fins/m and one spine-tube with a fin density of 1378 fins/m. The fluids employed in the testing were R-11, n-pentane, and water. In addition, they tested a Thermoexcel-C tube with a fin density of 1417

25

fins/m and R-11 as the working fluid. This model is based on the assumptions used for their previous model (equation (2.3)). This work resulted in the following equation to predict the condensate retention angle:

$$\psi = \cos^{-1}\left[1 - \frac{2\sigma\,(P - t_b)}{D_f\,\rho_l\,g\,[(t_b + s)e - A_p]}\right]$$

(2.7)

where

P = wetted perimeter of fin cross section,

t_b = fin base thickness, and

A_p = profile area of fin over fin cross section.

From equation (2.7), the retention angle increases with an increase in the surface tension to density ratio of the liquid, fin density, or with a decrease in tube diameter. For the case of a horizontal tube with rectangular-shaped fins, equation (2.7) reduces to equation (2.4). The experimental deviation from the predicted value of equation (2.7) was within 10 percent.

Honda et al. [9], in 1987, presented a new model which included the effects of condensate flow and heat transfer on the fin root tube surface in the unflooded region of the tube, and the wall temperature variation between the fin root and the fin root tube surface. This work resulted in the extension of the expression for the flooding angle to include the case of relatively large fin spacing as compared with the fin height which is equation (2.8) as follows:

$$\psi = \cos^{-1}\left(1 - X\right) \quad for \quad 0 \leq X \leq 2$$

$$\psi = 0 \quad for \quad 2 < X \qquad\qquad (2.8)$$

$$where \quad X = \frac{4\sigma}{\rho_l g D_f s} \quad for \ s \leq 2e$$

$$X = \frac{\left(\dfrac{4\sigma}{\rho_l g D_f s}\right)\left(\dfrac{s}{e}\right)}{1 + \left(\dfrac{s}{2e}\right)^2} \quad for \ s > 2e$$

where s is the fin spacing and e is the fin height.

In 1987, Masuda and Rose [15] considered four separate "flooding" conditions. These four conditions were based on the meniscus profile at various locations around the tube. The conditions considered were as follows:

(a) when the interfin space is just filled by the meniscus but the fin flanks are not fully wetted,

(b) when the fin flanks are fully wetted but the interfin space is not,

(c) when the entire interfin space is just wetted and the contact angle of the meniscus at the fin tip is non-zero, and

(d) when the flanks of the fin are just wetted with a finite film thickness at the center of the interfin space.

Separate expressions were developed for each of these conditions. The last condition considered corresponds to the condensate retention angle which is given by:

$$\psi = \cos^{-1}\left(\frac{2\sigma_l \cos\beta}{\rho_l \, g \, s \, tr_t} - 1\right) \qquad (2.9)$$

2. Heat Transfer on Finned Tubes

Initial studies of condensation heat transfer on finned tubes began in 1948 when Beatty and Katz [16] performed experiments with propane, n-butane, sulfur-dioxide, methyl chloride, and R-22 on single finned tubes with densities from 422 to 630 fins/m. They reported enhancements as high as 2.3 on the overall condensation heat-transfer coefficient for the finned tubes compared to smooth tubes using R-22, with a water-side velocity of 6 ft/sec. However, they did not compare the enhancement on the vapor-side heat-transfer coefficient, which were approximately six.

Using Nusselt [17] expressions for a horizontal smooth tube and for a vertical flat plate to represent the interfin tube area and the fin surface, respectively, and by modifying the leading coefficient from 0.728 to 0.689 to fit their experimental data, Beatty and Katz arrived at the following simple correlation equation (2.10) as follows:

$$h_{BK} = 0.689 \left[\frac{k_l^3 \rho_l^2 g \, h_{fg}}{\mu_l \Delta T \, D_{eq}}\right]^{1/4} \qquad (2.10)$$

$$where \quad \left[\frac{1}{D_{eq}}\right]^{1/4} = 1.30 \, \eta_f \frac{A_f}{A_{ef}} \frac{1}{\overline{L}^{1/4}} + \frac{A_o}{A_{ef}} \frac{1}{D_r^{1/4}}$$

$$\overline{L} = \frac{\pi [D_f^2 - D_r^2]}{4 \, D_f}$$

28

$$A_{ef} = A_o + \eta_f A_f.$$

This correlation was shown to predict their data for low-surface-tension fluids within about 10 percent. However, recent studies [18] have shown that this correlation could significantly overpredict the data for high-surface-tension fluids, such as water.

In 1971, Karkhu and Brrovkov [19] obtained data for condensation of steam at near-atmospheric pressure on four horizontal tubes having different configurations of trapezoidally shaped fins. For both steam and R-113, they reported a 50-100 percent increase in the condensing heat-transfer coefficient on three tubes compared to a smooth tube. The fourth tube with a fin height of 2.05 mm, a fin root thickness of 1.35 mm, a fin semivertex angle of 16.5 degrees and a fin density of 670 fins/m resulted in no heat-transfer enhancement. Unfortunately, the authors did not elaborate on the reasons why no heat-transfer enhancement was observed for the fourth tube. Their results showing nearly the same heat-transfer enhancement for both steam and R-113 appear to be somewhat surprising, based on the recent data as discussed in this section.

In 1980, Carnavos [20] tested a wide variety of finned tubes using R-11 and discovered increases in the condensing heat-transfer coefficient as much as 5 times that of the smooth-tube values. Rudy and Webb [4], in

1983, reported data for R-11 condensing on four tubes with different fin geometries. Their results indicated that the vapor-side coefficients exceeded Nusselt values by factors of approximately 7 to 9 (for a constant temperature drop across the condensate film). Honda et al. [5], in 1983, tested four low-fin tubes with different fin geometries using methanol and R-113 as condensing fluids. Vapor-side enhancements of 9 for R-113 and 6 for methanol were found. Yau et al. [1], in 1984, reported heat-transfer coefficients for steam at atmospheric pressure condensing on thirteen tubes with rectangular-section fins for which the fin spacing was the only variable, while the fin height and thickness were constant at 1.6 mm and 0.5 mm, respectively. These tubes had a root diameter of 12.7 mm and the fin spacings were 0.5, 1.0, 1.5, 2.0, 4.0, 6.0, 8.0, 10.0, 12.0, 14.0, 16.0, 18.0, and 20.0 mm. They reported an optimum vapor-side enhancement (computed at a heat flux of 0.5 Mw/m2 of around 4.4 for the tube with a fin spacing of 1.5 mm.

In 1981, Rudy and Webb [4] proposed a modification to the Beatty and Katz correlation as shown below by taking the condensate retention angle into consideration:

$$h_{RW} = h_{BK} \left[\frac{\pi - \psi}{\pi} \right], \qquad (2.11)$$

where ψ is the condensate retention angle. As can be seen from this equation, they neglected any heat transfer through the flooded portion of the tube. Even though this assumption

appeared sound at that time, they showed that equation (2.11) underpredicted their R-11 data by 10 to 60 percent.

In 1983, Owen et al. [8] extended the Rudy and Webb model to include heat conduction through the composite fins and condensate film (which has a thickness equal to the fin height) in the flooded portion of the tube. Even though this model made a slight improvement over the Rudy and Webb model, none of these simple models were capable of adequately addressing the complex physical problem at hand.

As discussed earlier, surface tension has been recognized to play an important role in the unflooded portion of the tube. In this manner, any successful model must recognize the effects of surface tension fully toward heat transfer and in fluid flow around a finned tube circumference. Gregorig [21] introduced the concept of condensate film thinning as a result of surface-tension-caused pressure gradients, and Karkhu and Borovkov [19] applied this concept to a simplified case involving tubes with trapezoidal fins.

Over the past few years, a number of studies involving theoretical or numerical approaches have shown considerable promise towards complete understanding of this phenomenon. In fact, in 1983 Honda and Nozu [5] presented a complex numerical model, which included proper consideration to surface-tension effects, to compute the condensing heat-transfer coefficient on finned tubes. They numerically

31

solved their fourth-order differential equation for the condensate film thickness. They showed this model to predict most of the data for 11 fluids and 22 tubes within a range of 20 percent. However, this model disagreed by up to 40 percent with steam data.

In 1985, Webb, Kedzierski and Rudy [22] formulated a new model based on an expansion developed by Adamek [23] for the average heat-transfer coefficient over the fin surface for a family of special fin shapes. They treated the interfin area in the flooded portion of the tube as condensation on a smooth tube. They made a correction to account for the additional condensate loading owing to the flow of condensate from the fin surfaces to the interfin area. Also, they computed the heat-transfer coefficient in the flooded portion of the tube using a two-dimensional conduction model. Webb et al. [22] have showm that their model agreed with their data for R-11 within 20 percent for finned tubes.

In 1987, Honda et al. [9] improved upon their earlier model by including the effects of condensate flow and heat transfer on the fin root tube surface in the unflooded region of the tube, and the wall temperature variation between the fin root and the fin root tube surface. They compared their predictions with experiemental heat-transfer coefficients for 12 fluids and 31 tubes. Most of the data agreed within about 20 percent. However, this model was shown to underpredict

32

the data on a fully flooded tube (i.e., when condensing steam on a finned tube with fin spacing of 0.5 mm) by up to 40 percent. As discussed later in this section, their predictions for this tube appear to be quite impressive though further improvements are necessary. Despite the considerable success shown by Honda et al., it appears somewhat impractical to use this model as a design tool owing to its complexity.

During the last four years, a wide variety of data has been obtained at the Naval Postgraduate School (NPS) for film condensation of steam on horizontal finned tubes under a grant from the National Science Foundation. The basic test apparatus was constructed by Krohn [24]. Graber [25] provided the instrumentation and took preliminary data as the system experienced problems with non-condensing gases and partial dropwise condensation on copper tubes. Poole [26] made further improvements on the apparatus, especially in achieving leak tightness. He operated the apparatus both under low pressure and at atmospheric pressure, and tested a otal of six finned tubes, with different fin spacings, as ell as a smooth tube. Poole experienced problems due to the occurrence of partial dropwise condensation. Using this system, Georgiadis [27] was able to obtain complete filmwise condensation on a smooth tube and on 21 finned copper tubes with rectangular-section fins. Based on both low pressure (approximately 85 mm Hg) and atmospheric runs, Georgiadis

33

reported an optimum fin spacing of 1.5 mm and an optimum thickness of 0.75 to 1.0 mm. Among the finned tubes with a fin height of 1.0 mm, the tube with a fin spacing of 1.5 mm and fin thickness of 1.0 mm provided the best heat-transfer performance. This tube resulted in a steam-side enhancement (i.e., the ratio of steam-side coefficient for the finned tube to the value for the smooth tube for the same heat flux) of about 4 and 5.7 at low pressure and at atmospheric pressure, respectively. In 1985, Flook [28] tested 19 additional tubes. These tubes included two sets of four tubes with fin heights of 0.5 and 1.5 mm, respectively. He found an optimum fin spacing of about 2.0 mm for rectangular-shaped fins with a fin thickness of 1.0 mm, and fin height of 0.5 mm and 1.5 mm. He obtained maximum enhancements of about 4.8 and 6.9 at low and atmospheric pressures, respectively.

Mitrou [10] obtained data for 26 copper tubes with circular fins of rectangular, triangular, trapezoidal and parabolic cross sections, for spiral fins of triangular cross section and for wire-wrapped tubes. A near-parabolic fin shape that provides a gradually decreasing curvature from fin tip to fin root resulted in a 10 to 15 percent increase in steam-side heat-transfer coefficient over other fin shapes. Therefore, he concluded that fin shape does not appear to be as crucial a variable as fin spacing [3].

Continuing with this research project, Cakan [29] performed measurements for filmwise condensation of steam

34

under low pressure and at near-atmospheric pressure on horizontal finned tubes attached with bronze porous and solid drainage strips. The purpose of this study was to measure the effects of these strips on the condensing heat-transfer performance, through the reduction of condensate retention angle. In addition, the effects of drainage strip type, height, and thickness were investigated. A total of 16 drainage strips were manufactured and tested on two finned tubes each with a fin thickness and height of 1.0 mm and with a fin spacing of 0.5 mm and 1.0 mm. The heat-transfer performance generally increased with increasing porous strip height up to a possible optimum value between 11 and 15 mm. Of the pore diameters tested (0.05-0.013 mm, 0.025-0.05 mm and 0.0025-0.013 mm), the strip with an average pore diameter of 0.025-0.05 mm gave the best heat-transfer performance. This optimum strip type showed an optimum strip thickness of 5.2 mm. The solid strips showed an optimum strip thickness of 1.5 mm. The optimum porous strip gave a 9% and 17% greater steam-side enhancement than the optimum solid strip for low and atmospheric pressures, respectively. For the finned tube with a fin spacing of 0.5 mm, a maximum enhancement of about 1.6 was found when it was attached with a 5.2-mm-thick, 8-mm-high porous strip having a pore diameter of 0.025-0.05 mm.

Because of the low thermal conductivity of non-metallic liquids, heat transfer through the flooded portion

of a finned tube should be considerably lower than that through the unflooded portion. However, as stated in Chapter I, Wanniarachchi et al. [4] showed considerable enhancement for a finned tube with a fin spacing of 0.5 mm, which was fully flooded by condensate both at low and atmospheric pressures.

3. Comparison of Predictive Models with Heat-Transfer Data

Rudy and Webb [4] suggested that the successful predictions of heat-transfer data for low-surface-tension fluids by the Beatty and Katz correlation was fortuitous. They reasoned that the degradation of the heat-transfer performance owing to the lower flooded (though small for low-surface-tension fluids) portion was perhaps compensated by the increased heat-transfer performance through the unflooded portion owing to thinning of the condensate film by surface-tension forces. Because of these unsettled issues, it is important that a truly successful model be capable of predicting the condensing heat-transfer coefficient of steam on finned tubes.

As shown in Table 1 [18], four heat-transfer models have been compared with experimental results obtained at the Naval Postgraduate School. This table lists the computed condensate retention angles and the ratios of experimental heat-transfer coefficient to predicted values for the six finned tubes. From the data listed in Table 1, the following observations can be made:

36

(a) In comparing the Beatty and Katz model [16] (column 3) with the experimental data, it is demonstrated that this model highly overpredicts the data for tubes with smaller fin spacings. This is a result of neglecting the presence of a flooded, low-heat-transfer portion of the tube. As the fin spacing increases, the extent of overprediction decreases as a result of decreasing condensate retention angle. For tubes with a fin spacing of 4 mm or more, the Beatty and Katz correlation underpredicts the heat-transfer performance. This observation appears to be a result of additional thinning of condensate film owing to the existence of surface-tension forces.

(b) The Rudy and Webb model [4] (column 4) which is an extension of the Beatty and Katz model is not valid for a fully flooded tube. This model underpredicts considerably the data for all other five tubes under both pressure conditions. This strongly suggests that there exists considerable heat transfer through the flooded portion.

(c) Another extension of the Beatty and Katz model is the Owen et al. [8] (column 5) model. The initial presentation of this model appeared to be in error due to the incorrect combination of the unflooded and flooded portions of the finned tube. The model presented in this thesis is the corrected version which provides

37

somewhat improved predictions over the Rudy and Webb model (column 4). Yet, it underpredicts the data by up to about 60 percent, while for the fully flooded tube, it underpredicts the data by a factor of up to 3.3.

(d) The last column in Table 1 represents predictions made by the Webb et al. model [22]. As can be seen, except for the fully flooded tube, their model is seen to predict the data within about 20 percent. It is very encouraging to see a fairly simple model predicting the data successfully. A more realistic representation of the heat-transfer performance through the flooded portion, together with the Webb et al. model, appears to show considerable promise for the future. It is important to note that heat-transfer models which do not consider the effects of surface-tension-induced flow in the unflooded portion of the finned tube provide inaccurate predictions of the experimental data as demonstrated by the first three models used in the above comparison (columns 3,4,5).

TABLE 1

COMPARISON OF HEAT-TRANSFER DATA WITH PREDICTIVE MODELS

Fin Spacing (mm)	Condensate Retention Angle (deg)	$\dfrac{h_o}{h_{BK}}$	$\dfrac{h_o}{h_{RW}}$	$\dfrac{h_o}{h_O}$	$\dfrac{h_o}{h_W}$
Vacuum runs, $q = 0.25$ MW/m^2					
0.5	180	0.323	∞	2.264	2.264
1.0	110	0.619	1.602	1.247	0.978
1.5	84	0.808	1.520	1.281	0.962
2.0	71	0.797	1.318	1.139	0.852
4.0	49	1.093	1.497	1.335	1.029
9.0	32	1.275	1.550	1.415	1.033
Atmospheric runs, $q = 0.75$ MW/m^2					
0.5	180	0.475	∞	3.316	3.316
1.0	103	0.741	1.744	1.402	1.103
1.5	79	0.993	1.786	1.526	1.161
2.0	67	1.014	1.627	1.419	1.076
4.0	46	1.312	1.772	1.585	1.214
9.0	31	1.368	1.653	1.509	1.073

III. DESCRIPTION OF TEST APPARATUS

A. TEST APPARATUS

The test apparatus used for this investigation was essentially the same as used by Georgiadis [27], Flook [28], and Mitrou [10]. A schematic of this apparatus is shown in Figure 3.1. Steam was generated using distilled water in a 304.8 mm (12 in.) Pyrex glass section which was fitted with ten 4000-watt, 440-volt Watlow immersion heaters. The steam from the boiler flowed upward and passed through a 304.8 mm (12 in.) to 152.4 mm (6 in.) reducing section into a 2.44 m (8 ft.) long section of Pyrex glass piping. The steam flowed through a 180-degree bend and entered into a 1.52 m long section before finally entering the stainless-steel test section, which is shown in Figure 3.2. The test tube was mounted horizontally in the test section. A portion of the steam condensed on the test tube, while the excess steam travelled downward and condensed in the auxiliary condenser. The condensate drained back to the boiler by gravity, completing the closed-loop operation of the system.

The exit side of the test tube was provided with a mixing chamber for accurate measurement of the outlet temperature of the coolant. A view port was provided in the test section to allow visual observation of the condensation mode to ensure complete filmwise condensation during each

40
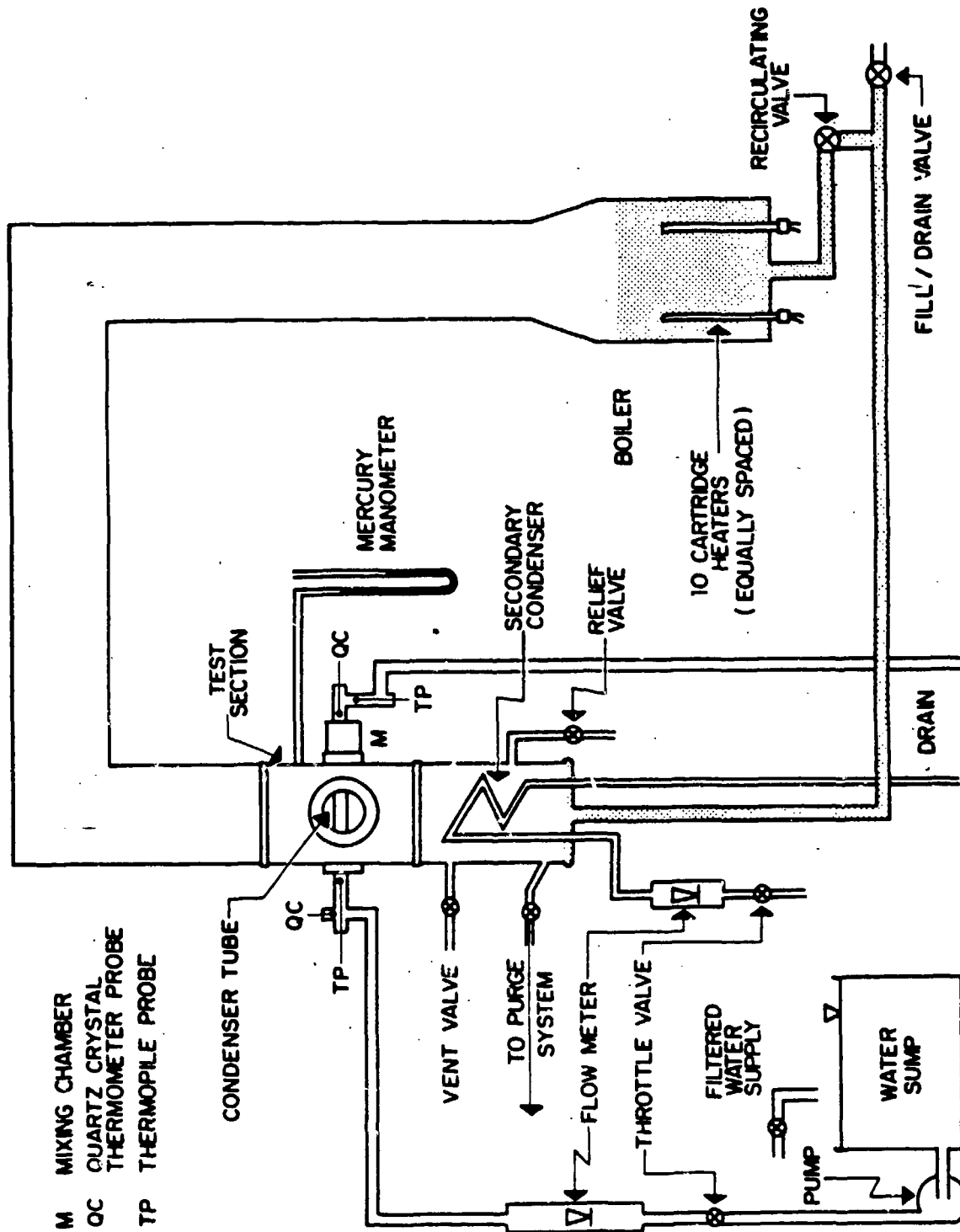
Figure 3.1   Schematic of Test Apparatus.
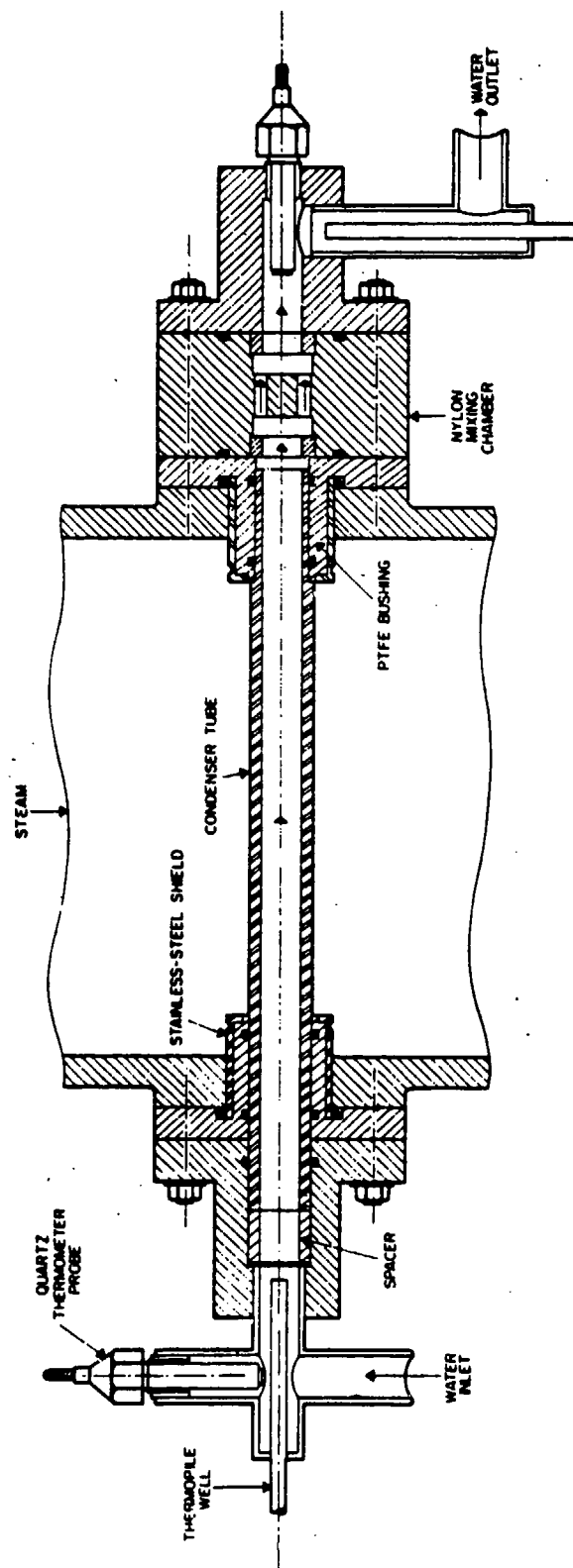
Figure 3.2   Schematic of Test Section.

run. The auxiliary condenser consisted of two 9.5 mm (3/8 in.) diameter water-cooled copper tubes helically coiled to a height of 457 mm (18 in.). The auxiliary condenser was cooled by a continuous supply of tap water through a flow meter. A throttle valve was provided to control the flow rate through the auxiliary condenser, thus keeping the system at the desired internal pressure. For example, when the flow rate through the test tube was decreased, the flow rate through the auxiliary condenser had to be increased. Filtered tap water was collected in a large sump with a capacity of about 0.4 cubic meters (Figure 3.3), and was used to cool the test tube. Two centrifugal pumps, connected in series, took the water from the sump and passed it through a flow meter into the test tube. A valve on the discharge side of the second pump, and before the flow meter, allowed the velocity of the water flowing through the test tube to be varied from 0 to 4.4 m/s (14.4 ft/sec).

A vacuum pump was operated continuously during the operation of the apparatus to remove non-condensing gases from the test section. The system used to remove non-condensing gases is shown in Figure 3.3. It was unavoidable that the vacuum pump mainly drew steam with trace amounts of air (non-condensing gases). To minimize the contamination of the pump by the steam, another condenser was provided to condense as much steam as possible. This
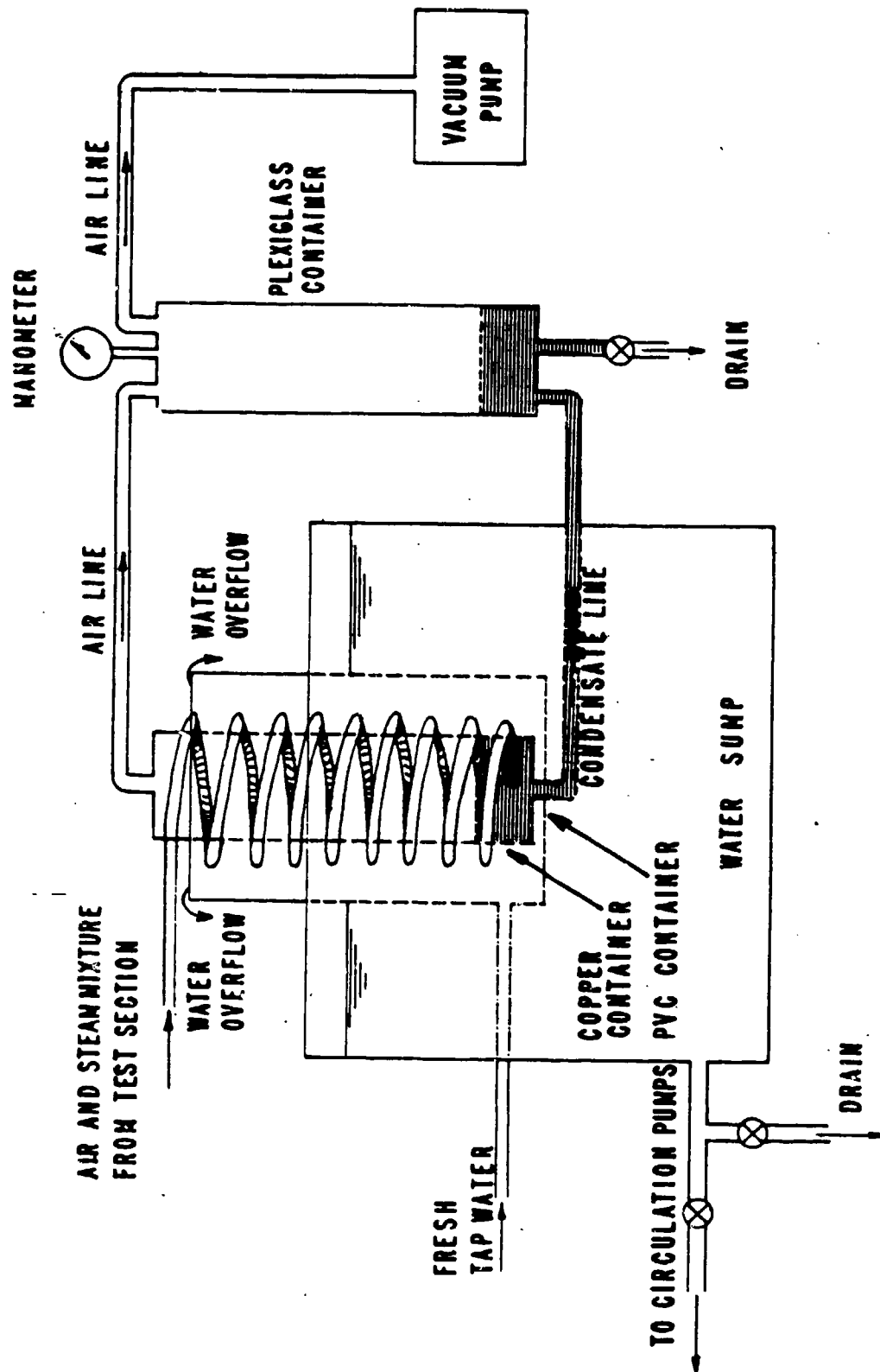
Figure 3.3 Purging System and Cooling Water Sump.

condenser was cooled with the filtered tap water before entering the large sump. The condensate from this steam collected in a Plexiglas cylinder to be drained later.

B. APPARATUS MODIFICATIONS

The original outside stainless steel casing of the auxiliary condenser was replaced by a Pyrex glass section which allowed visual observation of the auxiliary condenser operation, In addition, it allowed increased ability to detect possible system leaks. Following the installation of this section, a leak was identified on the auxiliary condenser drain lines. The detection and repair of the leak reduced the system leak rate corresponding to a previous pressure rise of 12 mmHg in 24 hours to the present value leak rate of about 1 mmHg in 24 hours.

C. INSTRUMENTATION

The electrical power input to the boiler immersion heaters was controlled by a panel-mounted potentiometer. In order to compute the input power to the boiler, a root-mean-square converter with an input voltage of 440 VAC generated a signal which was fed to the data-acquisition system. A more detailed description of the boiler power supply is provided by Poole [26]. The temperatures of the steam, condensate and the ambient were measured using calibrated copper-constantan thermocouples made of 0.25 mm diameter wires. Two of them were used for the steam temperature, one for the returning

45

condensate and one for the ambient temperature. These thermocouples had an accuracy range of within 0.1 K when compared against a platinum-resistance thermometer. Since the temperature rise of the coolant through the test tube is the most critical measurement, considerable attention was paid to obtaining the highest possible accuracy. For this purpose, two independent temperature measurement techniques were employed: a Hewlett-Packard (HP) 2804A quartz thermometer with two probes having a resolution of 0.0001 K, along with a 10-junction, series-connected copper-constantan thermopile with a resolution of 0.003 K. For all of the data collected, the quartz thermometers and the thermopile agreed to within 0.03 K, and when the difference was outside 0.03 K, the data set was disregarded and a repeat set was made. The cooling water flow rate was measured using a calibrated rotameter and the value was fed manually to the computer. Another rotameter was provided to adjust the cooling water flow rate through the auxiliary condenser.

A pressure tap located about 50 mm above the test tube was connected to a U-tube, mercury-in-glass manometer, graduated in millimeters, to measure the absolute pressure of the system. At the beginning and at the end of each test run, an accurate pressure reading was made and entered into the computer. The measured system pressure and the saturation pressure corresponding to the measured steam

temperature were used to compute the concentration of any air that might be present. For this purpose, a Gibbs-Dalton-type relationship was used. The computed non-condensing gas concentration was found to be within - 1.5 to 0 percent. Such a value revealed that major air leaks did not take place following the last vacuum test on the apparatus. Notice that a negative value for the non-condensing gas concentration represents the existence of vapor superheat, which arises mainly from the uncertainties associated with measured quantities.

D. VACUUM INTEGRITY

Vacuum tightness for any condensation system, especially at low pressures similar to large steam plant condensers which operate at an absolute pressure of about 50 mm Hg, is very important. This is because even a small amount of air or other non-condensing gas present with the condensing vapor tends to accumulate at the liquid-vapor interface. When this phenomenon takes place, an added thermal resistance occurs at the interface, which will degrade the heat-transfer performance considerably. Therefore, in order to be able to collect consistent and reliable data, extreme care was taken to ensure a leak-tight apparatus. In fact, as discussed earlie during initial system operation prior to the conducting of any testing for this project, a relatively large leak was detected and repaired in a drain line for the auxiliary condenser. The detection of the source of this

47

leak was made easier following the replacement of the auxilary condenser outer casing with one constructed entirely of Pyrex glass. A photograph of the auxiliary condenser section with the glass outer casing is included as Figure 3.4. Following the repair of the leak, a leak rate which corresponds to a pressure rise of about 1 mm Hg in 24 hours at a pressure of about 85 mmHg was measured. In addition, since the vacuum pump was operating continuously during the testing, any accumulation of non-condensing gases within the apparatus was effectively eliminated.

E. DATA ACQUISITION SYSTEM

An HP-9826A computer was used to control an HP-3497A Data Acquisition System to monitor the system temperatures and boiler input power (using the converter signal). Raw data were processed immediately using an assumed value for the Sieder-Tate-type coefficient (representing the tube-side heat-transfer coefficient) and stored on a diskette for reprocessing at a later time. After all the sets were collected, the data were reprocessed using a new Sieder-Tate-type coefficient found by using the modified Wilson method.

F. TUBES TESTED

For this thesis investigation, three copper tubes having integral, rectangular-section fins were tested. These tubes had dimensions of 1.0 mm for fin thickness and height and fin

48
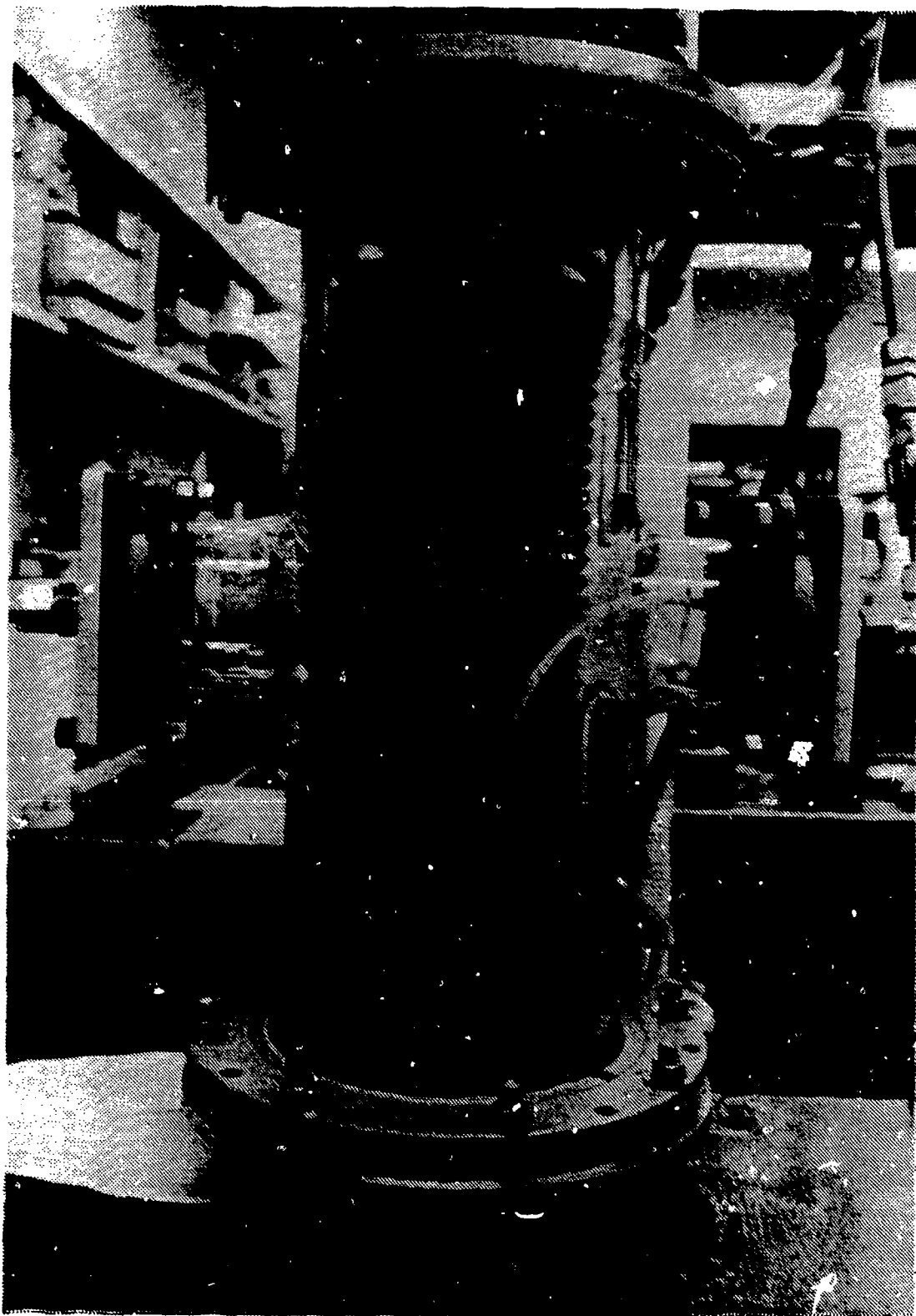
Figure 3.4 A Photograph of Auxiliary Condenser.

spacings of 0.5 mm, 1.0 mm and 1.5 mm. The upper sections of these tubes were ~ystematically insulated using Teflon pieces with angles of approximately 30, 60, 90, 150 and 210 degrees. The Teflon material used as insulation was located both between the fins and over top of the fins as shown in Figure 3.5. An inner insulating piece was also used on the water side of the tube.

The installation of the tube insulation used to test the finned tubes is listed below:

(a) The interfin insulation was installed first on the finned tube as shown in the photograph in Figure 3.6.

(b) Next, the fin tip insulation was installed and secured (using fine stainless steel wires) to the finned tube as shown by the photograph in Figure 3.7 and the tube side view in Figure 3.8.

(c) The inner insulation and insert were installed inside the tube as shown in Figure 3.9.
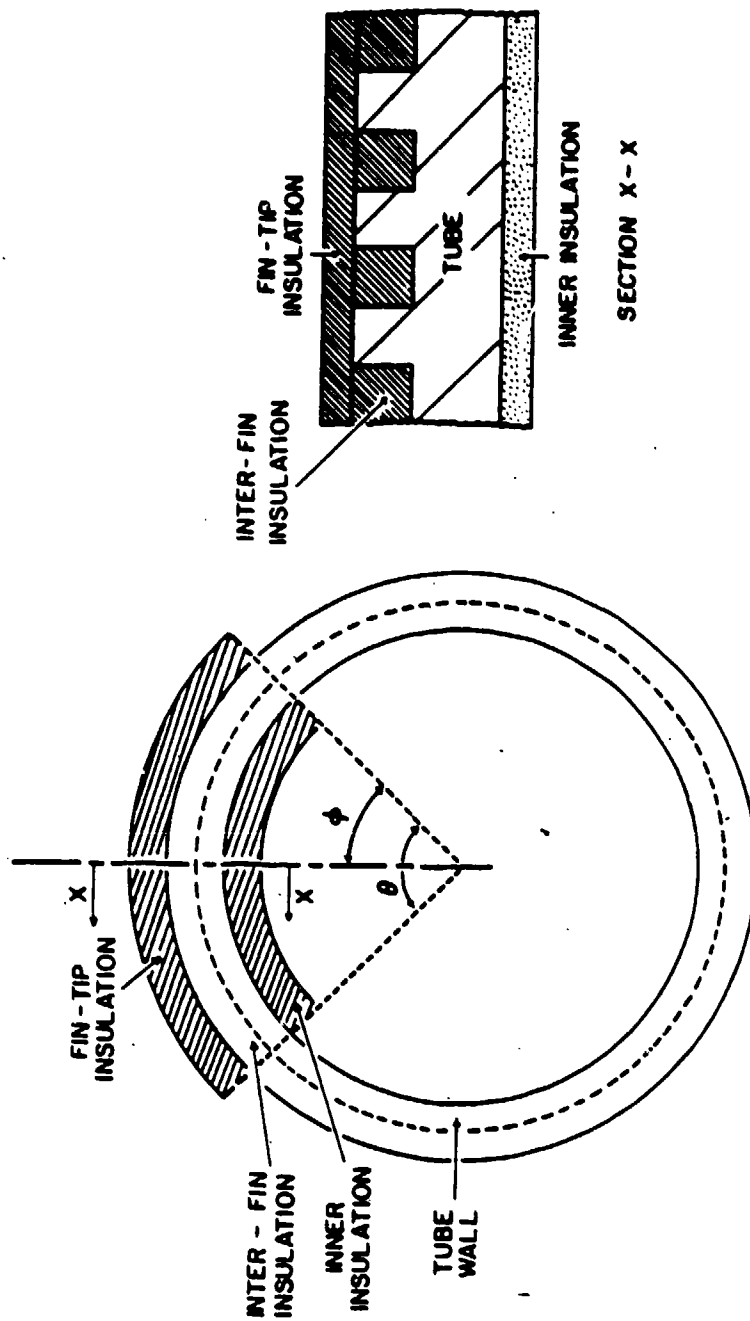
Figure 3.5 Schematic of Tube Cross-Section Showing Insulation.

51
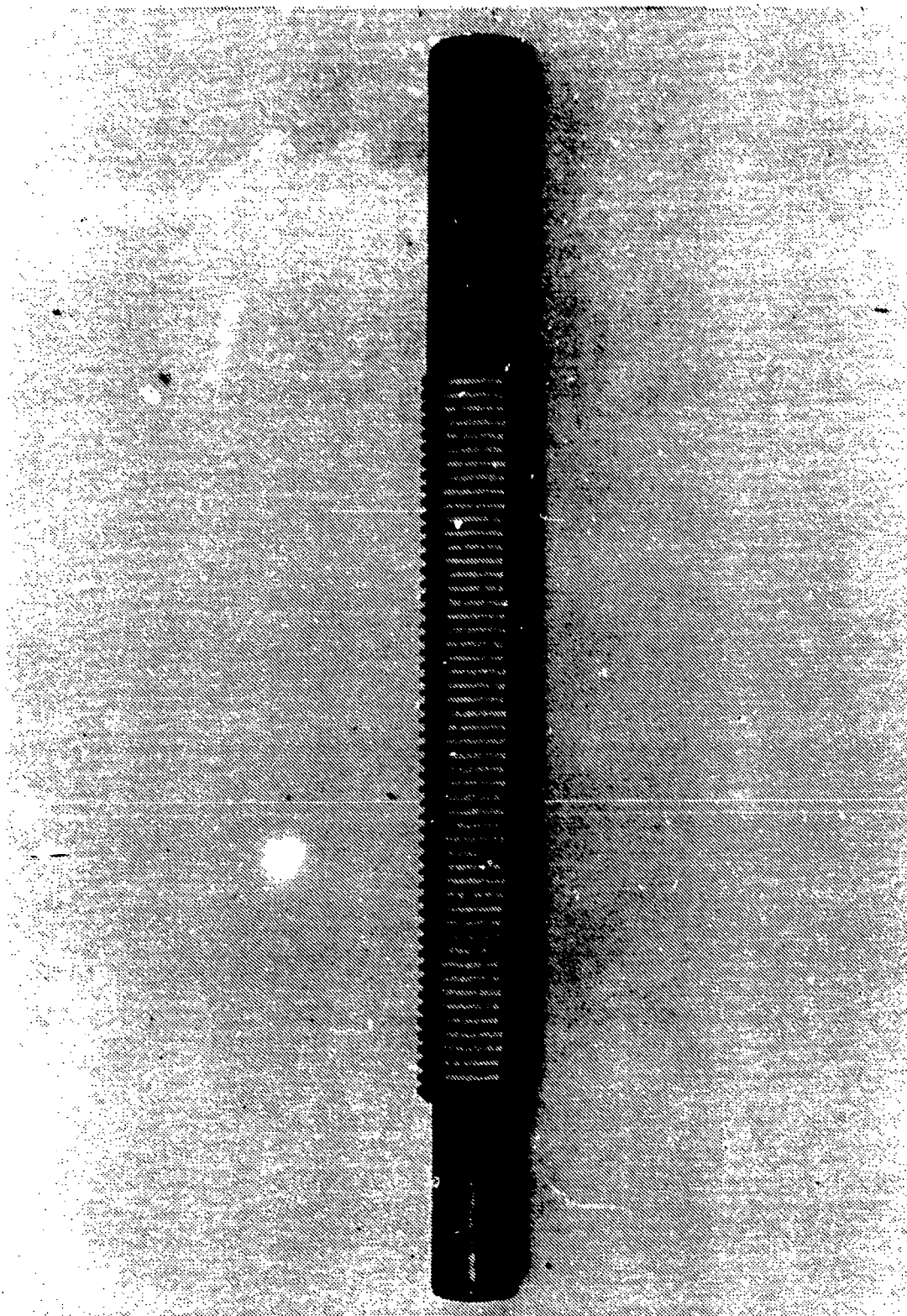
Figure 3.6   A Photograph of Finned Tube with Interfin
Insulation Installed.
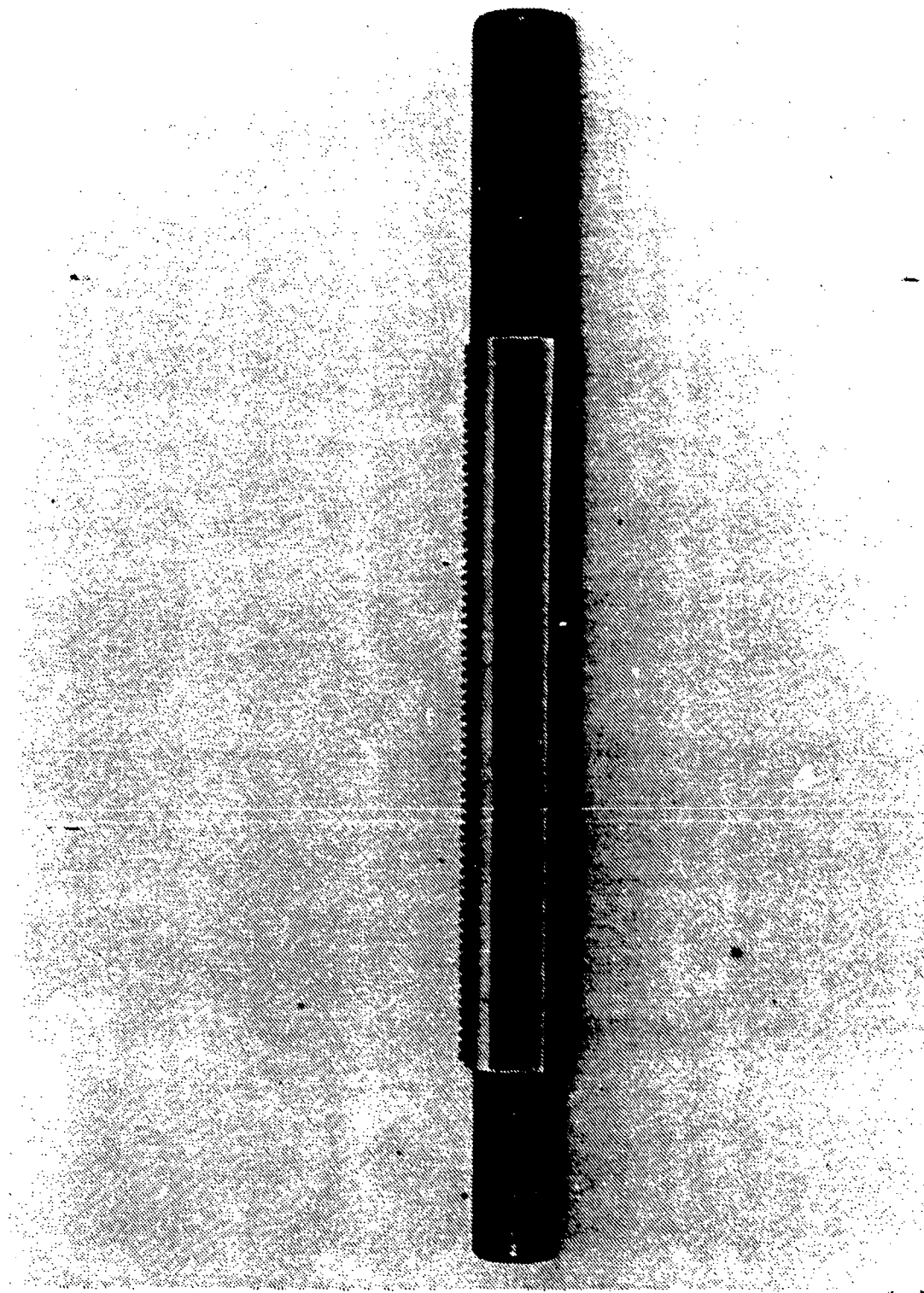
Figure 3.7   A Photograph of Top View of Finned Tube with
Fin Tip Insulation Installed.

53
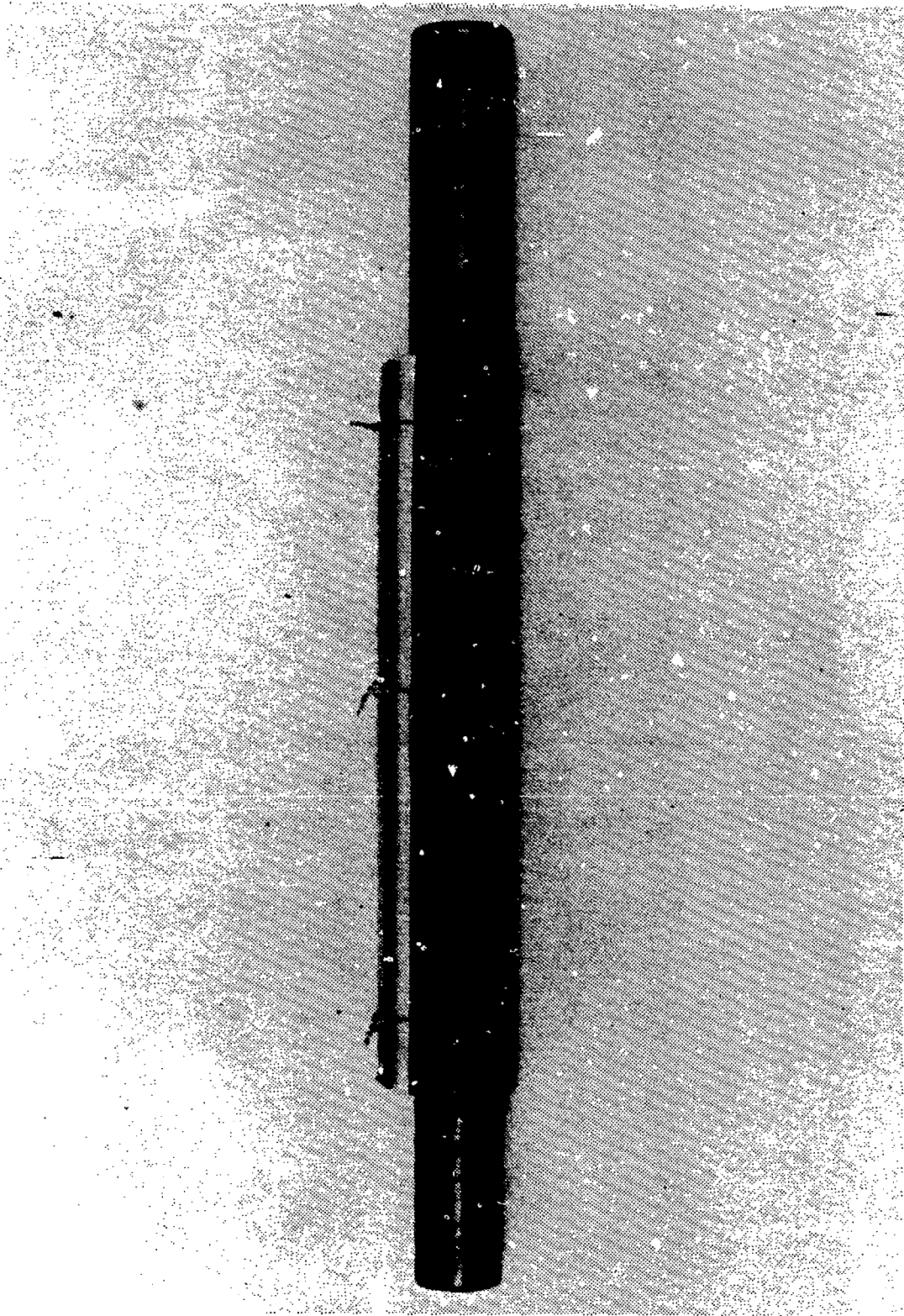
Figure 3.8   A Photograph of Side View of Finned Tube with
Fin Tip Insulation Installed.
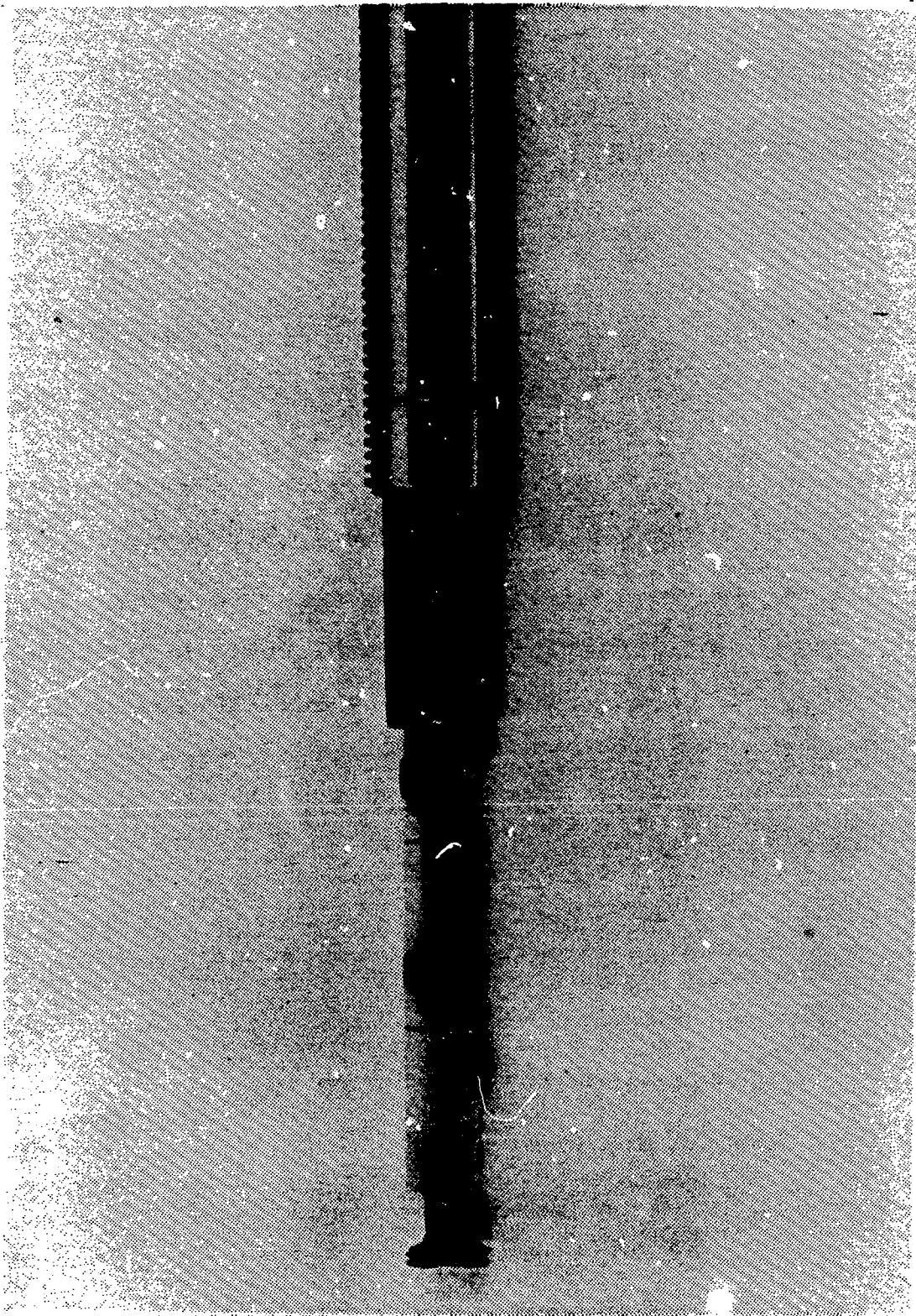
Figure 3.9   A Photograph of Finned Tube Showing All Three
Types of Insulation Present.

IV. SYSTEM OPERATION AND DATA REDUCTION

A. SYSTEM OPERATION

The general procedures employed in the preparation and testing of the condenser tubes are outlined below.

The exterior and interior surfaces of the tube- were thoroughly brushed and rinsed with water. Then, considering the poor wetting characteristics of copper with water, the exterior surface was treated with a solution consisting of equal volumes of sodium hydroxide and ethyl alcohol. This solution was applied while the tube was heated using a steam bath. The initial treatment for each tube was to apply the solution approximately every ten minutes for a period of about one hour to allow an initial base coating (an oxide layer) to form on the tube surface. Before re-testing an already oxidized tube on a later day, this same procedure was performed every five minutes for a period of 15-20 minutes to ensure a continuous oxide layer and to remove any foreign materials, such as oils, from the tube surface. Following treatment of the tube with the above-mentioned solution, the tube was rinsed with distilled water to remove any excess solution. This treatment was required since copper has poor wetting characteristics with water. Therefore, steam will normally condense on copper under a partial dropwise condensation mode, which is more effective than the filmwise condensation mode. Since the purpose of

56

this investigation was to collect data on tubes undergoing filmwise condensation and the tubes were copper, great care had to be taken to ensure complete wettability through the use of the above-mentioned treatment of the external tube surfaces. Since the oxide layer provided in this manner is very thin, its thermal resistance was negligible.

Following cleaning, the Teflon insulation was installed first between the tube's fins and then covering the tube fin tips. Following the installation of the insulation between the fins, the external surface of the tube was cleaned as before for about fifteen minutes. This cleaning process was again repeated following the installation of the Teflon section which covered the fin tips.

Upon the completion of the cleaning process, the tube was installed into the test section of the apparatus. A spiral insert and plastic insulation strip were installed on the inside of the tube. The purpose of the insert and plastic strip was to enhance the inside heat-transfer coefficient and insulate the upper section of the tube inner surface, respectively.

Following the installation of the tube in the apparatus, the system was brought to operating pressure and temperature by adjusting the input power to the boiler heaters, the cooling water flow rate through the tube, and the cooling water flow rate to the auxiliary condenser. Steady-state conditions were assumed when the operating conditions were

57

stabilized within a steam temperature variation corresponding to 2 microvolts and a variation of the temperature rise of the cooling water in the range of 0.005 K and 0.01 K for atmospheric and vacuum, respectively.

Once steady-state conditions were achieved, the data collection process could begin. The cooling water through the tube was entered manually into the computer starting each data measurement. The temperature rise of the cooling water through the tube, vapor pressure and temperature were gathered automatically by the data-acquisition system. For the first and last data points, the concentration of non-condensing gases (believed to be air) were computed to ensure that the apparatus was free of leaks. The sequence of data points was based on the percent flow rate of cooling water through the flowmeter and the test tube: 20, 26, 35, 45, 54, 62, 70, 80, 20. Notice that an 80% flow rate resulted in a water velocity of 4.4 m/s through the tube. The repeating of the 20% data point at the end of the run was useful to ensure that the data were not affected by dropwise condensation or by any air that could have leaked into the system. In addition, two readings were taken at each flow rate also to demonstrate data repeatability.

B. DATA REDUCTION

The data were collected and processed using the same program used by both Mitrou [10] and Cakan [29]. This program incorporates property functions, calibration curves

58

for the cooling water flowmeter and for all thermocouples as well as the temperature rise due to frictional heating within the mixing chamber.

The overall heat-transfer resistance is given by equation (4.1) which is composed of the inside resistance, steam-side resistance, and the tube wall resistance. This equation (4.1) is as follows:

$$\frac{1}{U_o A_o} = \frac{1}{h_i A_i} + \frac{1}{h_o A_o} + \frac{R_w}{A_o} \qquad (4.1)$$

where

$$R_w = \frac{D_o \, ln\left(\frac{D_o}{D_i}\right)}{2 k_m}$$

$$A_i = \pi D_i (L + L_1 \eta_1 + L_2 \eta_2) \quad , \quad and$$

$$A_o = \pi D_o L$$

η_1 , η_2 = fin efficiencies at the inlet and outlet portions of the tube inside the Teflon bushings [14]

$\overline{L}$ = length of condenser test tube

L_1 = length of tube portion (not exposed to vapor) inside nylon bushing at the inlet

L_2 = length of tube portion (not exposed to vapor) inside nylon bushing at the outlet.

The separation of the overall heat-transfer resistance into the three individual thermal resistances become neccessary to obtain the steam-side heat-transfer coefficient. The steam-side heat-transfer coefficient was based on the smooth-tube

59

area (i.e., the surface area of a smooth tube having an outside diameter equal to the fin root diameter). The inside heat-transfer coefficent is given by a Sieder-Tate-type equation (4.2) and is determined using the modified Wilson plot method for the finned tube.

$$Nu_i = \frac{h_i D_i}{k_c} = C_i Re^{0.8} Pr^{1/3} \left(\frac{\mu_c}{\mu_w} \right)^{0.14}$$
(4.2)

The accuracy of the steam-side heat-transfer coefficient from equation (4.1) tends to increase as the inside resistance term becomes a smaller fraction of the overall resistance. In order to increase the steam-side coefficient accuracy, a coiled insert was installed inside all tested tubes. This insert provided a smaller flow area (therefore, a higher Reynolds number for a given mass flow rate) and a swirl within the tube resulting in improved mixing of the coolant and enhanced heat transfer.

1. **Modified Wilson Plot on Finned Tubes**

This method, which was previously discussed by Mitrou [10] and Cakan [29], was employed in this study to calculate the inside heat-transfer coefficient. The data were always collected by assuming a reasonable approximation for the Sieder-Tate-type coefficent. Upon the completion of a run, the data were reprocessed using the Modified Wilson Plot analysis to determine a more accurate value for the Sieder-Tate-type coefficient. Based on this new Sieder-Tate-

60

type coefficient, the condensing heat-transfer coefficients were computed.

2. Determination of Finned-Tube Enhancement

In this investigation, the finned tube enhancement based on a fixed steam-side temperature difference was used as an important measure of the improvement of the heat-transfer performance of the finned tube when compared to that of the smooth tube. In the course of these measurements and calculations, a number of different tube enhancements were used, and are defined in this section. In general, the tube enhancement is defined as the ratio of the heat-transfer coefficient of the finned tube to the heat-transfer coefficient of the smooth tube. A list of definitions for the different enhancements used in this thesis are provided as follows using Figure 3.5 as visual support:

(a) $\bar{\varepsilon}_{n-\phi}$ represents the average enhancement of the uninsulated or bottom portion of the tube.

(b) $\bar{\varepsilon}_n$ represents the average enhancement for the entire tube with no insulation present.

(c) $\bar{\varepsilon}_\phi$ is the average enhancement of the insulated or top portion of the tube. Notice that this value was not measured directly, but was inferred from $\bar{\varepsilon}_n$ and $\bar{\varepsilon}_{n-\phi}$ as given by the following equation:

$$\bar{\varepsilon}_\phi = \frac{n}{\phi} \left[\bar{\varepsilon}_n - \left(\frac{n}{n-\phi} \right) \bar{\varepsilon}_{n-\phi} \right] \tag{4.3}$$

61

(d) ε_ϕ is the local value of the tube enhancement with no insulation present.

In order to determine the local enhancement (ε_ϕ) around the finned tube surface, a polynomial of the form of equation (4.4) was assumed.

$$\varepsilon_\phi = a_o + a_1\phi + a_2\phi^2 + a_3\phi^3 \qquad (4.4)$$

Thus, the average enhancement was determined as follows:

$$\bar{\varepsilon}_\phi = \frac{1}{\phi} \int_0^\phi \varepsilon_\phi \, d\phi \qquad (4.5)$$

The cubic polynomial assumed for the local enhancement relationship requires four boundary conditions in order to determine the coefficient values. These conditions are as follows:

(a) $\varepsilon_\phi = 0 \quad at \quad \phi = \pi$

(b) $\dfrac{d\varepsilon_\phi}{d\phi} = 0 \quad at \quad \phi = 0$

(c) $\bar{\varepsilon}_\phi = B \quad at \quad \phi = \pi.$

In addition to the above three boundary conditions, the least squares technique was applied to the relationship for the average enhancement to fulfill the conditions to define completely the coefficients of the equations. The specific steps required in these calculations and subsequent results for the average and local enhancement relationships are provided in Appendix C.

62

V. RESULTS AND DISCUSSION

A. INTRODUCTION

Data were collected on three horizontal finned tubes employing the procedure described in Chapter IV. As stated in Chapter IV, the three finned tubes tested had a fin height and fin thickness of 1.0 mm and fin spacings of 0.5, 1.0 and 1.5 mm. The data runs were performed at both low pressure (approx. 85 mmHg) and atmospheric pressure on each tube at least twice on different days to ensure data repeatabilty. If two runs showed larger than 5% disagreement in the condensing heat-transfer coefficient, an additional run was made to obtain reliable data. During all runs, the test tube was visually inspected to ensure filmwise condensation was occurring. Although some data runs suggested the presence of dropwise condensation by an increase of as much as 10 percent in the heat-transfer coefficient over previous runs, its presence was never visually evident. As discussed by Georgiadis [27], large increases in the heat-transfer coefficient appear to be as a result of the tube undergoing partial dropwise condensation with exposure to steam. Since visual observation of characteristic droplets never occurred, it is possible that dropwise condensation was taking place at a microscopic level especially near fin edges where a very thin condensate film exists. All data runs presented in this

63

thesis satisfied the requirement of 5 percent agreement between corresponding repeatability runs.

Initial data runs were performed on the three tubes without any insulation in order to establish heat-transfer coefficient values for the bare tubes. These initial runs for uninsulated tubes were necessary to show agreement with previous investigations and establish an independent basis for comparison of the effects of insulating the upper portions of the tubes. Additionally, these initial data runs provided values of the average enhancement ($\bar{\varepsilon}_\phi$) of the uninsulated tube.

Subsequent data runs were performed on the tubes with increasing portions of the upper tube section being insulated. The measurements were performed for nominal angles of 30, 60, 90, 150 and 210 degrees of the upper portion of the tube. Measurements were also performed using a smooth tube in order to ensure comparability with previous investigations.

B. COMPARISON OF DATA WITH PREVIOUS INVESTIGATIONS

Figure 5.1 shows the variation of the steam-side heat-transfer coefficient with the steam-side temperature drop for the three finned tubes in comparison with previous data obtained by Georgiadis [27] under low-pressure condition. Notice that the solid curves represent the least-squares fits to the present data, while the broken curves represent the

64
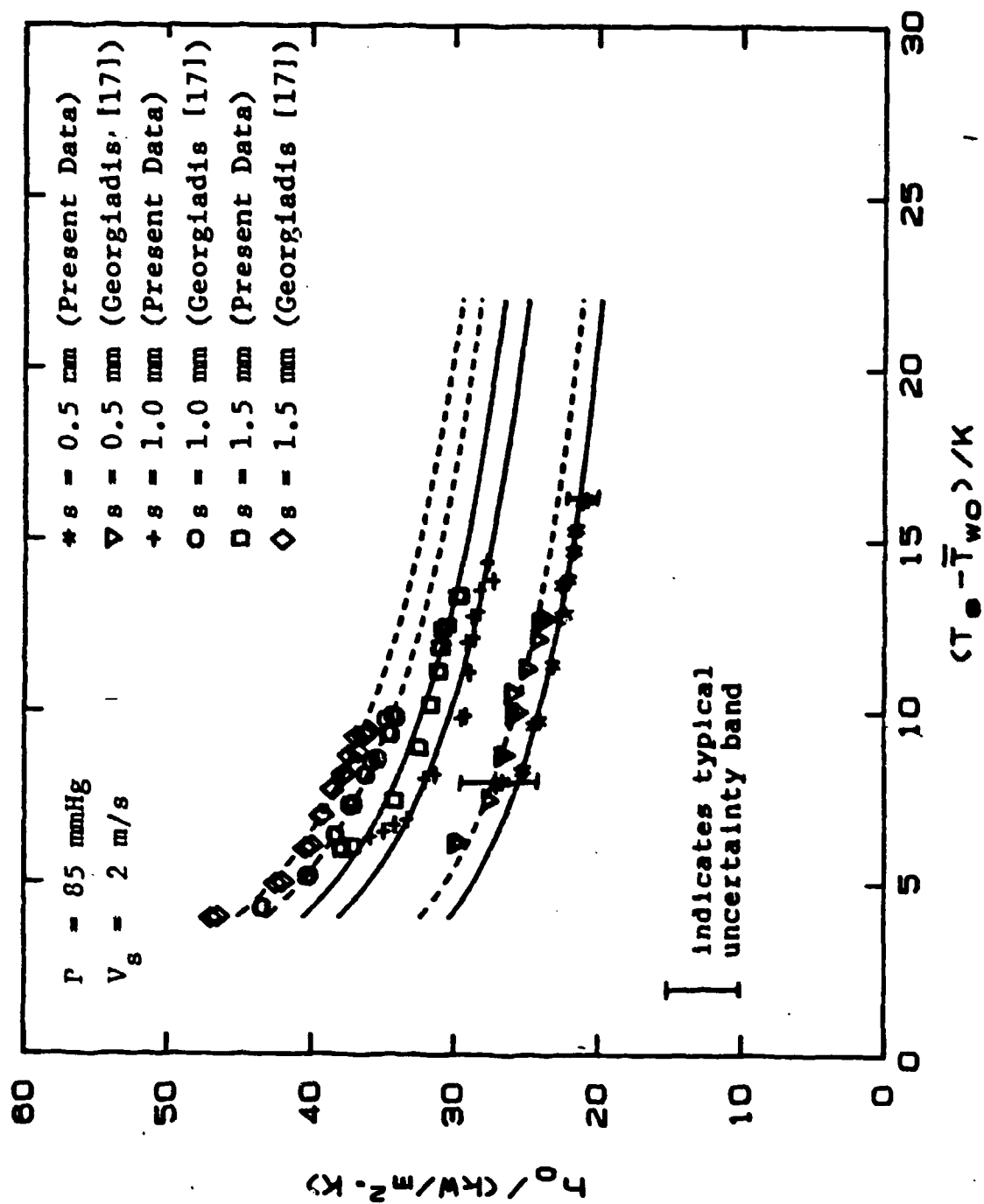
Figure 5.1 Comparison of Present Data with Data of
Georgiadis [17] for Low-Pressure Condition.

65

least-squares fit to the data of Georgiadis [27]. These least-squares fits were generated according to the following expression:

$$q = a \Delta T^{0.75} \qquad (5.1)$$

Slightly more improved fits were possible by allowing the exponent of the temperature difference to be a variable to be found by the least-squares technique. However, the use of a constant value of 0.75 makes it quite convenient when defining the enhancement ratio as discussed later in this Chapter. Figure 5.2 shows a comparison of data similar to that of Figure 5.1, but for near-atmospheric condition. As can be seen, both of these figures show that the data of Georgiadis lie consistently up to 10 percent higher than the present data. It is possible that the data of Georgiadis had been slightly affected by microscopic dropwise condensation as discussed earlier. With systematic improvements made to the apparatus and to the tube-cleaning process, the present data are believed to be least affected by microscopic dropwise condensation.

Figures 5.1 and 5.2 also show typical uncertainty bands for the steam-side heat-transfer coefficient computed using the procedures outlined in Appendix A. Notice that, while these uncertainties are 15.8% to 2.7% for the atmospheric condition, data were repeated to within 5%.

66
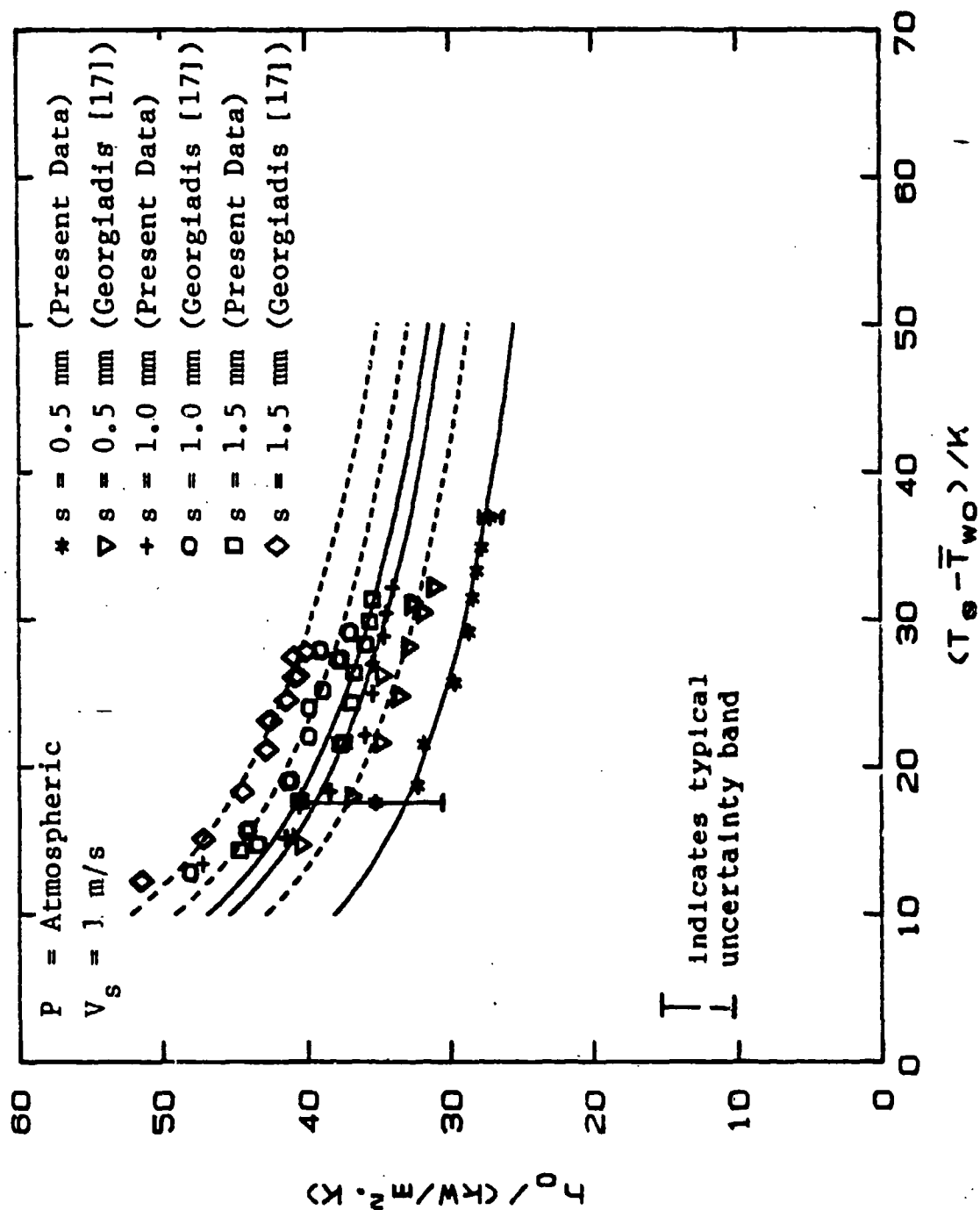
Figure 5.2　Comparison of Present Data with Data of
　　　　　　Georgiadis [17] for Atmospheric Condition.

67

C. MEASUREMENTS FOR PARTIALLY INSULATED FINNED TUBES

The tubes were insulated systematically up to 5 different angles as discussed in Chapter IV. The results of these measurements are presented in the format of outside heat-transfer coefficient versus the steam-side temperature difference. These results are shown in Figures 5.3 through 5.8. These curves, as expected, show that as the size of the insulated portion of the upper tube section increases, the outside heat-transfer coefficient decreases. Notice that the outside (i.e., steam-side) heat-transfer coefficient is based on the total area of the corresponding smooth tube, regardless of the extent of insulation. This heat-transfer coefficient represents the average value for the remaining uninsulated lower portion of the tube. As discussed before, the least-squares curves represent equation (5.1) where the coefficent (a) values are listed in Table 2.

Using the coefficients provided in Table 2, the heat-transfer coefficients for both smooth and finned tubes can be calculated. The heat-transfer coefficients can then be used to determine the tube enhancement based on the temperature difference. The heat-transfer coefficient for the smooth tube is calculated by dividing the smooth-tube coefficient from Table 2 by the temperature difference raised to the 0.25 power. The heat-transfer coefficient for the finned tube is calculated by using the finned-tube coefficient from Table 2 divided by the same temperature difference raise to the 0.25

68

TABLE 2

SUMMARY OF LEAST-SQUARES CURVES TO EXPERIMENTAL DATA
(equation (5.2))

Tube No.	Insulated Angle(deg)	Vacuum	Atmospheric
1	smooth	23200	25600
4	0	42800	67800
	30	37000	60100
	58	34800	56700
	90	30300	46400
	149	22600	31100
	210	12000	17900
5	0	53800	80700
	29	49300	71200
	88	35700	53500
	148	19000	29400
	210	10400	15400
6	0	57300	93400
	27	51200	75800
	38	36300	52000
	148	19300	32300
	211	9150	14400
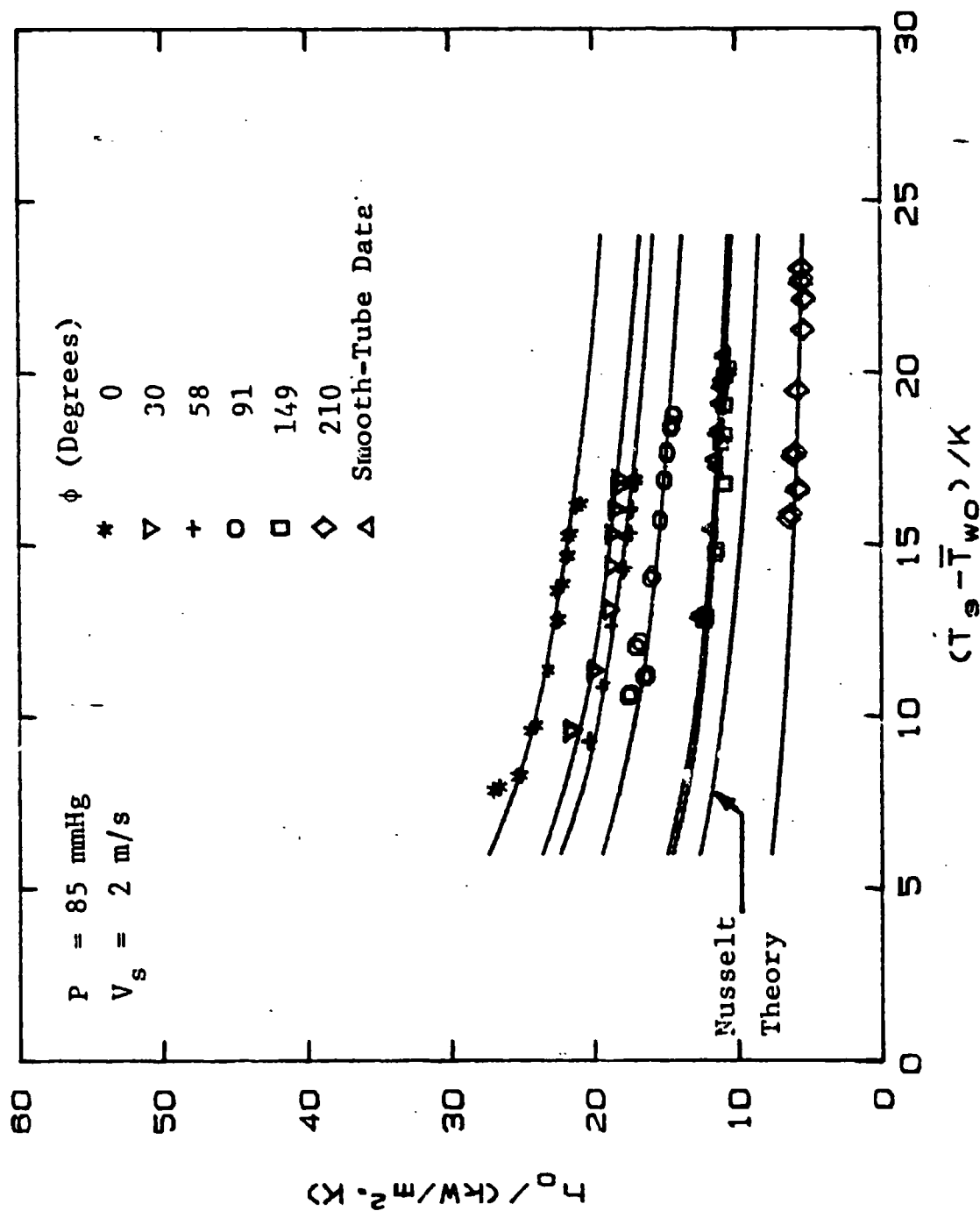
Figure 5.3 Effect of Insulating Tube on Condensing Heat-
Transfer Performance for Low-Pressure Condition
(s = 0.5 mm).

70
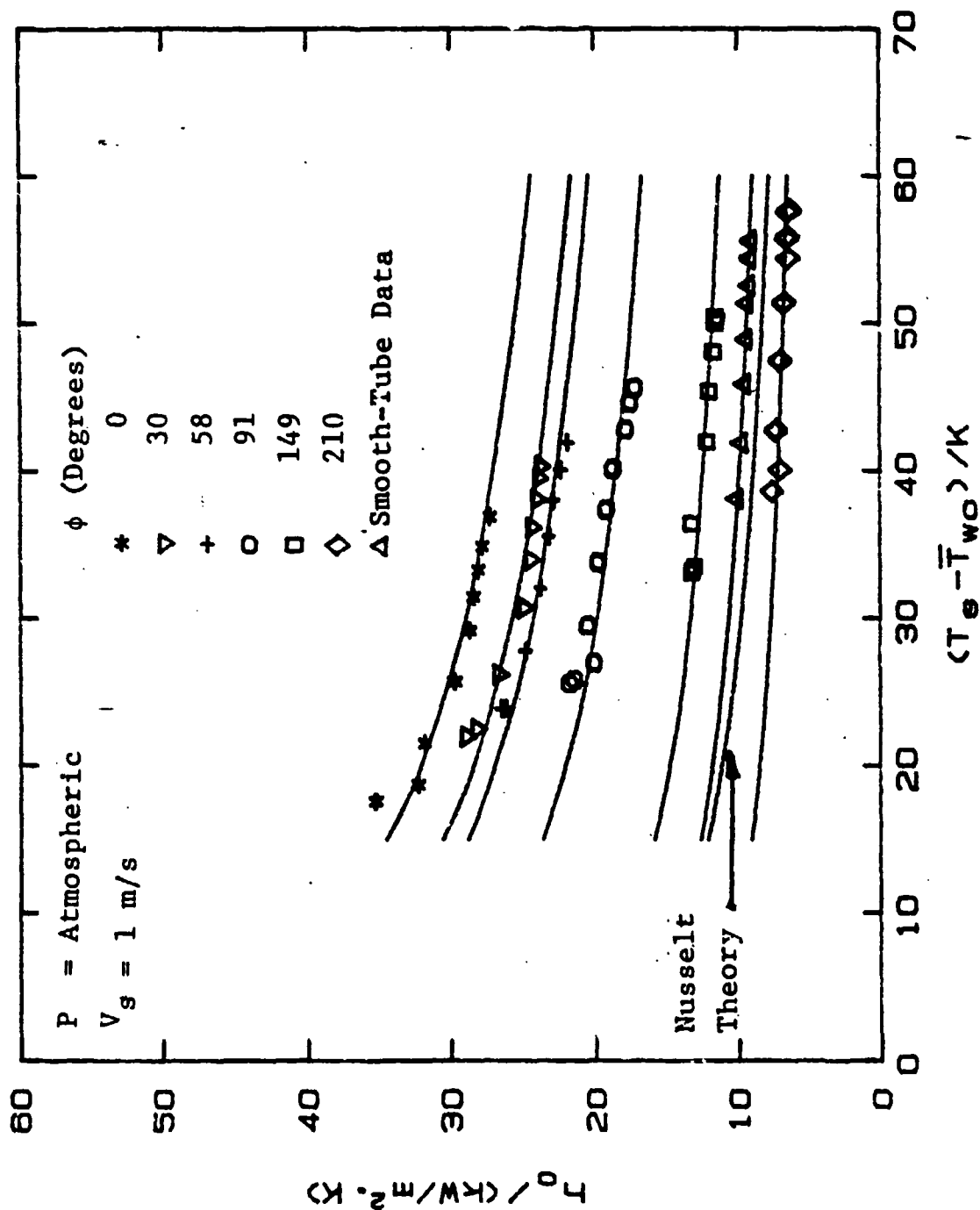
Figure 5.4 Effect of Insulating Tube on Condensing Heat-
Transfer Performance for Atmospheric Condition
(s = 0.5 mm).

71
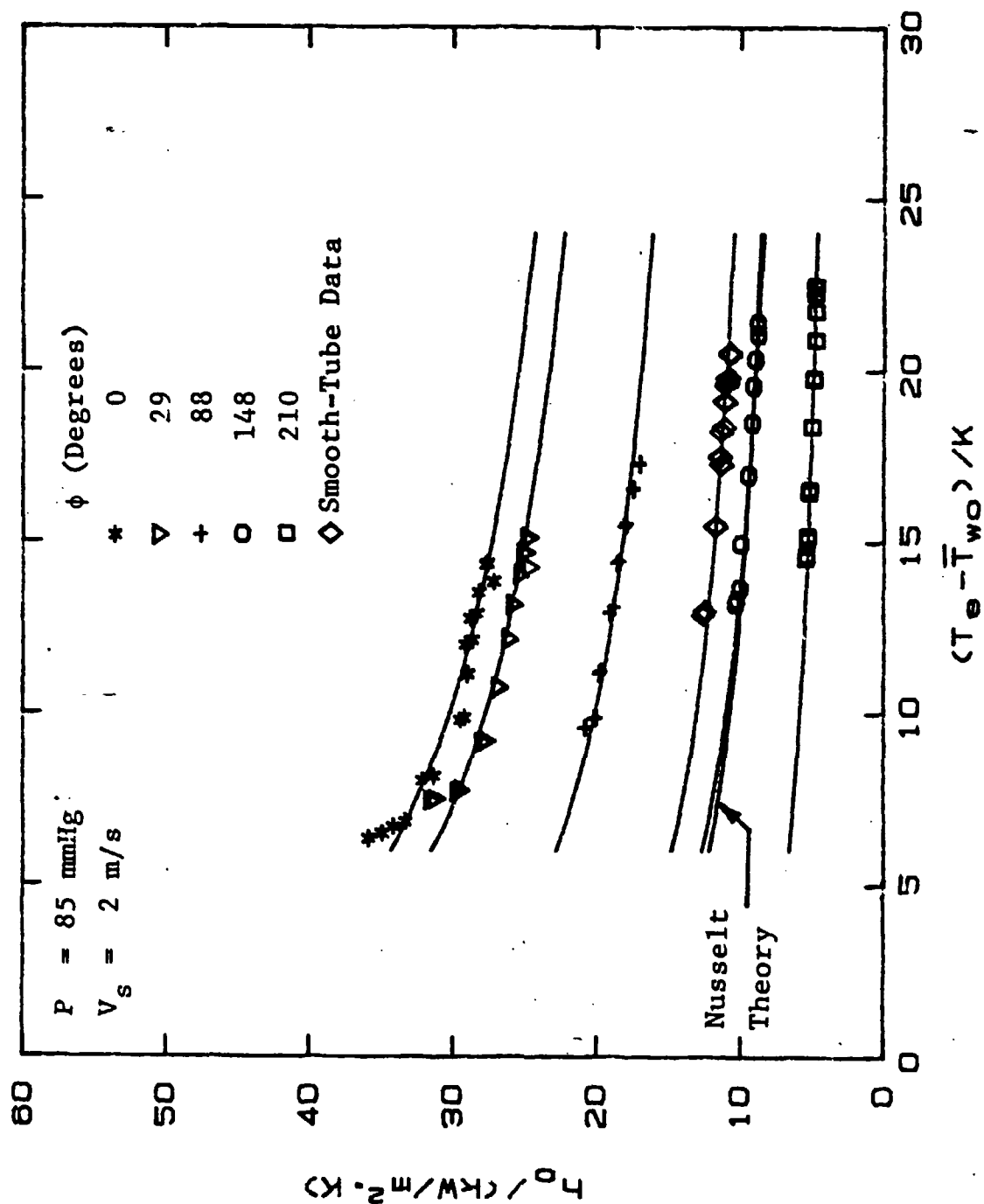
Figure 5.5   Effect of Insulating Tube on Condensing Heat-
Transfer Performance for Atmospheric Condition
(s = 1.0 mm).
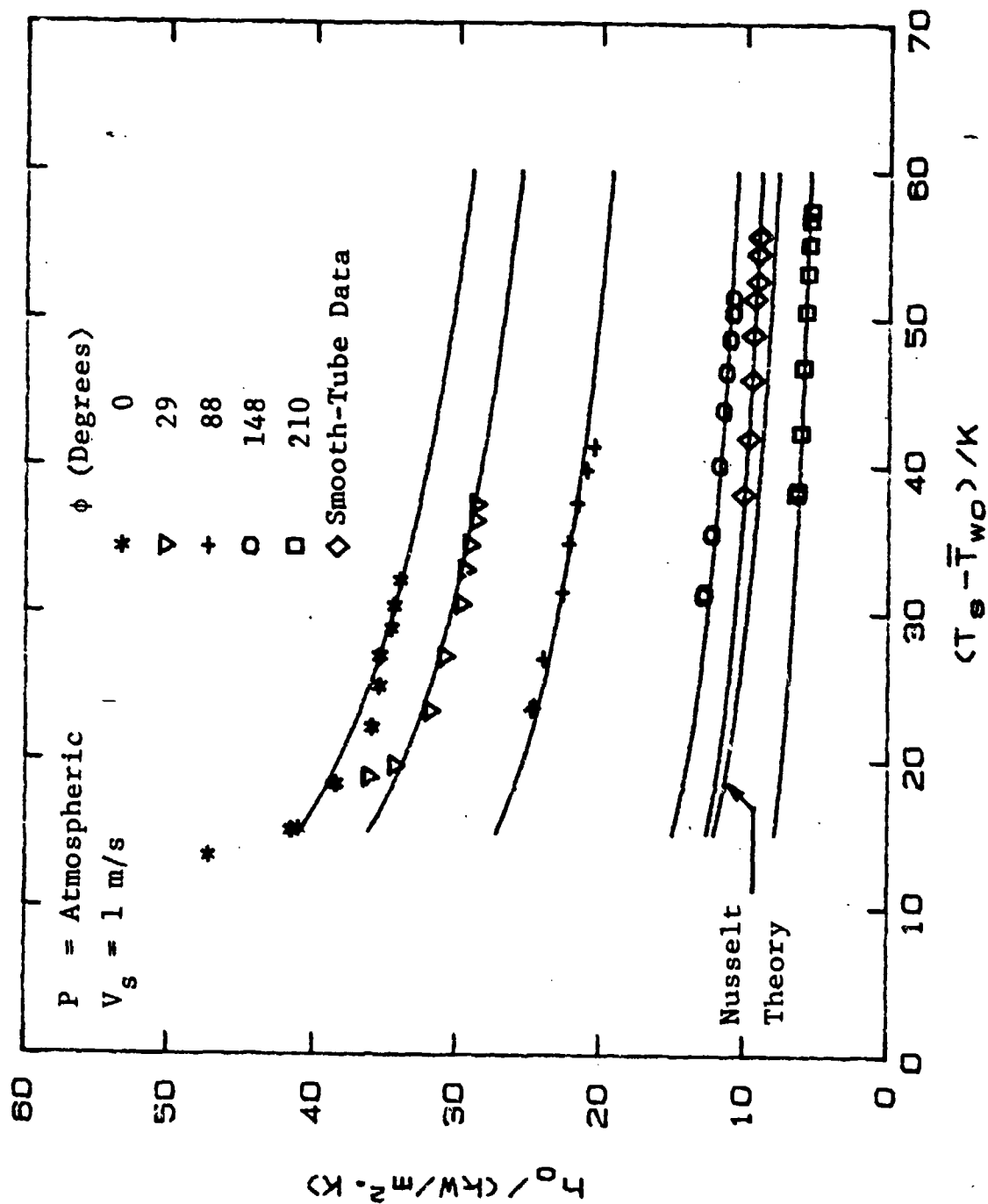
Figure 5.6 Effect of Insulating Tube on Condensing Heat-
Transfer Performance for Atmospheric Condition
(s = 1.0 mm).
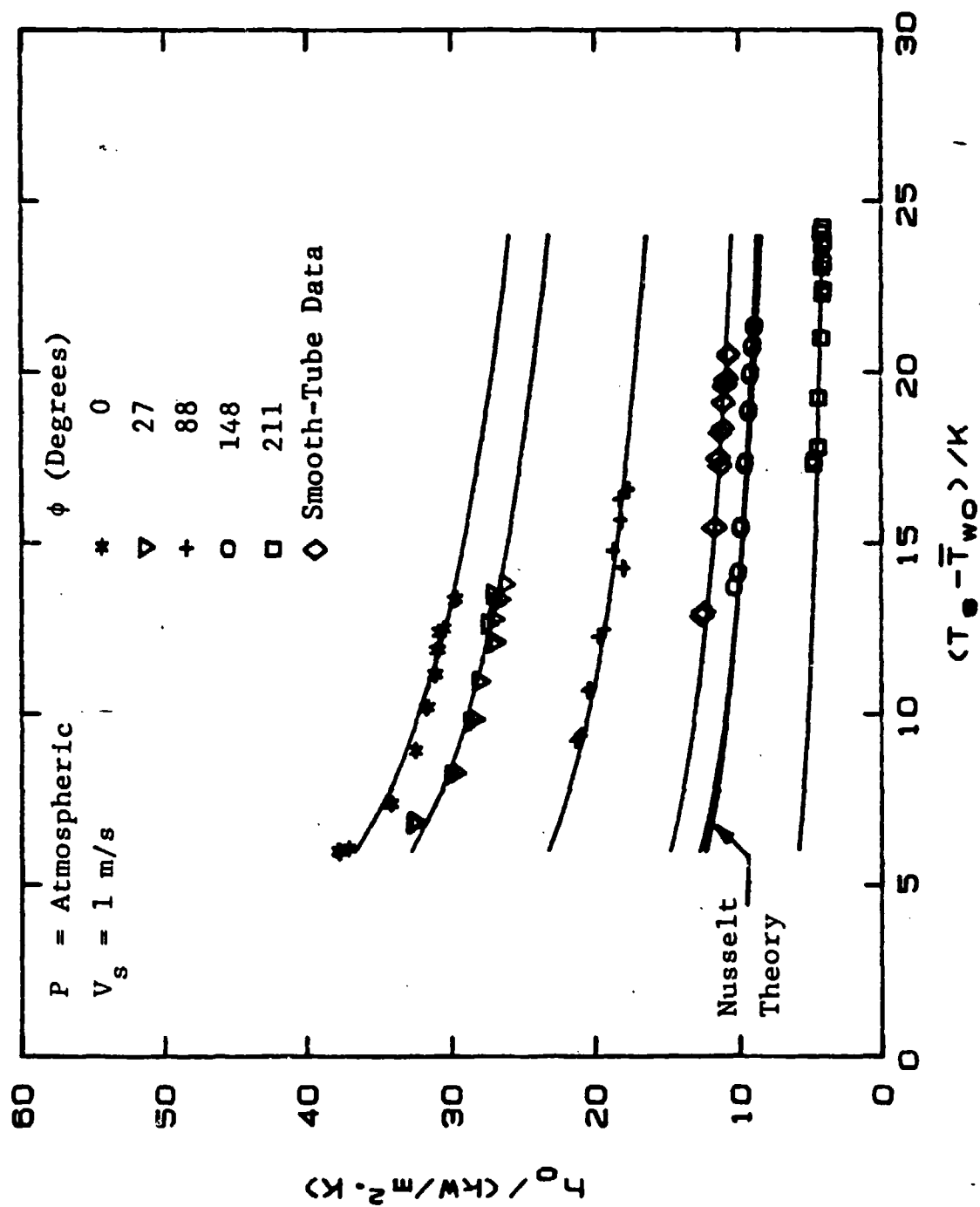
Figure 5.7 Effect of Insulating Tube on Condensing Heat-Transfer Performance for Atmospheric Condition (s = 1.5 mm).

74
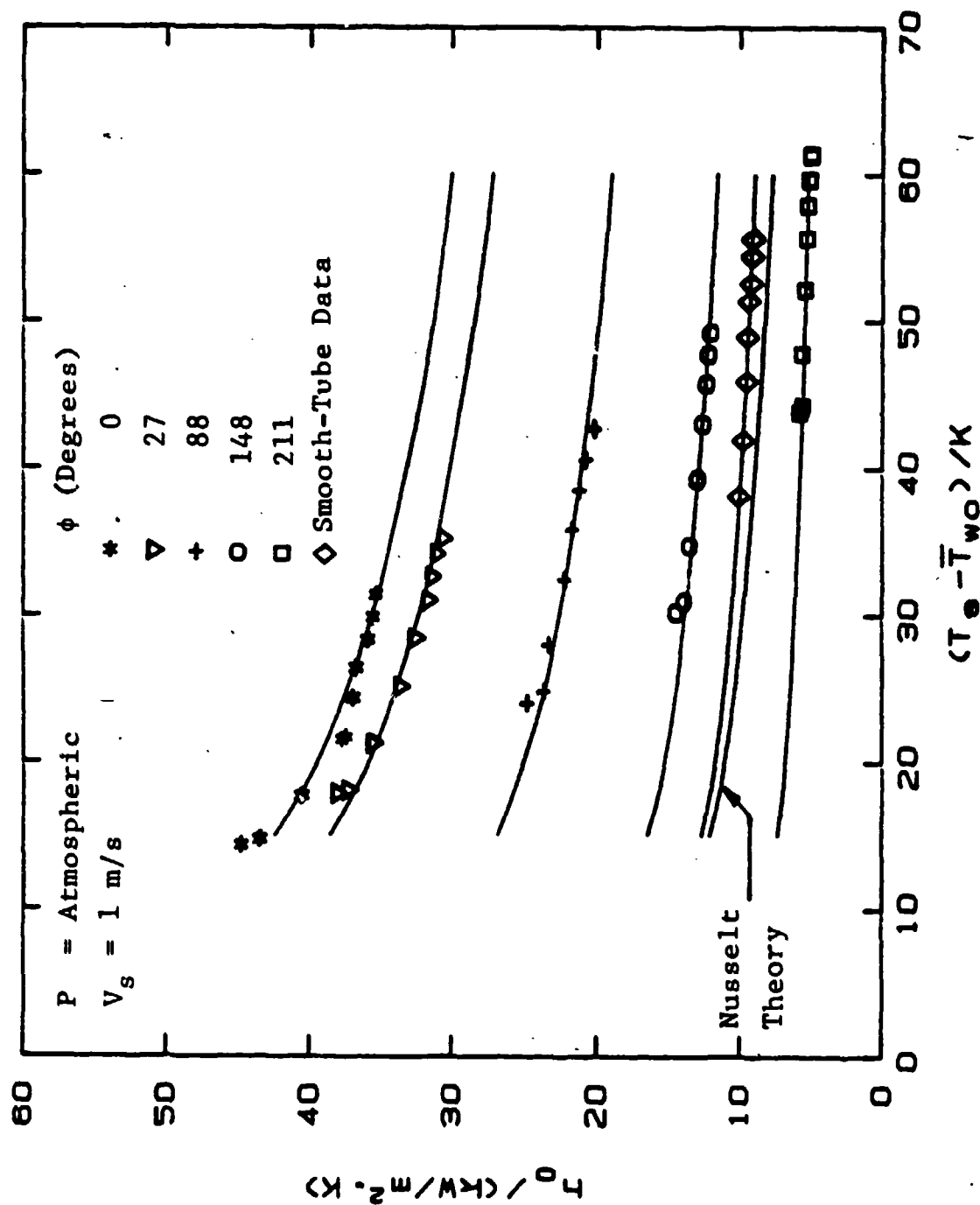
Figure 5.8   Effect of Insulating Tube on Condensing Heat-
Transfer Performance for Atmospheric Condition
(s = 1.5 mm).

75

power. The tube enhancement ($\varepsilon_{\Delta T}$) based on the temperature difference is then determined by dividing the finned tube heat-transfer coefficient by the smooth tube heat-transfer coefficient.

The Sieder-Tate-Type (C_i) constants for the inside heat-transfer coefficient and their modified values (C_{im}) are plotted in Figures 5.9 and 5.10 for low and atmospheric pressures, respectively. The modified values of the Sieder-Tate-type coefficient (C_{im}) are based on the actual heat-transfer area, after subtracting the area occupied by the internal plastic insulation, and is computed by the relationship;

$$C_{im} = C_i \left(\frac{\pi}{\pi - \phi} \right),$$ (5.2)

The curves shown in Figures 5.9 and 5.10, represent the average trends for the three tubes. The uncertainty in the Sieder-Tate-type constant was 2.5% and 2.8% for low pressure and atmospheric pressure, respectively. And the uncertainty in the modified Sieder-Tate-type constant ranges from 3.2% to 4.7% and from 2.8% to 4.9% for low pressure and atmospheric pressure, respectively. Notice that, as the angle of insulation increases, the measured coefficient (C_i) increases slightly up to an insulated angle of about 0.5 radians (28.6 degrees) then decreases, while the modified coefficient (C_{im}) increases and approaches a constant value of about 0.1.
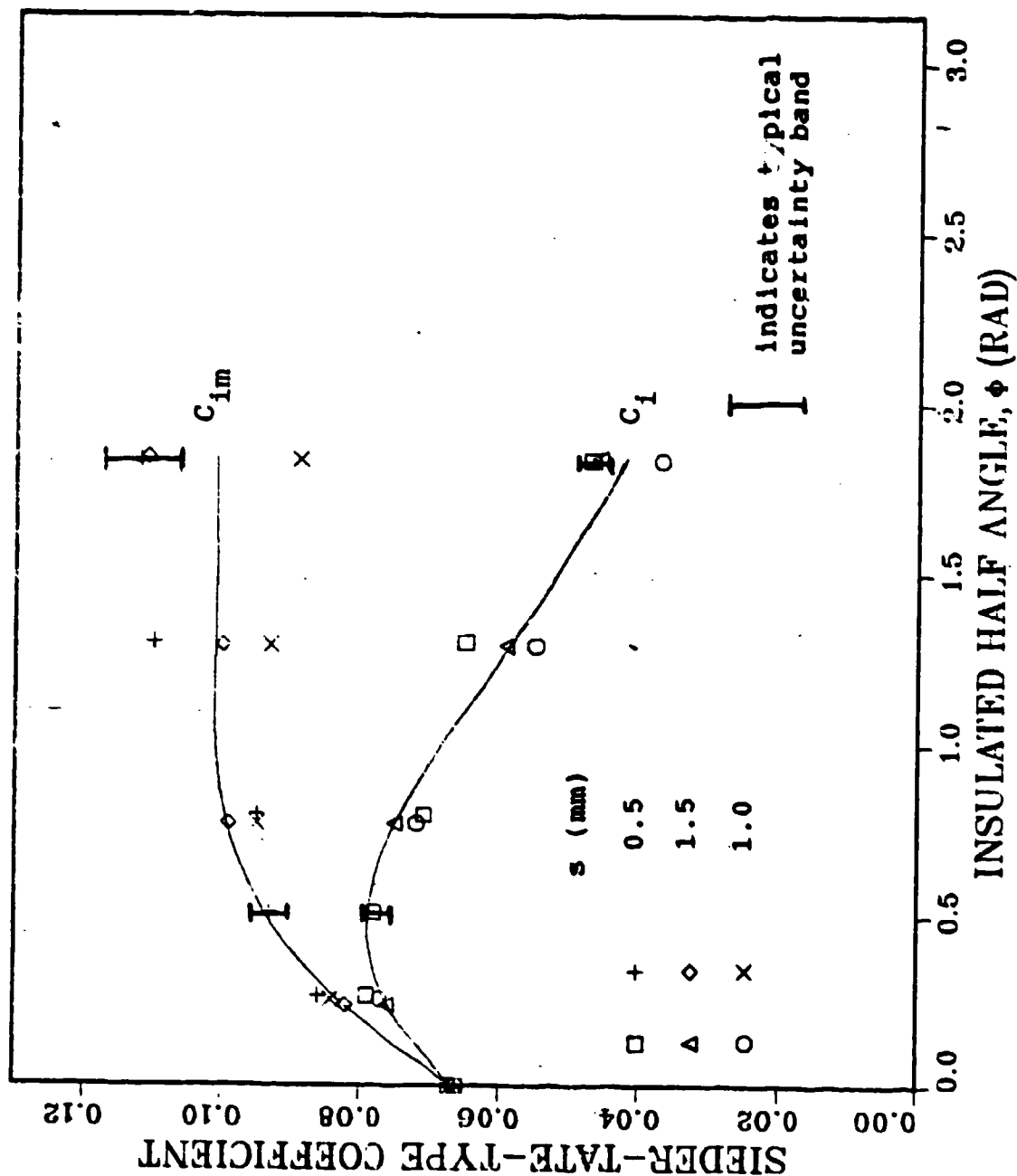
Figure 5.9   Effect of Tube Insulation on Sieder-Tate-Type Coefficient (C_i) and Modified Coefficient (C_{im}) for All Tubes at Low-Pressure Condition.

77
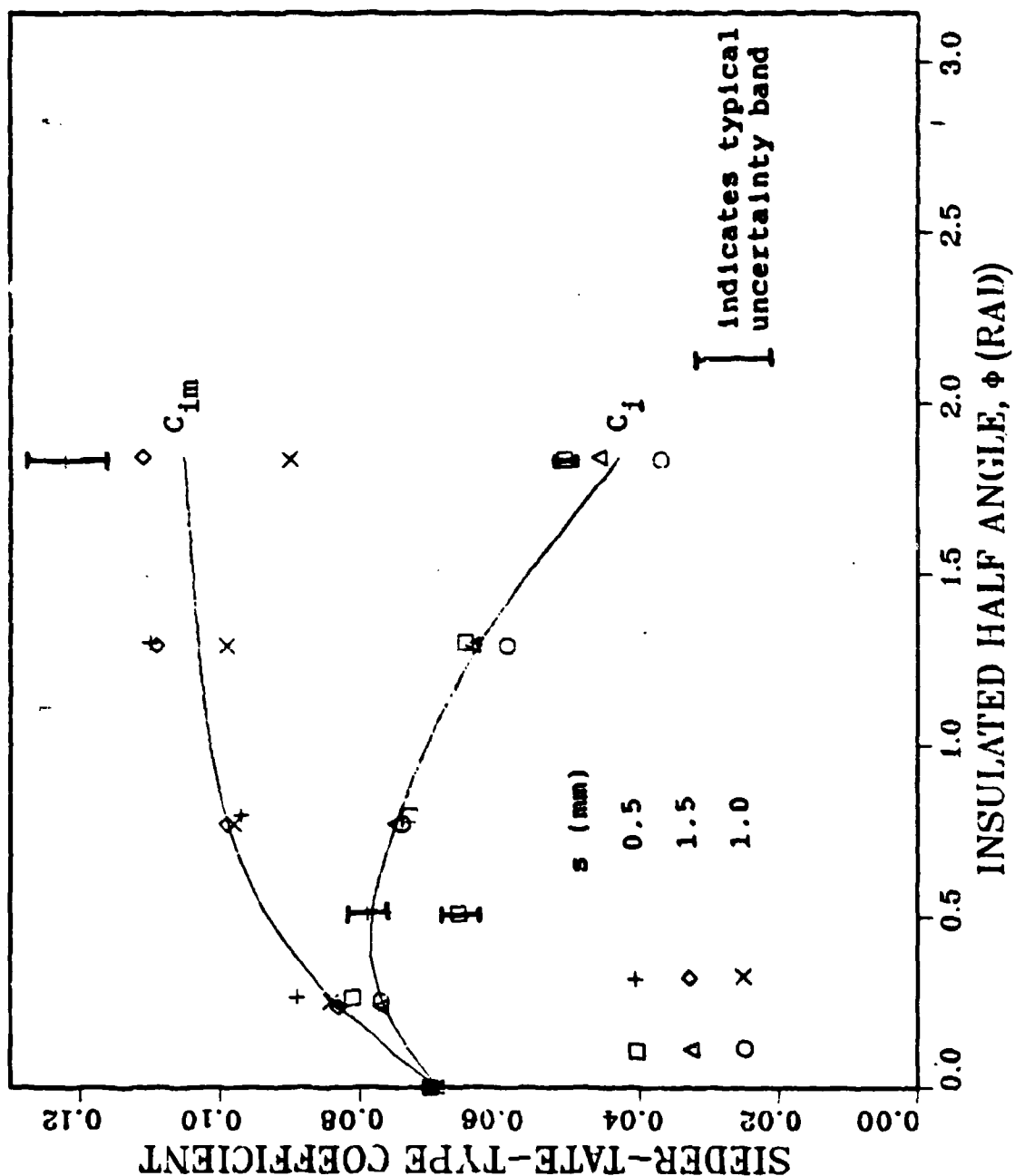
Figure 5.10   Effect of Tube Insulation on Sieder-Tate-Type
Coefficient (C_i) and Modified Coefficient (C_{im})
for All Tubes at Atmospheric Pressure Condition.

Notice that, as discussed in Chapter IV, the tubes were tested with a spiral insert, provided to enhance the inside heat-transfer coefficient. This insert had a single start spiral of a 3.2-mm-diameter copper wire wrapped around a 6.4-mm-diameter stainless steel rod allowing a pitch of about 40 mm. When this insert was placed inside a test tube, the water was forced to travel through this spiral channel. As a result, the water encountered heated and unheated sections repeatedly. While the thermal boundary layer develops during the heated portion, turbulent eddies would provide mixing during the unheated portion, thus resulting in a smaller water temperature in the near vicinity of the tube wall. Notice also that the spiral motion creates a centrifugal force, which directs the denser and colder water toward the interior tube surface, thus supplementing the mixing process. For these reasons, the average heat-transfer coefficient in the next heated portion would be somewhat more enhanced than if the unheated portion was not present. Based on this observation, it is possible that the enhancement in the heated portion (based on the heated surface area) of the tube increases with increasing length of the unheated portion as this would allow more and more mixing. Also, an upper limit to the length of the unheated portion must exist as complete mixing will be achieved within a finite distance of travel depending on the local conditions, such as the Reynolds

number. The above-mentioned explanations are only qualitative, and quantitative explanations are beyond the scope of this investigation.

D. DISCUSSION OF STEAM-SIDE ENHANCEMENT

To summarize the data presented in Figures 5.3 through 5.8, steam-side enhancement ratios were defined as outlined below, as proposed by Masuada and Rose [15]. From equation (5.1),

$$q_s = a_s \Delta T_s^{0.75} = h_s \Delta T_s \qquad (5.3)$$

$$q_f = a_f \Delta T_f^{0.75} = h_f \Delta T_f$$

therefore,
$$h_f = a_f \Delta T_f^{-0.25}$$

$$h_s = a_s \Delta T_s^{-0.25}$$

$$\varepsilon = \frac{h_f}{h_s} = \frac{a_f}{a_s} \left[\frac{\Delta T_s}{\Delta T_f} \right]^{0.25} \qquad (5.4)$$

For constant steam-side temperature drop (i.e., $\Delta T_f = \Delta T_s$),

$$\varepsilon_{\Delta T} = \frac{a_f}{a_s} \qquad (5.5)$$

As can be seen, the use of a constant exponent value of 0.75 in equation (5.1) results in a simple expression for enhancement based on the temperature difference. Notice, however, this enhancement ratio does not depend on the vapor-side temperature difference.

80

Further, when considering the case of constant heat-flux condition (i.e., $q_f = q_s$),

$$a_f \Delta T_f^{0.75} = a_s \Delta T_s^{0.75} \qquad (5.6)$$

$$\frac{\Delta T_s}{\Delta T_f} = \left[\frac{a_f}{a_s}\right]^{4/3}$$

Substituting in equation (5.4),

$$\varepsilon_q = \frac{a_f}{a_s}\left[\frac{a_f}{a_s}\right]^{1/3} = \left[\frac{a_f}{a_s}\right]^{4/3}$$

$$\varepsilon_q = \varepsilon_{\Delta T}^{3/4} \qquad (5.7)$$

Once again, ε_q is independent of ΔT or q. Since there exists a unique and simple relationship between ε_q and $\varepsilon_{\Delta T}$ as shown in equation (5.7), only $\varepsilon_{\Delta T}$ will be presented during this Chapter.

The average tube enhancement ($\varepsilon_{\Delta T}$) for the three tubes is plotted separately in Figures 5.11, 5.12, and 5.13. These Figures show that, for each of the tubes, the average enhancement is larger for the atmospheric condition. The smaller surface tension value at 100 °C (0.069 N/m) compared to the value at 48 °C (0.058 N/m) may be responsible for the larger enhancement at atmospheric pressure. Notice that a smaller surface tension results in a smaller condensate retention angle, thus increasing the heat-transfer performance. The average enhancements are shown again in Figures 5.14 and 5.15 comparing the results for the three tubes. The uncertainty in the average enhancement data is

81
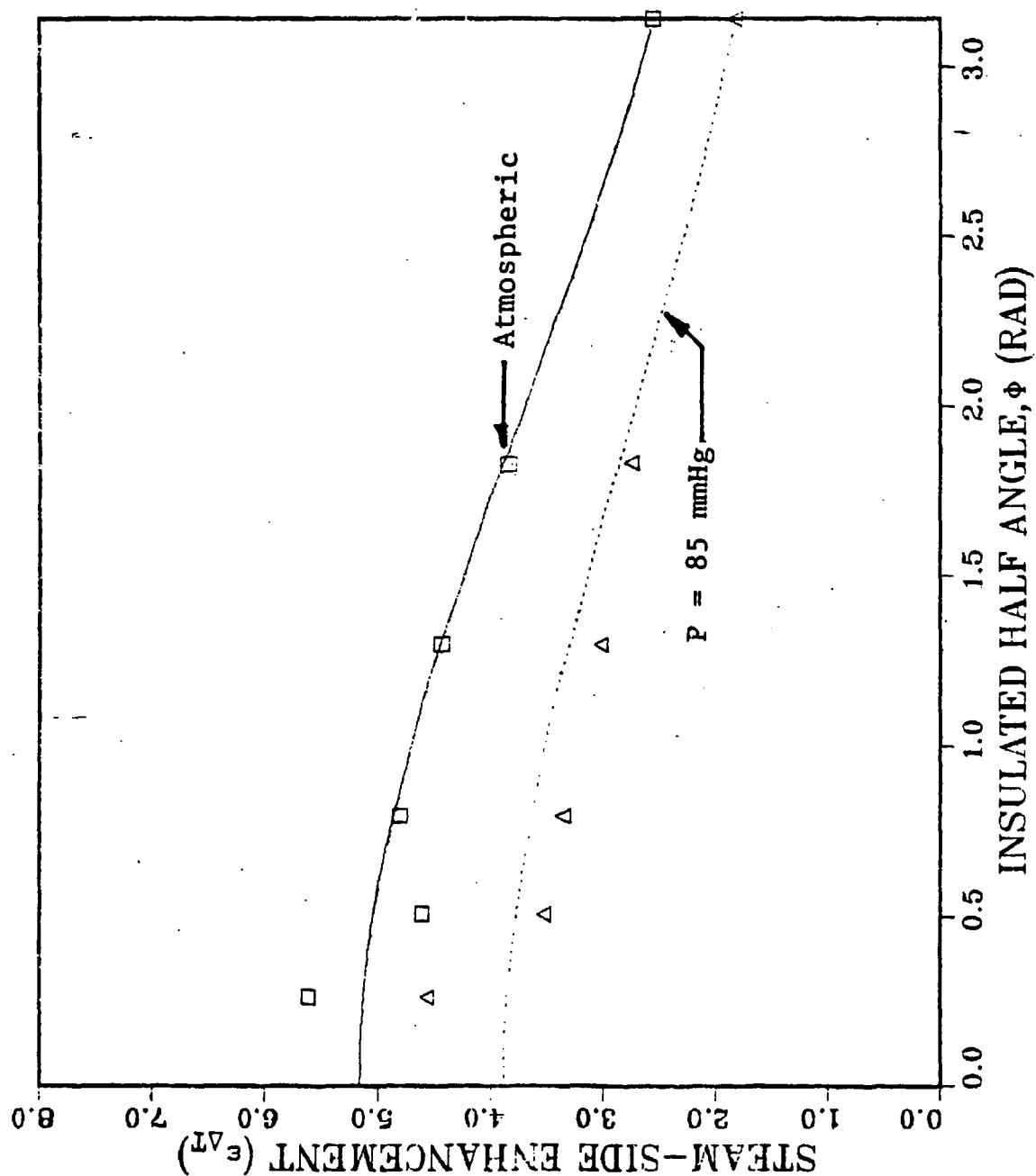
Figure 5.11   Variation of Average Enhancement with Angular
Position for Tube with s = 0.5 mm for Both
Pressure Conditions.
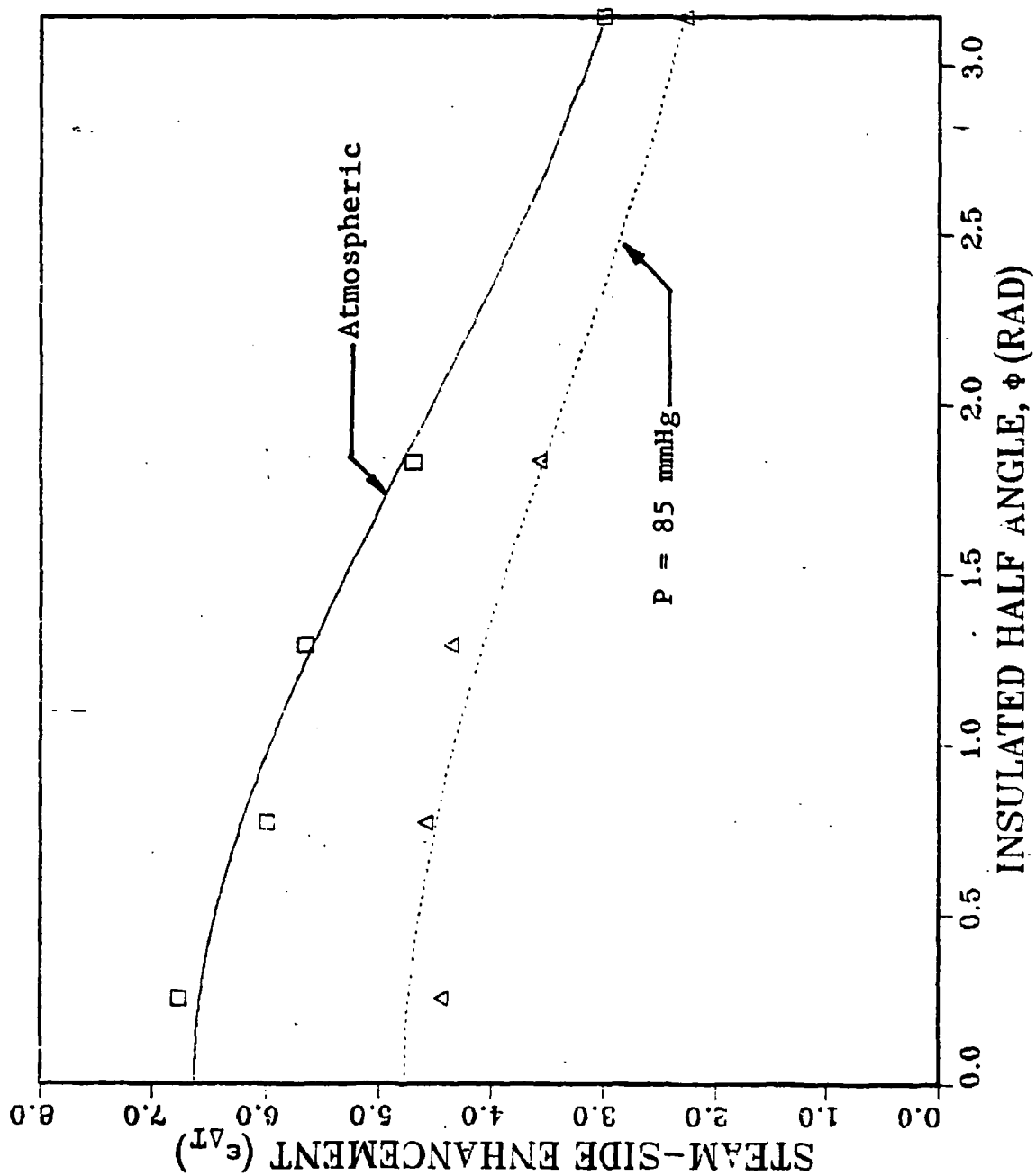
Figure 5.12   Variation of Average Enhancement with Angular
               Position for Tube with s = 1.0 mm for Both
               Pressure Conditions.

83
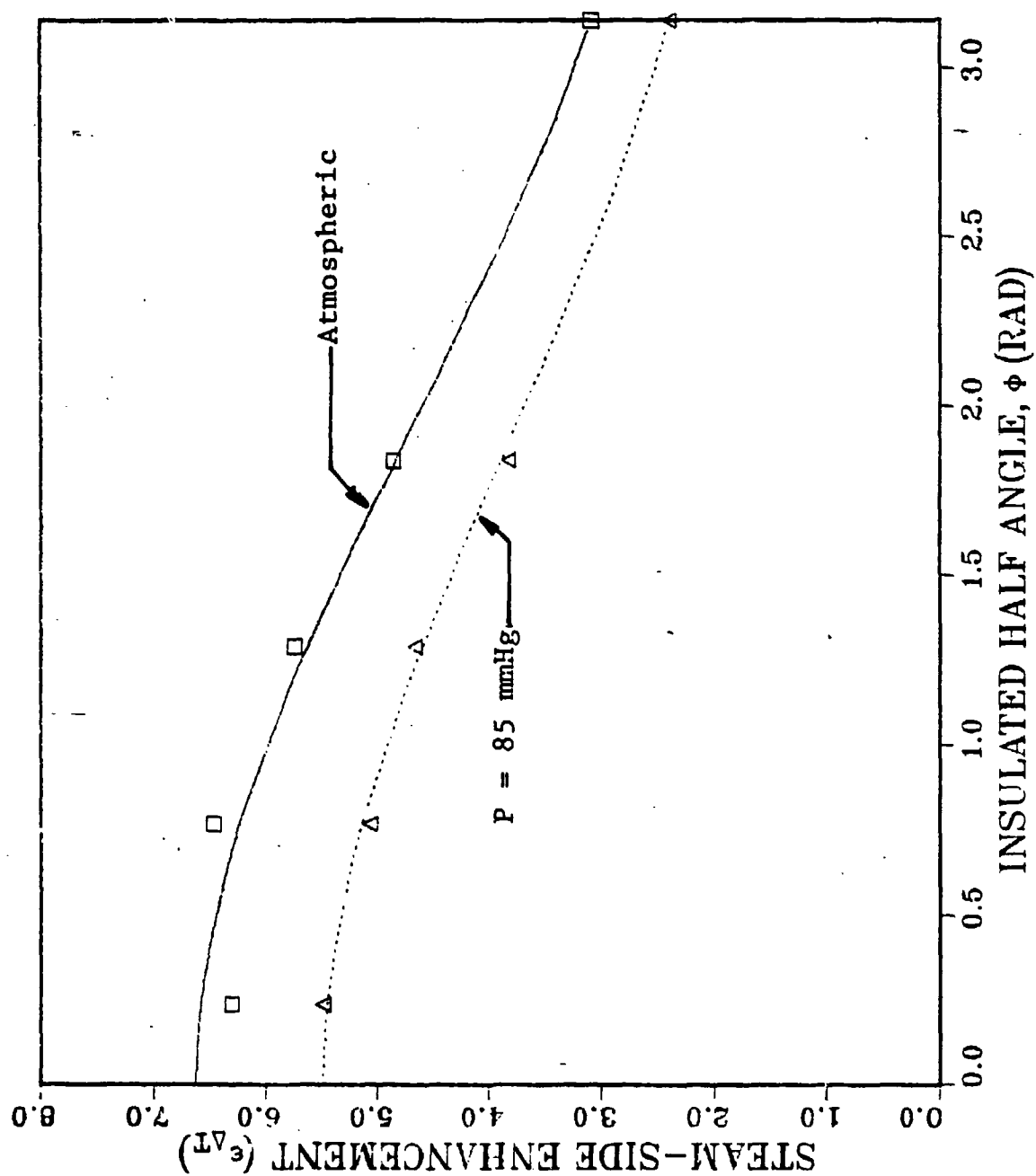
Figure 5.13 Variation of Average Enhancement with Angular
Position for Tube with s = 1.5 mm for Both
Pressure Conditions.
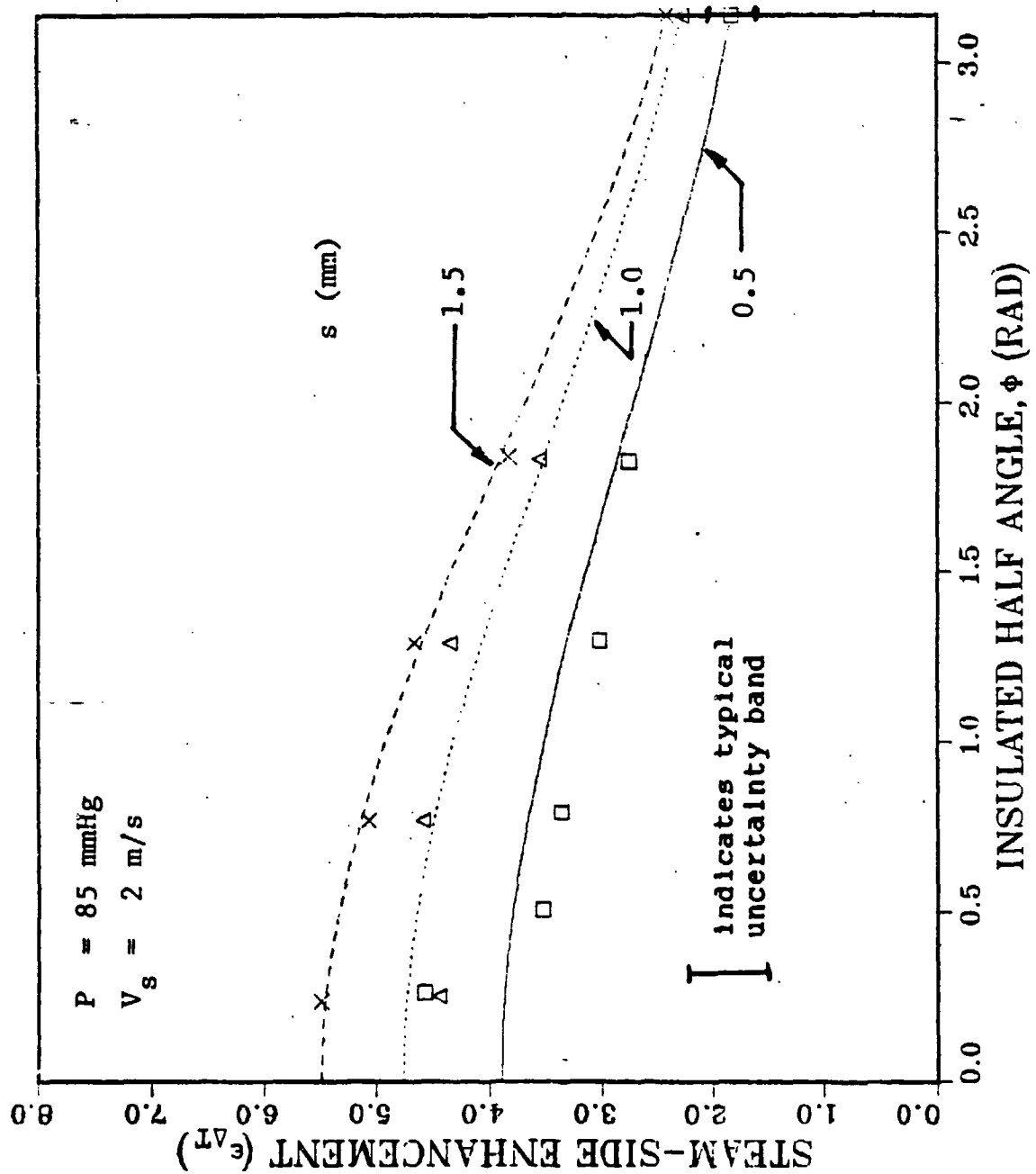
Figure 5.14   Comparison of Average Enhancement for All Three
Tubes Under Low-Pressure Condition.
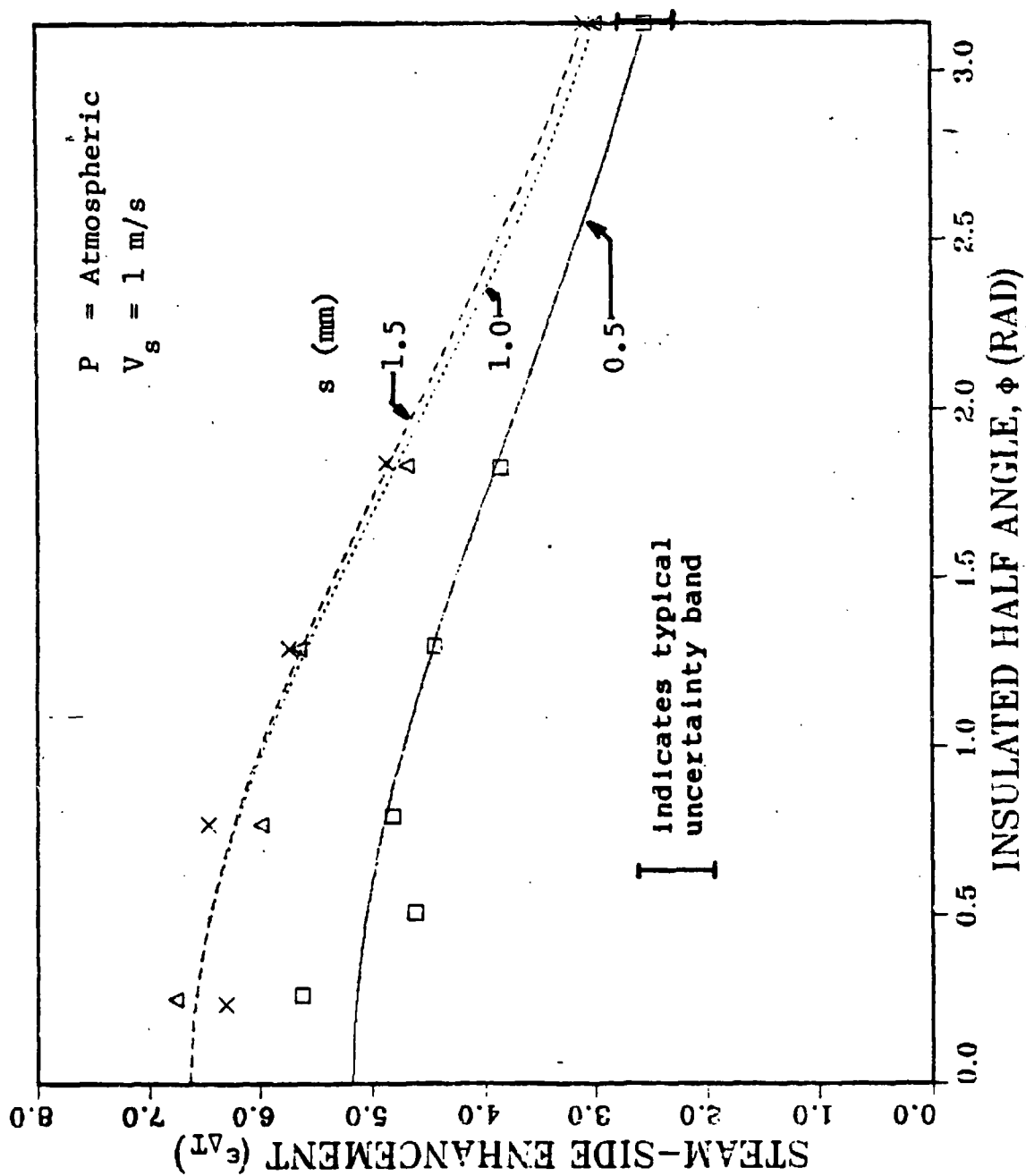
Figure 5.15 Comparison of Average Enhancement for All Three
Tubes At Atmospheric Condition.

10.7% and 10.2% for the low pressure and atmoshperic pressure, respectively. The results of the comparison are:

(a) For the low pressure condition, the tube with a 1.5 mm fin spacing yielded the largest average enhancement, followed by the 1.0 mm and 0.5 mm spacing, respectively.

(b) For the atmospheric condition, the tubes with 1.5 mm and 1.0 mm fin spacing provided the same average enhancement except in the lower sections of the tube where the 1.5 mm spacing out-performed the 1.0 mm tube. The tube with fin spacings of 0.5 mm provided the lowest average enhancement.

Using the average enhancement data together with the analysis described in Appendix C, the local enhancements of the tubes were calculated as shown in Figures 5.16 and 5.17 for low and atmospheric conditions, respectively. The results of the comparison of the local enhancement for each of the tubes are:

(a) For the low pressure condition, the tube with a fin spacing of 1.5 mm yields the largest local enhancement followed by the 1.0 mm and the 0.5 mm fin spacings.

(b) At atmospheric conditions, the local enhancement curves for the tubes with fin spacing of 1.5 mm and 1.0 mm coincide at angles less than about 0.8 radians and separate slightly as the angle increases with the curve for the 1.5 mm tube remaining slightly larger. These

87
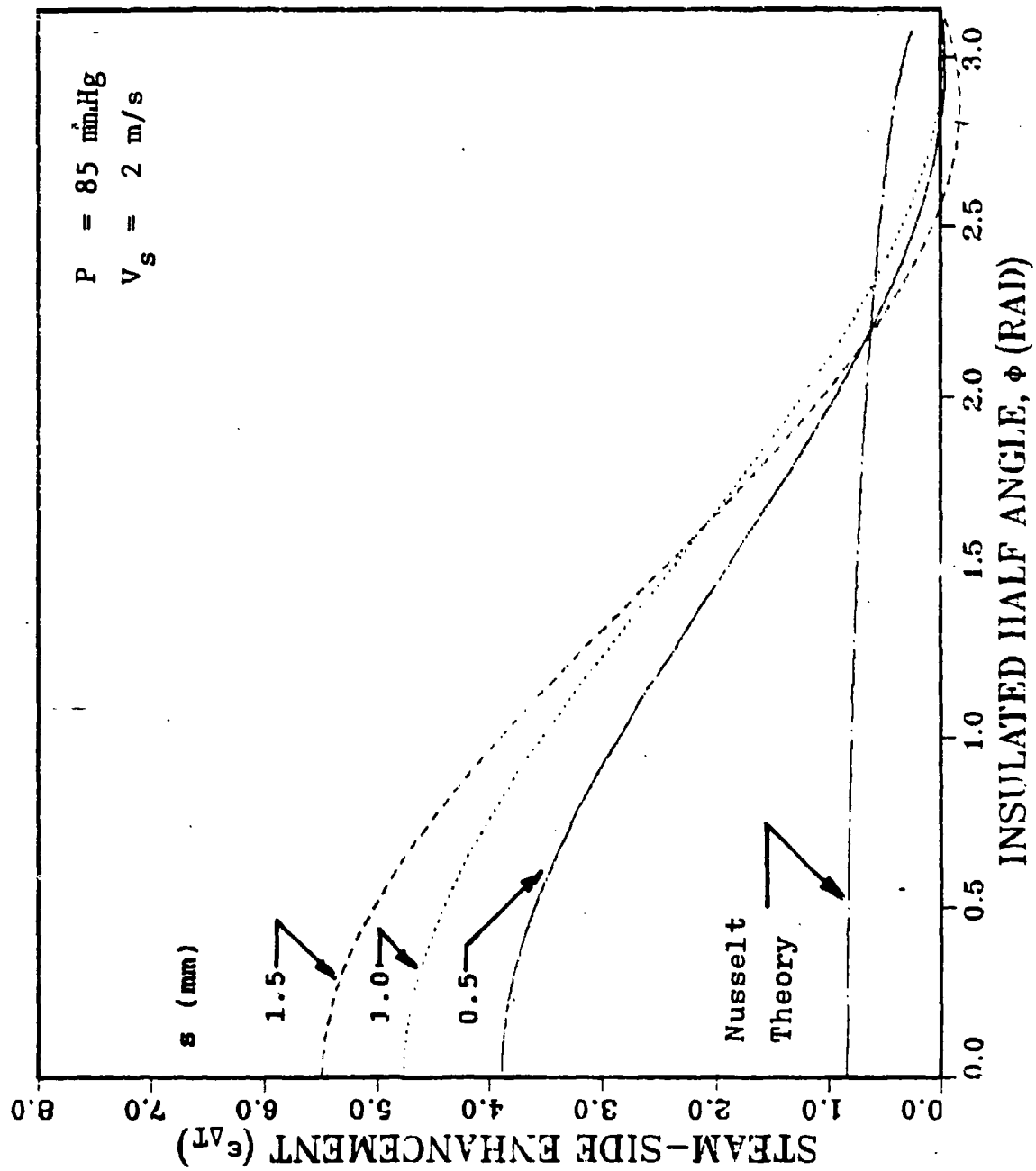
Figure 5.16   Comparison of Local Enhancement Curves for All
Three Tubes At Low-Pressure Condition.
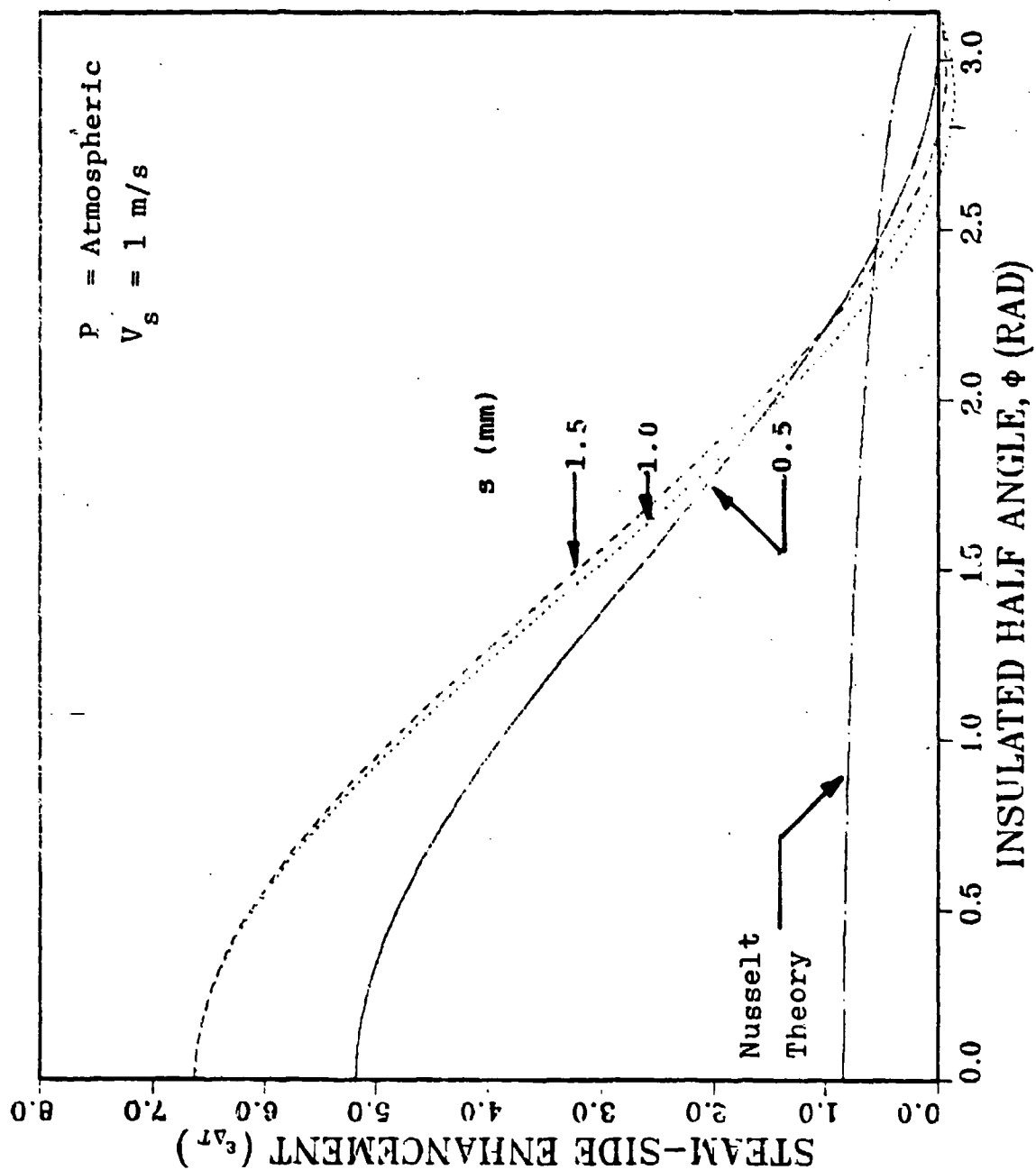
Figure 5.17   Comparison of Local Enhancement Curves for All
               Three Tube At Atmospheric Condition.

curves both cross the 0.5 mm curve at angles approximately 2.0 and 2.1 radians for the 1.0 mm and 1.5 mm tubes, respectively.

Notice that the enhancements shown in Figures 5.16 and 5.17 drop below zero as the angle approaches $\phi = \pi$. The negative values of enhancement are attributed to experimental uncertainty. Notice also that the shape of these local enhancemnt curves is dependent on the type of polynomial chosen. A more realistic curve, probably guided by theoretical considerations, which includes an inflection point at the flooding condition is expected to yield an improved expression for the local heat-transfer coefficient.[1]

E. DISCUSSION OF OUTSIDE HEAT-TRANSFER COEFFICIENT

The local heat-transfer coefficient was compared to its value at the top of the tube. This ratio was achieved by dividing the local enhancement at the position of concern by the local enhancement at the top of the tube. The results of these calculations are contained in Figures 5.18 and 5.19 for the low pressure and atmospheric conditions for all three finned tubes. The heat-transfer coefficient ratio in these

---

[1] Additional attempts were made using MATLAB on the mainframe computer together with the following expressions: (a) sixth-order polynomial, (b) sum of cosine terms i.e.,

$$\varepsilon_\phi = a_0 + a_1 \cos\phi + a_2 \cos 2\phi + a_3 \cos 3\phi + a_4 \cos 4\phi + a_5 \cos 5\phi + a_6 \cos 6\phi \,,$$

(c) sixth-order polynomial of $\cos\phi$. Unfortunately, none of these expressions gave results superior to those presented in this thesis using the third-order polynomial.
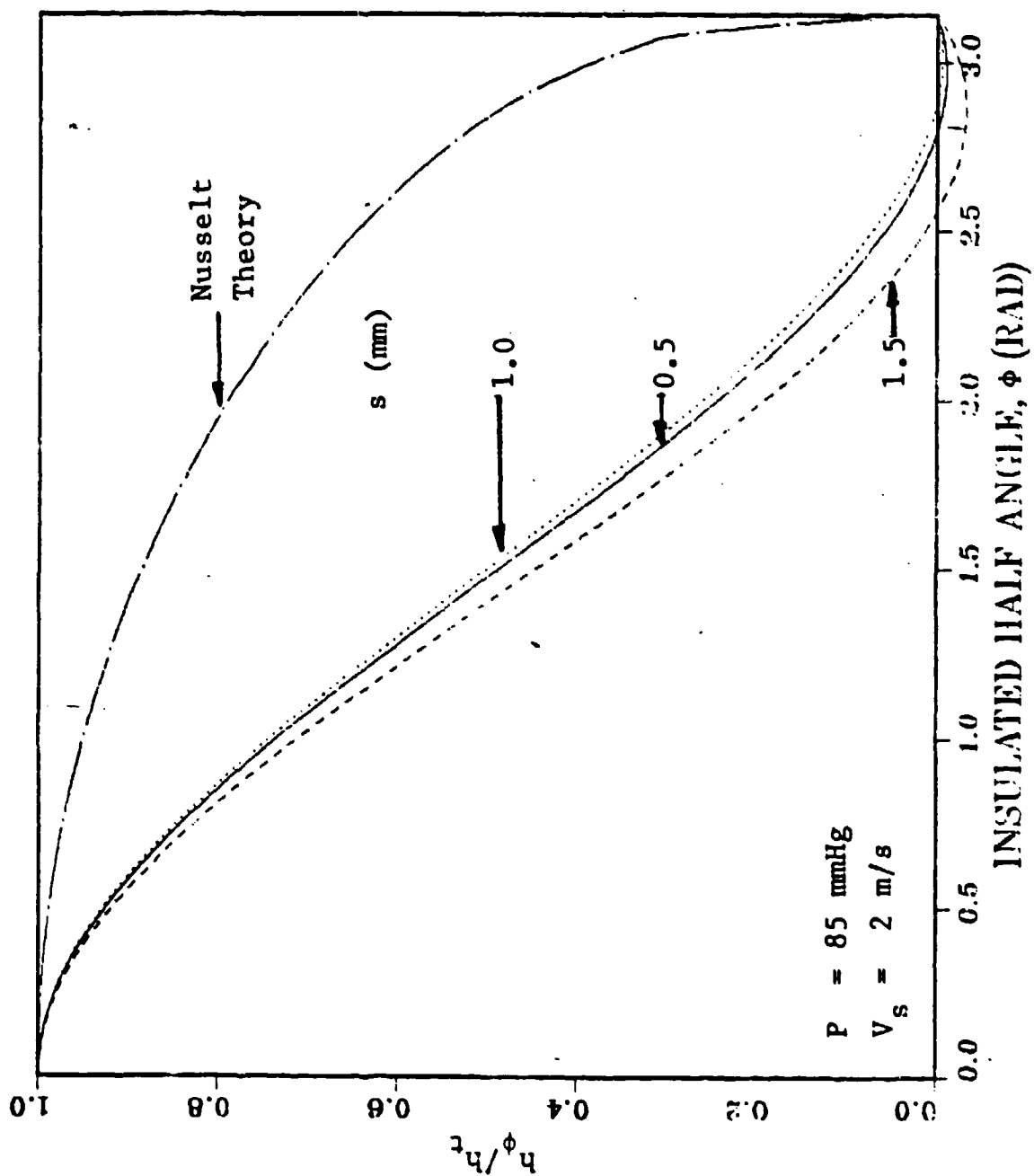
Figure 5.18 Comparison of Normalized Heat-Transfer
Coefficient for All Three Tubes At Low-Pressure
Condition and Normalized Nusselt Theory.
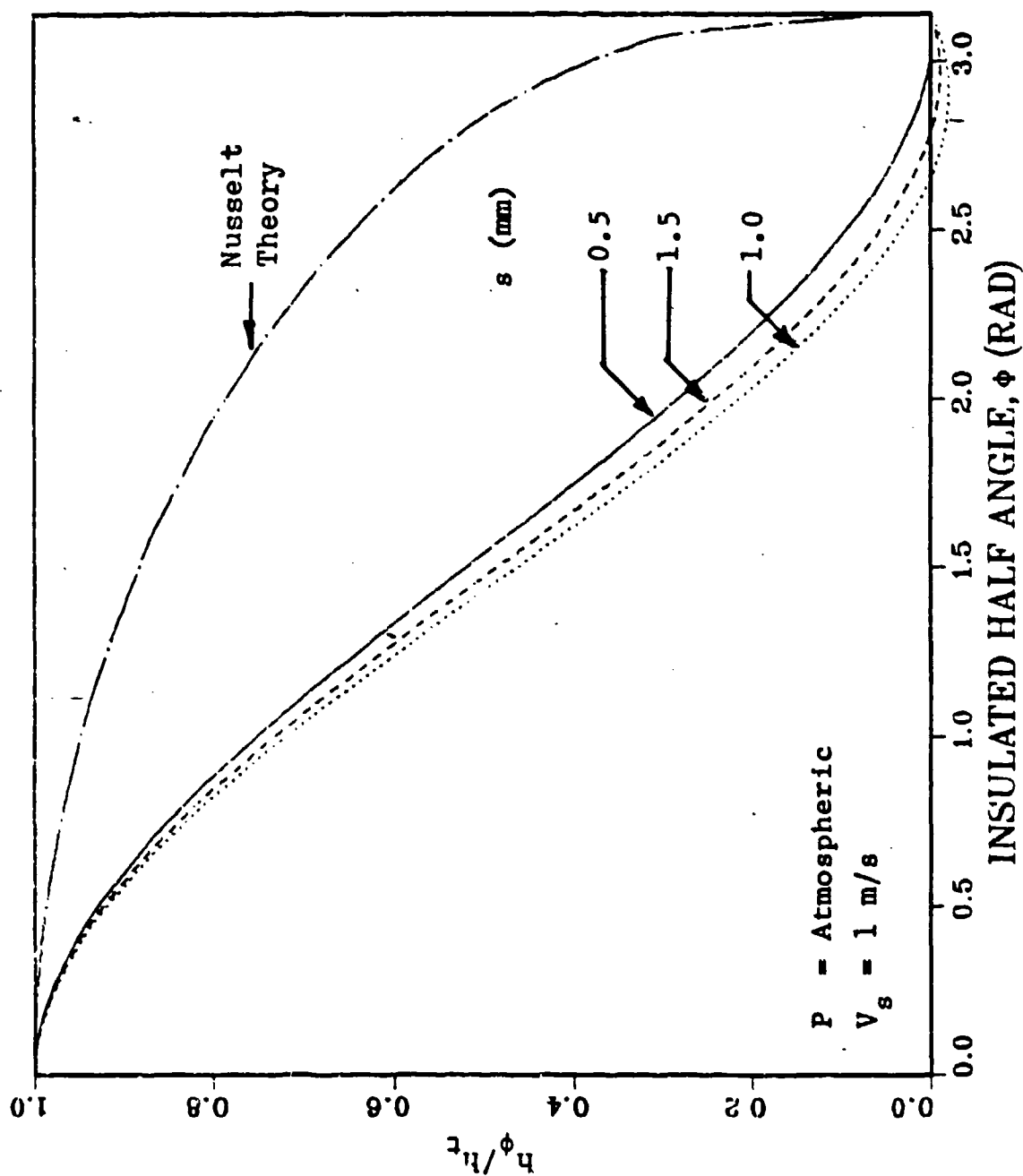
Figure 5.19 Comparison of Normalized Heat-Transfer
Coefficient for All Three Tubes At Atmospheric
Condition and Normalized Nusselt Theory.

Figures shows the variation in the heat-transfer coefficient along the surface of the tube. In addition, a curve representing the Nusselt theory is also plotted in Figures 5.18 and 5.19 to allow comparison of the experimental results to the theoretical model. The results of the comparison of the heat-transfer coefficient for the - three tubes to each other shows that, for both pressure conditions, the local heat-transfer coefficients remain relatively close together across the entire surface of the tube. The comparison of the heat-transfer coefficient for the three finned tubes with the curve generated using the Nusselt theory shows that the values decrease gradually along the surface of the tube while the predictions by Nusselt theory decreases slowly with a large decrease at the bottom of the tube. Notice that a rapid decrease in the heat-transfer coefficient indicates a sharp rate of increase in condensate film thickness. For finned tubes, a rapid increase in film thickness is expected at the flooding point. On the other hand, for smooth tubes, such a rapid increase in film thickness occurs only near the bottom of the tube. These agreements agree quite well with the trends shown in Figure 5.19.

VI   CONCLUSIONS AND RECOMMENDATIONS

A.   CONCLUSIONS

1. The procedure used during this study by insulating various portions of the upper section of finned tubes, together with a third-order polynomial, resulted in a representative variation for the local heat-transfer coefficient around the circumference of the tubes.

2. The average enhancement for the tubes with fin spacings of 0.5, 1.0. and 1.5 mm were 2.5, 3.0 and 3.1, respectively, for the atmospheric pressure conditions. And they were 1.8, 2.3 and 2.4 for the low pressure condition.

3. For the fully flooded tube (i.e., s = 0.5 mm), the local enhancements at the top of the tube were 5.2 and 3.8 for atmospheric and low pressure conditions, respectively. For the tube with a fin spacing of 1.0 mm, these values were 6.6 and 4.8, respectively. And for the tube with a fin spacing of 1.5 mm, these values were 6.6 and 5.5, respectively.

4. The Sieder-Tate-type coefficient (C_i) undergoes changes as the insulated angle is increased. This coefficient (C_i) increases to a maximum of approximately 0.075 at an angle of 0.5 radians (28.6 degrees) and then decreases as the angle of insulation continues to increase toward the

94

bottom of the finned tube. The modified Sieder-Tate-type coefficient (C_{im}) (i.e., the value based on the actual heated area) increased as the insulated angle increases up to a value of approximately 0.1 at an angle of 1.0 radians (57.2 degrees) where it remains relatively constant. The increase in the modified coefficient (C_{im}) with the increasing insulated angle is believed to be due to the turbulent mixing during the unheated portion.

5. The local-heat-transfer coefficient for the finned tube rapidly decreases along the surface of the tube when compared to the Nusselt theory for the smooth tube. This occurrence is due to the slow build up of condensate fil. thickness along the surface of the finned tube, thus decreasing the local heat-transfer coefficent more rapidly. For the smooth tube, the condensate build up is more sudden near the bottom of the tube.

B. RECOMMENDATIONS

1. Using the same techniques, the measurements should be repeated using smaller and more numerous angles of insulation. This should allow for a more detailed picture of the behavior of the local heat-transfer coefficient around the circumference of the finned tube.

2. Investigations should be performed using different fluids such as R-113 and ethylene glycol, to generate data for obtaining further insight to the local heat-transfer coefficient.

3. A study of the effect of the outside insulation on the condensate flow field around the surface of the tube should be conducted.

APPENDIX A

LISTING OF RAW DATA

The following pages contain raw data obtained for tubes # 4, # 5, and # 6 at low and atmospheric pressures.

TABLE 3

RAW DATA FROM FIN SPACING 0.5 MM TUBE
WITH AN INSULATED HALF ANGLE OF 0 DEGREES.

Tube Number: 04
File Name: F04V17
Pressure Condition: Vacuum
Steam Velocity: 2.0 (m/s)

Data #	Vw (m/s)	Tin (C)	Tout (C)	Ts (C)
1	1.17	17.30	20.02	48.50
2	1.17	17.28	20.02	48.48
3	1.50	17.03	19.09	48.46
4	1.50	17.02	19.38	48.56
5	1.99	16.80	18.80	48.51
6	1.99	16.80	18.80	48.48
7	2.53	16.66	18.37	48.47
8	2.53	16.65	18.36	48.44
9	3.02	16.56	18.09	48.48
10	3.02	16.56	18.10	48.43
11	3.46	16.49	17.89	48.52
12	3.46	16.50	17.89	48.54
13	3.89	16.43	17.72	48.49
14	3.89	16.43	17.71	48.50
15	4.44	16.37	17.53	48.49
16	4.44	16.37	17.51	48.39
17	1.17	17.17	19.86	48.44
18	1.17	17.18	19.87	48.47

Tube Number: 04
File Name: F04A12
Pressure Condition: Atmospheric
Steam Velocity: 1.0 (m/s)

Data #	Vw (m/s)	Tin (C)	Tout (C)	Ts (C)
1	1.17	17.32	25.30	99.91
2	1.17	17.34	25.31	99.82
3	1.50	17.19	24.08	99.86
4	1.50	17.20	24.11	99.98
5	1.99	17.14	22.94	99.85
6	1.99	17.15	22.96	99.92
7	2.53	17.07	22.07	99.95
8	2.53	17.09	22.07	99.83
9	3.02	17.03	21.49	99.83
10	3.02	17.03	21.50	99.90
11	3.45	17.00	21.09	99.86
12	3.45	17.01	21.09	99.77
13	3.89	17.00	20.75	99.89
14	3.89	17.00	20.76	99.89
15	4.43	16.98	20.39	100.05
16	4.43	16.98	20.40	99.99
17	1.17	17.84	25.63	99.88
18	1.17	17.83	25.62	99.78

TABLE 4

RAW DATA FROM FIN SPACING 0.5 MM TUBE
WITH AN INSULATED HALF ANGLE OF 30 DEGREES.

Tube Number: 04
File Name: F04V114
Pressure Condition: Vacuum
Steam Velocity: 2.0 (m/s)

Data #	Vw (m/s)	Tin (C)	Tout (C)	Ts (C)
1	1.17	18.55	21.23	48.39
2	1.17	18.55	21.24	48.47
3	1.49	18.34	20.64	48.51
4	1.49	18.34	20.64	48.46
5	1.98	18.16	20.04	48.34
6	1.98	18.16	20.04	48.29
7	2.53	18.03	19.64	48.31
8	2.53	18.03	19.64	48.41
9	3.01	17.96	19.40	48.45
10	3.01	17.96	19.39	48.43
11	3.45	17.91	19.20	48.36
12	3.45	17.91	19.21	48.33
13	3.88	17.87	19.05	48.39
14	3.88	17.88	19.06	48.38
15	4.02	17.87	19.03	48.47
16	4.02	17.88	19.04	48.50
17	1.17	18.68	21.37	48.52
18	1.17	18.69	21.37	48.43

Tube Number: 04
File Name: F04A115
Pressure Condition: Atmospheric
Steam Velocity: 1.0 (m/s)

Data #	Vw (m/s)	Tin (C)	Tout (C)	Ts (C)
1	1.17	19.42	27.64	100.01
2	1.17	19.44	27.65	100.07
3	1.49	19.28	26.33	99.96
4	1.49	19.30	26.35	99.93
5	1.98	19.15	24.98	99.89
6	1.98	19.17	25.00	99.93
7	2.52	19.08	24.05	99.93
8	2.52	19.10	24.06	99.98
9	3.01	19.06	23.47	99.97
10	3.01	19.06	23.48	100.00
11	3.44	19.05	23.05	100.04
12	3.44	19.07	23.07	99.95
13	3.88	19.05	22.72	99.87
14	3.88	19.06	22.73	99.86
15	4.09	19.07	22.60	100.00
16	4.09	19.07	22.59	100.02
17	1.17	19.96	28.19	99.90
18	1.17	19.97	28.21	99.94

TABLE 5

RAW DATA FROM FIN SPACING 0.5 MM TUBE
WITH AN INSULATED HALF ANGLE OF 58 DEGREES.

Tube Number: 04
File Name: F04V39
Pressure Condition: Vacuum
Steam Velocity: 2.0 (m/s)

Data #	Vw (m/s)	Tin (C)	Tout (C)	Ts (C)
1	1.17	17.14	19.58	48.39
2	1.17	17.14	19.59	48.45
3	1.50	16.90	19.01	48.51
4	1.50	16.89	19.02	48.52
5	1.99	16.68	18.47	48.53
6	1.99	16.67	18.47	48.58
7	2.53	16.52	18.03	48.51
8	2.53	16.52	18.04	48.47
9	3.02	16.43	17.76	48.35
10	3.02	16.43	17.77	48.32
11	3.46	16.37	17.58	48.29
12	3.46	16.38	17.56	48.33
13	3.89	16.32	17.43	48.36
14	3.89	16.32	17.43	48.36
15	4.00	16.32	17.41	48.39
16	4.00	16.32	17.41	48.43
17	1.17	17.16	19.59	48.33
18	1.17	17.16	19.60	48.35

Tube Number: 04
File Name: F04A48
Pressure Condition: Atmospheric
Steam Velocity: 1.0 (m/s)

Data #	Vw (m/s)	Tin (C)	Tout (C)	Ts (C)
1	1.17	17.26	25.39	100.04
2	1.17	17.29	25.41	100.01
3	1.50	17.15	24.09	99.88
4	1.50	17.16	24.11	99.87
5	1.99	17.07	22.85	99.87
6	1.99	17.09	22.87	99.92
7	2.53	16.98	21.88	100.05
8	2.53	17.00	21.90	100.02
9	3.02	16.93	21.27	99.96
10	3.02	16.96	21.28	99.94
11	3.45	16.96	20.85	99.87
12	3.45	16.96	20.86	99.87
13	3.86	16.97	20.54	100.04
14	3.86	16.98	20.56	100.12
15	1.17	17.83	25.89	99.90
16	1.17	17.83	25.88	99.83

TABLE 6

RAW DATA FROM FIN SPACING 0.5 MM TUBE
WITH AN INSULATED HALF ANGLE OF 91 DEGREES.

Tube Number: 04
File Name: F04V60
Pressure Condition: Vacuum
Steam Velocity: 2.0 (m/s)

Data #	Vw (m/s)	Tin (C)	Tout (C)	Ts (C)
1	1.17	18.08	20.46	48.52
2	1.17	18.05	20.44	48.48
3	1.50	17.75	19.80	48.36
4	1.50	17.73	19.79	48.29
5	1.98	17.40	19.09	48.33
6	1.98	17.38	19.08	48.30
7	2.53	17.16	18.60	48.42
8	2.53	17.16	18.58	48.44
9	3.02	17.03	18.28	48.49
10	3.02	17.01	18.27	48.53
11	3.45	16.91	18.04	48.50
12	3.45	16.89	18.03	48.45
13	3.89	16.81	17.84	48.46
14	3.89	16.80	17.84	48.47
15	4.05	16.75	17.75	48.49
16	4.05	16.75	17.74	48.44
17	1.17	17.46	19.80	48.28
18	1.17	17.45	19.81	48.33

Tube Number: 04
File Name: F04A59
Pressure Condition: Atmospheric
Steam Velocity: 1.0 (m/s)

Data #	Vw (m/s)	Tin (C)	Tout (C)	Ts (C)
1	1.17	19.08	26.24	100.05
2	1.17	19.08	26.20	100.04
3	1.49	18.87	24.96	99.87
4	1.49	18.86	24.96	99.79
5	1.98	18.63	23.70	99.85
6	1.98	18.62	23.68	99.94
7	2.52	18.46	22.74	99.88
8	2.52	18.46	22.72	99.84
9	3.01	18.36	22.11	99.94
10	3.01	18.36	22.10	99.92
11	3.45	18.29	21.61	100.04
12	3.45	18.29	21.61	99.97
13	3.88	18.21	21.24	99.95
14	3.88	18.20	21.21	99.95
15	4.10	18.17	21.21	99.96
16	4.10	18.18	21.05	99.92
17	1.17	18.95	25.93	100.02
18	1.17	18.97	25.93	100.03

TABLE 7

RAW DATA FROM FIN SPACING 0.5 MM TUBE
WITH AN INSULATED HALF ANGLE OF 149 DEGREES.

Tube Number: 04
File Name: F04V70
Pressure Condition: Vacuum
Steam Velocity: 2.0 (m/s)

Data #	Vw (m/s)	Tin (C)	Tout (C)	Ts (C)
1	1.17	16.83	18.85	48.44
2	1.17	16.83	18.85	48.38
3	1.50	16.58	18.28	48.54
4	1.50	16.57	18.27	48.44
5	1.99	16.34	17.71	48.41
6	1.99	16.33	17.71	48.42
7	2.53	16.16	17.33	48.49
8	2.53	16.16	17.34	48.36
9	3.02	16.03	17.06	48.32
10	3.02	16.03	17.05	48.29
11	3.46	15.93	16.86	48.46
12	3.46	15.33	16.86	48.45
13	3.49	15.88	16.79	48.42
14	1.17	16.60	18.64	48.46
15	1.17	16.60	18.64	48.41

Tube Number: 04
File Name: F04A73
Pressure Condition: Atmospheric
Steam Velocity: 1.0 (m/s)

Data #	Vw (m/s)	Tin (C)	Tout (C)	Ts (C)
1	1.17	18.49	24.13	100.05
2	1.17	18.49	24.15	99.98
3	1.49	18.28	23.16	99.93
4	1.49	18.30	23.17	99.91
5	1.98	18.09	21.96	100.04
6	1.98	18.08	21.95	100.06
7	2.53	17.95	21.19	99.98
8	2.53	17.95	21.19	99.89
9	3.01	17.86	20.67	99.83
10	3.01	17.97	20.67	99.87
11	3.45	17.80	20.32	99.90
12	3.45	17.80	20.30	99.88
13	3.59	17.80	20.24	99.88
14	3.59	17.80	20.24	99.89
15	1.17	18.54	24.20	99.88
16	1.17	18.55	24.21	99.81

TABLE 8

RAW DATA FROM FIN SPACING 0.5 MM TUBE WITH AN INSULATED HALF ANGLE OF 210 DEGREES.

Tube Number: U4
File Name: F04V83
Pressure Condition: Vacuum
Steam Velocity: 2.0 (m/s)

Data #	Vw (m/s)	Tin (C)	Tout (C)	Ts (C)
1	1.17	18.16	19.44	48.53
2	1.17	18.13	19.43	48.48
3	1.49	17.85	18.91	48.48
4	1.49	17.83	18.90	48.46
5	1.98	17.57	13.42	48.51
6	1.98	17.56	13.42	48.47
7	2.53	17.36	18.04	48.51
8	2.53	17.35	18.03	48.50
9	3.02	17.22	17.81	48.40
10	3.02	17.22	17.81	48.41
11	3.45	17.10	17.65	48.48
12	3.45	17.09	17.63	48.50
13	3.78	17.01	17.52	48.50
14	3.78	17.01	17.52	48.47
15	1.17	17.76	18.99	48.31
16	1.17	17.76	18.99	48.30

Tube Number: 04
File Name: F04A85
Pressure Condition: Atmospheric
Steam Velocity: 1.0 (m/s)

Data #	Vw (m/s)	Tin (C)	Tout (C)	Ts (C)
1	1.17	19.74	22.51	99.98
2	1.17	18.74	22.51	99.87
3	1.49	18.50	21.64	99.86
4	1.49	18.50	21.63	99.94
5	1.98	18.25	20.76	100.06
6	1.98	18.24	20.76	99.94
7	2.53	18.09	20.15	99.98
8	2.53	18.09	20.14	100.04
9	3.01	17.97	19.71	99.94
10	3.01	17.97	19.72	100.02
11	3.45	17.88	19.46	99.92
12	3.45	17.88	19.47	99.90
13	3.88	17.80	19.21	100.03
14	3.88	17.81	13.22	100.06
15	3.91	17.80	19.22	100.03
16	3.91	17.79	19.21	99.94
17	1.17	18.57	22.19	99.89
18	1.17	18.58	22.20	99.96

TABLE 9

RAW DATA FROM FIN SPACING 1.0 MM TUBE
WITH AN INSULATED HALF ANGLE OF 0 DEGREES.

Tube Number: 05
File Name: F05V16
Pressure Condition: Vacuum
Steam Velocity: 2.0 (m/s)

Data #	Vw (m/s)	Tin (C)	Tout (C)	Ts (C)
1	1.17	17.03	19.95	48.47
2	1.17	16.95	19.88	48.31
3	1.50	16.42	19.00	48.48
4	1.50	16.41	19.00	48.44
5	1.99	16.07	18.25	48.29
6	1.99	16.06	18.25	48.30
7	2.53	15.88	17.81	48.43
8	2.53	15.88	17.80	48.48
9	3.02	15.75	17.49	48.51
10	3.02	15.74	17.47	48.50
11	3.46	15.67	17.26	48.49
12	3.46	15.67	17.27	48.46
13	3.90	15.60	17.07	48.44
14	3.90	15.60	17.05	48.51
15	4.44	15.53	16.88	48.50
16	4.44	15.53	16.83	48.48
17	1.17	16.31	19.26	48.31
18	1.17	16.30	19.24	48.33

Tube Number: 05
File Name: F05A08
Pressure Condition: Atmospheric
Steam Velocity: 1.0 (m/s)

Data #	Vw (m/s)	Tin (C)	Tout (C)	Ts (C)
1	1.17	19.27	27.39	100.03
2	1.17	19.23	27.43	98.82
3	1.49	18.87	25.99	99.98
4	1.49	18.87	25.98	99.84
5	1.98	18.62	24.69	100.03
6	1.98	18.62	24.69	99.92
7	2.52	18.45	23.74	99.89
8	2.52	18.44	23.73	99.98
9	3.01	18.32	23.11	100.05
10	3.01	18.32	23.11	100.00
11	3.45	18.23	22.60	99.90
12	3.45	18.22	22.60	99.86
13	3.88	18.13	22.19	100.05
14	3.88	18.13	22.19	99.99
15	4.43	18.05	21.77	99.99
16	4.43	18.05	21.77	100.02
17	1.17	18.81	26.97	100.02
18	1.17	18.80	26.95	99.91

TABLE 10

RAW DATA FROM FIN SPACING 1.0 MM TUBE
WITH AN INSULATED HALF ANGLE OF 29 DEGREES.

Tube Number: 05
File Name: F05V43
Pressure Condition: Vacuum
Steam Velocity: 2.0 (m/s)

Data #	Vw (m/s)	Tin (C)	Tout (C)	Ts (C)
1	1.17	17.42	20.38	48.51
2	1.17	17.39	20.35	48.42
3	1.50	17.06	19.63	48.35
4	1.50	17.05	19.63	48.35
5	1.99	16.80	19.00	48.36
6	1.99	16.79	18.98	48.25
7	2.53	16.58	18.47	48.32
8	2.53	16.57	18.47	48.31
9	3.02	16.46	18.16	48.33
10	3.02	16.45	18.15	48.35
11	3.46	16.37	17.92	48.46
12	3.46	16.36	17.90	48.49
13	3.89	16.29	17.72	48.44
14	3.89	16.29	17.71	48.38
15	4.22	16.24	17.58	48.30
16	4.22	16.23	17.58	48.29
17	1.17	17.01	20.04	48.42
18	1.17	17.02	20.04	48.44

Tube Number: 05
File Name: F05A44
Pressure Condition: Atmospheric
Steam Velocity: 1.0 (m/s)

Data #	Vw (m/s)	Tin (C)	Tout (C)	Ts (C)
1	1.17	17.33	26.01	99.99
2	1.17	17.35	26.04	100.03
3	1.50	17.21	24.71	100.00
4	1.56	17.22	24.71	100.01
5	1.99	17.07	23.41	99.85
6	1.99	17.09	23.42	99.84
7	2.53	17.00	22.41	99.88
8	2.53	17.00	22.42	99.89
9	3.02	16.95	21.80	100.03
10	3.02	16.97	21.81	100.04
11	3.45	16.95	21.36	99.99
12	3.45	16.96	21.37	99.93
13	3.89	16.92	20.97	99.90
14	3.89	16.93	20.97	99.94
15	4.24	16.93	20.74	100.06
16	4.24	16.94	20.76	100.00
17	1.17	17.79	26.57	99.99
18	1.17	17.80	26.56	99.90

TABLE 11

RAW DATA FROM FIN SPACING 1.0 MM TUBE
WITH AN INSULATED HALF ANGLE OF 88 DEGREES.

Tube Number: 05
File Name: F05V62
Pressure Condition: Vacuum
Steam Velocity: 2.0 (m/s)

Data #	Vw (m/s)	Tin (C)	Tout (C)	Ts (C)
1	1.17	17.73	20.29	48.27
2	1.17	17.72	20.29	48.33
3	1.50	17.50	19.73	48.44
4	1.50	17.49	19.72	48.49
5	1.99	17.26	19.13	48.48
6	1.99	17.25	19.12	48.57
7	2.53	17.08	18.68	48.38
8	2.53	17.08	18.66	48.35
9	3.02	16.95	18.34	48.36
10	3.02	16.95	18.34	48.31
11	3.45	16.86	18.12	48.52
12	3.45	16.85	18.11	48.53
13	3.86	16.78	17.93	48.51
14	3.86	16.77	17.92	48.41
15	1.17	17.53	20.08	48.31
16	1.17	17.53	20.09	48.36

Tube Number: 05
File Name: F05A65
Pressure Condition: Atmospheric
Steam Velocity: 1.0 (m/s)

Data #	Vw (m/s)	Tin (C)	Tout (C)	Ts (C)
1	1.17	18.78	26.29	100.03
2	1.17	18.77	26.29	99.98
3	1.49	18.55	25.05	99.91
4	1.49	18.55	25.05	99.88
5	1.98	18.33	23.72	99.90
6	1.98	18.33	23.72	99.93
7	2.53	18.19	22.79	100.02
8	2.53	18.19	22.78	99.92
9	3.01	18.08	22.13	99.92
10	3.01	18.08	22.12	100.05
11	3.45	18.01	21.66	100.06
12	3.45	18.01	21.66	100.00
13	3.80	17.97	21.33	99.91
14	3.80	17.96	21.31	99.83
15	1.17	18.73	26.24	100.07
16	1.17	18.74	26.24	100.01

TABLE 12

RAW DATA FROM FIN SPACING 1.0 MM TUBE
WITH AN INSULATED HALF ANGLE OF 148 DEGREES.

Tube Number: 05
File Name: F05V75
Pressure Condition: Vacuum
Steam Velocity: 2.0 (m/s)

Data #	Vw (m/s)	Tin (C)	Tout (C)	Ts (C)
1	1.17	17.66	19.40	48.29
2	1.17	17.64	19.38	48.40
3	1.50	17.38	18.88	48.49
4	1.50	17.37	18.87	48.53
5	1.99	17.05	18.25	48.42
6	1.99	17.04	18.25	48.42
7	2.53	16.86	17.86	48.36
8	2.53	16.84	17.85	48.36
9	3.02	16.72	17.60	48.43
10	3.02	16.71	17.59	48.50
11	3.46	16.62	17.42	48.48
12	3.46	16.61	17.40	48.43
13	3.89	16.53	17.25	48.42
14	3.89	16.53	17.24	48.42
15	4.14	16.47	17.15	48.44
16	4.14	16.46	17.15	48.39
17	1.17	17.24	19.00	48.51
18	1.17	17.25	19.00	48.56

Tube Number: 05
File Name: F05A77
Pressure Condition: Atmospheric
Steam Velocity: 1.0 (m/s)

Data #	Vw (m/s)	Tin (C)	Tout (C)	Ts (C)
1	1.17	18.29	23.45	99.88
2	1.17	18.29	23.46	99.93
3	1.49	18.09	22.46	99.96
4	1.49	18.08	22.44	99.99
5	1.98	17.86	21.42	100.03
6	1.98	17.85	21.42	100.04
7	2.53	17.69	20.67	100.00
8	2.53	17.69	20.67	99.97
9	3.02	17.57	20.18	99.92
10	3.02	17.57	20.17	99.89
11	3.45	17.49	19.82	99.91
12	3.45	17.47	19.80	99.95
13	3.89	17.41	19.53	100.03
14	3.89	17.41	19.52	100.01
15	4.18	17.38	19.36	99.93
16	4.18	17.38	19.37	99.97
17	1.17	18.18	23.33	100.04
18	1.17	18.17	23.31	99.91

TABLE 13

RAW DATA FROM FIN SPACING 1.0 MM TUBE
WITH AN INSULATED HALF ANGLE OF 210 DEGREES.

Tube Number: 05
File Name: F05V105
Pressure Condition: Vacuum
Steam Velocity: 2.0 (m/s)

Data #	Vw (m/s)	Tin (C)	Tout (C)	Ts (C)
1	1.17	18.91	19.94	48.30
2	1.17	18.78	19.80	48.28
3	1.49	18.46	19.32	48.53
4	1.49	18.43	19.29	48.46
5	1.98	18.12	18.81	48.49
6	1.98	18.09	18.79	48.45
7	2.53	17.86	18.43	48.37
8	2.53	17.84	18.41	48.33
9	3.02	17.66	18.16	48.40
10	3.02	17.65	18.15	48.41
11	3.45	17.48	17.93	48.48
12	3.45	17.48	17.93	48.53
13	3.89	17.38	17.78	48.45
14	3.89	17.36	17.77	48.44
15	3.97	17.30	17.70	48.50
16	3.97	17.28	17.69	48.54
17	1.17	18.02	19.06	48.29
18	1.17	18.01	19.05	48.41

Tube Number: 05
File Name: F05A108
Pressure Condition: Atmospheric
Steam Velocity: 1.0 (m/s)

Data #	Vw (m/s)	Tin (C)	Tout (C)	Ts (C)
1	1.17	18.91	22.06	99.94
2	1.17	18.93	22.09	100.05
3	1.49	18.72	21.36	100.07
4	1.49	18.72	21.35	100.04
5	1.98	18.53	20.66	99.98
6	1.98	19.53	20.65	99.99
7	2.52	18.39	20.14	100.06
8	2.52	18.38	29.14	100.05
9	3.01	18.29	19.80	99.90
10	3.01	18.30	19.81	99.94
11	3.45	18.22	19.57	99.89
12	3.45	18.23	19.56	99.81
13	3.88	18.17	19.38	99.96
14	3.88	18.17	19.39	99.99
15	4.02	18.15	19.33	99.99
16	4.02	18.14	19.31	100.00
17	1.17	18.92	22.05	99.99
18	1.17	18.93	22.07	99.97

TABLE 14

RAW DATA FROM FIN SPACING 1.5 MM TUBE WITH AN INSULATED HALF ANGLE OF 0 DEGREES.

Tube Number: 06
File Name: F06V04
Pressure Condition: Vacuum
Steam Velocity: 2.0 (m/s)

Tube Number: 06
File Name: F06A06
Pressure Condition: Atmospheric
Steam Velocity: 1.0 (m/s)

Data #	Vu (m/s)	Tin (C)	Tout (C)	Ts (C)	Data #	Vu (m/s)	Tin (C)	Tout (C)	Ts (C)
1	1.17	17.36	20.26	48.48	1	1.17	19.41	27.69	99.74
2	1.17	17.31	20.22	48.35	2	1.17	19.47	27.74	99.62
3	1.50	17.04	19.59	48.30	3	1.49	19.37	26.62	99.93
4	1.50	17.02	19.57	48.25	4	1.49	19.39	26.64	99.88
5	1.99	16.76	18.97	48.39	5	1.98	19.30	25.47	99.99
6	1.99	16.75	18.95	48.37	6	1.98	19.30	25.48	100.21
7	2.53	16.57	18.49	48.33	7	2.52	19.03	24.41	99.87
8	2.53	16.56	18.48	48.33	8	2.52	19.00	24.36	99.72
9	3.02	16.46	18.19	48.35	9	3.01	18.82	23.68	99.90
10	3.02	16.46	18.19	48.45	10	3.01	18.82	23.67	99.80
11	3.46	16.39	18.00	48.50	11	3.45	18.69	23.15	99.93
12	3.46	16.39	17.99	48.43	12	3.45	18.68	23.13	99.84
13	3.89	16.34	17.81	48.31	13	3.88	18.64	22.77	100.03
14	3.89	16.34	17.82	48.27	14	3.88	18.65	22.78	100.01
15	4.44	16.29	17.63	48.36	15	4.42	18.61	22.40	100.00
16	4.44	16.29	17.64	48.37	16	4.42	18.61	22.40	100.10
17	1.17	17.11	20.03	48.41	17	1.17	19.43	27.70	99.98
18	1.17	17.11	20.05	48.50	18	1.17	19.44	27.73	100.17

TABLE 15

RAW DATA FROM FIN SPACING 1.5 MM TUBE
WITH AN INSULATED HALF ANGLE OF 27 DEGREES.

Tube Number: 06
File Name: F06V54
Pressure Condition: Vacuum
Steam Velocity: 2.0 (m/s)

Data #	Vw (m/s)	Tin (C)	Tout (C)	Ts (C)
1	1.17	19.32	22.18	48.47
2	1.17	19.30	22.16	48.48
3	1.49	19.04	21.53	48.43
4	1.49	19.04	21.54	48.47
5	1.98	18.81	20.94	48.53
6	1.98	18.80	20.92	48.50
7	2.52	18.63	20.46	48.26
8	2.52	18.62	20.46	48.28
9	3.01	18.50	20.13	48.37
10	3.01	18.50	20.13	48.38
11	3.45	18.41	19.92	48.55
12	3.45	18.41	19.92	48.50
13	3.88	18.35	19.72	48.35
14	3.88	18.34	19.73	48.31
15	4.15	18.30	19.62	48.40
16	4.15	18.31	19.64	48.31
17	1.17	19.09	21.98	48.51
18	1.17	19.09	21.97	48.53

Tube Number: 06
File Name: F06A57
Pressure Condition: Atmospheric
Steam Velocity: 1.0 (m/s)

Data #	Vw (m/s)	Tin (C)	Tout (C)	Ts (C)
1	1.17	18.46	27.22	99.95
2	1.17	18.48	27.25	100.03
3	1.49	18.35	25.98	100.03
4	1.49	18.37	25.99	100.03
5	1.98	18.26	24.68	99.87
6	1.98	18.27	24.70	99.88
7	2.53	18.18	23.71	99.95
8	2.53	18.19	23.71	99.94
9	3.01	18.13	23.05	99.98
10	3.01	18.14	23.05	99.98
11	3.45	18.10	22.59	100.01
12	3.45	18.11	22.59	99.94
13	3.88	18.08	22.21	99.90
14	3.88	18.08	22.21	99.89
15	4.13	18.09	22.03	99.97
16	4.13	18.09	22.03	99.99
17	1.17	18.92	27.62	99.99
18	1.17	18.92	27.61	99.93

TABLE 16

RAW DATA FROM FIN SPACING 1.5 MM TUBE
WITH AN INSULATED HALF ANGLE OF 88 DEGREES.

Tube Number: 06
File Name: F06V66
Pressure Condition: Vacuum
Steam Velocity: 2.0 (m/s)

Data #	Vw (m/s)	Tin (C)	Tout (C)	Ts (C)
1	1.17	18.80	21.34	48.43
2	1.17	18.79	21.33	48.45
3	1.49	18.51	20.71	48.48
4	1.49	18.50	20.71	48.46
5	1.98	18.28	20.11	48.31
6	1.98	18.27	20.11	48.30
7	2.52	18.12	19.64	48.44
8	2.52	18.11	19.65	48.61
9	3.01	18.02	19.41	48.35
10	3.01	18.02	19.41	48.32
11	3.45	17.95	19.19	48.30
12	3.45	17.95	19.20	48.40
13	3.88	17.88	19.02	48.50
14	3.88	17.88	19.04	48.50
15	3.96	17.85	18.96	48.34
16	3.96	17.84	18.95	48.32
17	1.17	18.59	21.13	48.43
18	1.17	18.60	21.13	48.38

Tube Number: 06
File Name: F06A69
Pressure Condition: Atmospheric
Steam Velocity: 1.0 (m/s)

Data #	Vw (m/s)	Tin (C)	Tout (C)	Ts (C)
1	1.17	19.10	26.78	99.86
2	1.17	19.10	26.79	99.97
3	1.49	18.82	25.41	99.97
4	1.49	18.81	25.40	99.95
5	1.98	18.59	24.08	100.23
6	1.98	18.58	24.05	100.04
7	2.52	18.42	23.04	100.00
8	2.52	18.40	23.04	100.00
9	3.01	18.29	22.37	100.01
10	3.01	18.29	22.36	99.95
11	3.45	18.21	21.89	99.52
12	3.45	18.20	21.88	99.95
13	3.88	18.14	21.47	109.02
14	3.88	18.14	21.47	100.00
15	3.96	18.12	21.41	99.90
16	3.96	18.11	21.39	99.87
17	1.17	18.90	26.50	100.03
18	1.17	18.91	26.51	100.04

TABLE 17

RAW DATA FROM FIN SPACING 1.5 MM TUBE
WITH AN INSULATED HALF ANGLE OF 148 DEGREES.

Tube Number: 06
File Name: F06V78
Pressure Condition: Vacuum
Steam Velocity: 2.0 (m/s)

Data #	Vw (m/s)	Tin (C)	Tout (C)	Ts (C)
1	1.17	18.02	19.83	48.51
2	1.17	17.99	19.81	48.53
3	1.50	17.64	19.18	48.51
4	1.50	17.62	19.15	48.49
5	1.98	17.33	18.57	48.49
6	1.98	17.31	18.55	48.45
7	2.53	17.08	18.12	48.44
8	2.53	17.06	18.09	48.39
9	3.02	16.92	17.82	48.49
10	3.02	16.90	17.81	48.51
11	3.45	16.79	17.60	48.47
12	3.45	16.78	17.58	48.47
13	3.75	16.66	17.41	48.49
14	3.75	16.65	17.40	48.53
15	1.17	17.37	19.20	48.47
16	1.17	17.37	19.18	48.43

Tube Number: 06
File Name: F06A81
Pressure Condition: Atmospheric
Steam Velocity: 1.0 (m/s)

Data #	Vw (m/s)	Tin (C)	Tout (C)	Ts (C)
1	1.17	18.60	24.10	100.04
2	1.17	18.58	24.09	100.03
3	1.49	18.33	23.03	100.00
4	1.49	18.32	23.02	100.00
5	1.98	18.08	21.93	99.99
6	1.98	18.06	21.89	99.97
7	2.53	17.89	21.10	99.87
8	2.53	17.89	21.10	99.92
9	3.02	17.77	20.58	99.99
10	3.02	17.77	20.58	99.94
11	3.45	17.68	20.21	99.94
12	3.45	17.68	20.20	100.01
13	3.80	17.62	19.95	100.01
14	3.80	17.62	19.95	99.98
15	1.17	18.40	24.01	99.96
16	1.17	18.40	24.02	100.09

TABLE 18

RAW DATA FROM FIN SPACING 1.5 MM TUBE
WITH AN INSULATED HALF ANGLE OF 211 DEGREES.

Tube Number: 06
File Name: F06V97
Pressure Condition: Vacuum
Steam Velocity: 2.0 (m/s)

Data #	Vw (m/s)	Tin (C)	Tout (C)	Ts (C)
1	1.17	18.10	19.11	48.45
2	1.17	18.09	19.11	48.46
3	1.49	17.83	18.68	48.51
4	1.49	17.82	18.68	48.49
5	1.98	17.59	18.26	48.41
6	1.98	17.58	18.25	48.39
7	2.53	17.41	17.96	48.41
8	2.53	17.41	17.95	48.51
9	3.02	17.30	17.79	48.48
10	3.02	17.29	17.77	48.45
11	3.45	17.21	17.64	48.43
12	3.45	17.21	17.63	48.43
13	3.89	17.13	17.52	48.49
14	3.89	17.13	17.52	48.45
15	1.17	17.88	18.93	48.37
16	1.17	17.89	18.95	48.33

Tube Number: 06
File Name: F06A99
Pressure Condition: Atmospheric
Steam Velocity: 1.0 (m/s)

Data #	Vw (m/s)	Tin (C)	Tout (C)	Ts (C)
1	1.17	18.35	21.63	100.08
2	1.17	18.37	21.63	100.01
3	1.49	18.22	20.92	100.05
4	1.49	18.23	20.93	100.04
5	1.98	18.06	20.20	99.96
6	1.98	18.07	20.21	99.95
7	2.53	17.95	19.70	99.98
8	2.53	17.96	19.71	100.00
9	3.01	17.91	19.42	100.03
10	3.01	17.91	19.41	100.01
11	3.45	17.88	19.21	99.99
12	3.45	17.89	19.21	99.84
13	3.88	17.85	19.03	99.96
14	3.88	17.84	19.03	100.15
15	1.17	18.65	21.86	99.93
16	1.17	18.66	21.86	100.06

APPENDIX B

UNCERTAINTY ANALYSIS

There is always an uncertainty associated with any measurement which is dependent on the measuring device accuracy, calibration of the device, and the operator's experience. Numerical data collected during this thesis effort were used together with theoretical formulations, so final values of the steam-side heat transfer coefficient may be distorted due to uncertainty propagation during calculations. In cases where the final results show large uncertainties, it may be unwise to accept the experimental results. The uncertainty on a computation can be determined using the following equation proposed by Kline and McClintok [30] shown below:

$$W_r = \left[\left(\frac{\partial R}{\partial x_1} W_1 \right)^2 + \left(\frac{\partial R}{\partial x_2} W_2 \right)^2 + \cdots \cdots + \left(\frac{\partial R}{\partial x_n} W_n \right)^2 \right]^{1/2} \qquad (b.1)$$

where

R is the result

W_r is the uncertainty of the desired dependent variable

$x_1, x_2, \ldots, x_n$ are the measured independent variables

$W_1, W_2, \ldots, W_n$ are the uncertainties in the measured variables.

A complete discussion covering the development of the uncertainty analysis used for this investigation is given by Georgiadis [27]. The uncertainties associated with various

quantities during this experiment were obtained using the program "UNA9" listed in Mitrou's thesis [10].

DATA FOR THE UNCERTAINTY ANALYSIS:

File Name: F04V17
Pressure Condition: Vacuum (11 kPa)
Steam Temperature   =   48.50   (Deg C)
Water Flow Rate (%)   =   20.00
Water Velocity   =   1.17   (m/s)
Heat Flux   =   2.115E+05   (W/m^2)
Tube-metal thermal conduc.   =   385.0   (W/m.K)
Sieder-Tate constant   =   0.0704

UNCERTAINTY ANALYSIS:

        VARIABLE   PERCENT UNCERTAINTY

Mass Flow Rate, Md   2.97
Reynolds Number, Re   3.06
Heat Flux, q   3.05
Log-Mean-Tem Diff, LMTD   0.53
Wall Resistance, Rw   2.67
Overall H.T.C., Uo   3.10
Water-Side H.T.C., Hi   2.58
Steam-Side H.T.C., Ho   13.44

DATA FOR THE UNCERTAINTY ANALYSIS:

File Name: F04V17
Pressure Condition: Vacuum (11 kPa)
Steam Temperature   =   48.49   (Deg C)
Water Flow Rate (%)   =   80.00
Water Velocity   =   4.44   (m/s)
Heat Flux   =   3.413E+05   (W/m^2)
Tube-metal thermal conduc.   =   385.0   (W/m.K)
Sieder-Tate constant   =   0.0704

UNCERTAINTY ANALYSIS:

        VARIABLE   PERCENT UNCERTAINTY

Mass Flow Rate, Md   0.78
Reynolds Number, Re   1.06
Heat Flux, q   1.52
Log-Mean-Tem Diff, LMTD   1.22
Wall Resistance, Rw   2.67
Overall H.T.C., Uo   1.95
Water-Side H.T.C., Hi   1.16
Steam-Side H.T.C., Ho   3.95

DATA FOR THE UNCERTAINTY ANALYSIS:

```
File Name:          F04A12
Pressure Condition: Atmospheric (101 kPa)
Steam Temperature            =   99.91       (Deg C)
Water Flow Rate (%)          =   20.00
Water Velocity               =    1.17        (m/s)
Heat Flux                    =    6.198E+05  (W/m^2)
Tube-metal thermal conduc.   =  385.0        (W/m.K)
Sieder-Tate constant         =    0.0667
```

UNCERTAINTY ANALYSIS:

VARIABLE	PERCENT UNCERTAINTY
Mass Flow Rate, Md	2.97
Reynolds Number, Re	3.07
Heat Flux, q	3.01
Log-Mean-Tem Diff, LMTD	0.18
Wall Resistance, Rw	2.67
Overall H.T.C., Uo	3.02
Water-Side H.T.C., Hi	2.60
Steam-Side H.T.C., Ho	15.79

DATA FOR THE UNCERTAINTY ANALYSIS:

```
File Name:          F04A12
Pressure Condition: Atmospheric (101 kPa)
Steam Temperature            =  100.05       (Deg C)
Water Flow Rate (%)          =   80.00
Water Velocity               =    4.43        (m/s)
Heat Flux                    =    1.004E+06  (W/m^2)
Tube-metal thermal conduc.   =  385.0        (W/m.K)
Sieder-Tate constant         =    0.0667
```

UNCERTAINTY ANALYSIS:

VARIABLE	PERCENT UNCERTAINTY
Mass Flow Rate, Md	0.79
Reynolds Number, Re	1.07
Heat Flux, q	0.99
Log-Mean-Tem Diff, LMTD	0.41
Wall Resistance, Rw	2.67
Overall H.T.C., Uo	1.07
Water-Side H.T.C., Hi	1.20
Steam-Side H.T.C., Ho	2.74

DATA FOR THE UNCERTAINTY ANALYSIS:

```
File Name:               SV14
Pressure Condition:      Vacuum (11 kPa)
Steam Temperature              =    49.15      (Deg C)
Water Flow Rate (%)            =    20.00
Water Velocity                 =     1.17      (m/s)
Heat Flux                      =     1.622E+05 (W/m^2)
Tube-metal thermal conduc.     = 385.0         (W/m.K)
Sieder-Tate constant           =     0.0687
```

UNCERTAINTY ANALYSIS:

VARIABLE	PERCENT UNCERTAINTY
Mass Flow Rate, Md	2.98
Reynolds Number, Re	3.07
Heat Flux, q	3.09
Log-Mean-Tem Diff, LMTD	0.68
Wall Resistance, Rw	2.67
Overall H.T.C., Uo	3.16
Water-Side H.T.C., Hi	2.59
Steam-Side H.T.C., Ho	8.14

DATA FOR THE UNCERTAINTY ANALYSIS:

```
File Name:               SV14
Pressure Condition:      Vacuum (11 kPa)
Steam Temperature              =    48.98      (Deg C)
Water Flow Rate (%)            =    76.25
Water Velocity                 =     4.22      (m/s)
Heat Flux                      =     2.208E+05 (W/m^2)
Tube-metal thermal conduc.     = 385.0         (W/m.K)
Sieder-Tate constant           =     0.0687
```

UNCERTAINTY ANALYSIS:

VARIABLE	PERCENT UNCERTAINTY
Mass Flow Rate, Md	0.82
Reynolds Number, Re	1.10
Heat Flux, q	2.02
Log-Mean-Tem Diff, LMTD	1.80
Wall Resistance, Rw	2.67
Overall H.T.C., Uo	2.71
Water-Side H.T.C., Hi	1.20
Steam-Side H.T.C., Ho	4.12

DATA FOR THE UNCERTAINTY ANALYSIS:

File Name: SIA111
Pressure Condition: Atmospheric (101 kPa)
Steam Temperature   =   99.62   (Deg C)
Water Flow Rate (%)   =   20.00
Water Velocity   =   1.16   (m/s)
Heat Flux   =   3.837E+05   (W/m^2)
Tube-metal thermal conduc.   =   385.0   (W/m.K)
Sieder-Tate constant   =   0.0710

UNCERTAINTY ANALYSIS:

VARIABLE	PERCENT UNCERTAINTY
Mass Flow Rate, Md	3.01
Reynolds Number, Re	3.11
Heat Flux, q	3.05
Log-Mean-Tem Diff, LMTD	0.28
Wall Resistance, Rw	2.67
Overall H.T.C., Uo	3.06
Water-Side H.T.C., Hi	2.62
Steam-Side H.T.C., Ho	6.43

DATA FOR THE UNCERTAINTY ANALYSIS:

File Name: SIA111
Pressure Condition: Atmospheric (101 kPa)
Steam Temperature   =   99.88   (Deg C)
Water Flow Rate (%)   =   80.00
Water Velocity   =   4.40   (m/s)
Heat Flux   =   5.043E+05   (W/m^2)
Tube-metal thermal conduc.   =   385.0   (W/m.K)
Sieder-Tate constant   =   0.0710

UNCERTAINTY ANALYSIS:

VARIABLE	PERCENT UNCERTAINTY
Mass Flow Rate, Md	0.79
Reynolds Number, Re	1.12
Heat Flux, q	1.22
Log-Mean-Tem Diff, LMTD	0.92
Wall Resistance, Rw	2.67
Overall H.T.C., Uo	1.47
Water-Side H.T.C., Hi	1.20
Steam-Side H.T.C., Ho	2.08

APPENDIX C

LEAST SQUARES CALCULATIONS

The derivation of the average and local enhancement relationships is summarized as follows:

(a) Assume a third-order polynomial for the local enhancement ratio:

$$\varepsilon_\phi = a_o + a_1 \phi + a_2 \phi^2 + a_3 \phi^3 \tag{c.1}$$

(b) Apply the first boundary condition,

$$\frac{d\varepsilon_\phi}{d\phi} = 0 \qquad at \qquad \phi = 0$$

$$\frac{d\varepsilon_\phi}{d\phi} = a_1 + 2 a_2 \phi + 3 a_3 \phi^2$$

$$a_1 = 0$$

$$\varepsilon_\phi = a_0 + a_2 \phi^2 + a_3 \phi^3$$

(c) Apply the second boundary condition,

$$\varepsilon_\phi = 0 \qquad at \qquad \phi = \pi$$

$$0 = a_o + a_2 \pi^2 + a_3 \pi^3$$

$$a_0 = -\left(a_2 \pi^2 + a_3 \pi^3 \right)$$

$$\varepsilon_\phi = -\left(a_2 \pi^2 + a_3 \pi^3 \right) + a_2 \phi^2 + a_3 \phi^3$$

(d) The average enhancement relationship is determined using the definition of the average value of a function

$$\bar{\varepsilon}_\phi = \frac{1}{\phi} \int_0^\phi \varepsilon_\phi \, d\phi$$

$$= \frac{1}{\phi} \int_0^{\phi} \left(-a_2 n^2 - a_3 n^3 + a_2 \phi^2 + a_3 \phi^3 \right) d\phi$$

yields,

$$\bar{\varepsilon}_\phi = -a_2 n^2 - a_3 n^3 + \frac{a_2}{3} \phi^2 + \frac{a_3}{4} \phi^3$$

(e) Apply the third boundary condition, $\bar{\varepsilon}_\phi = B$ at $\phi = n$ to the average enhancement function. B is defined as the value of the average enhancement for the uninsulated tube.

$$B = -a_2 n^2 - a_3 n^3 + \frac{a_2}{3} n^2 + \frac{a_3}{4} n^3$$

which simplifies to

$$a_3 = -\frac{4B}{3 n^3} - \frac{8}{9 n} a_2$$

Now,

$$\bar{\varepsilon}_\phi = -a_2 n^2 + \frac{a_2}{3} \phi^2 - \left(\frac{\phi^3}{4} - n^3 \right) \left(\frac{4B}{3 n^3} + \frac{8}{9 n} a_2 \right)$$

which simplifies to,

$$\bar{\varepsilon}_\phi = a_2 \left(-n^2 + \frac{\phi^2}{3} + \frac{8 n^2}{9} - \frac{2 \phi^3}{9 n} \right) + \frac{4B}{3} - \frac{B \phi^3}{3 n^3}$$

(f) Apply the final condition in the form of the least squares technique. Minimize the error as follows:

$$S = \Sigma E^2 = \Sigma \left\{ \bar{\varepsilon}_\phi - \left[a_2 \left(-n^2 + \frac{\phi^3}{3} + \frac{8 n^2}{9} - \frac{2 \phi^3}{9 n} \right) + \frac{4B}{3} - \frac{B \phi^3}{3 n^3} \right] \right\}^2$$

by

$$\frac{dS}{da_3} = 0$$

which yields,

$$a_2 = \frac{TERM1}{TERM2}$$

$$TERM1 = -n^2 \Sigma \bar{\varepsilon}_i + \frac{1}{3} \Sigma \bar{\varepsilon}_i \phi_i^2 + \frac{8 n^2}{9} \Sigma \bar{\varepsilon}_i - \frac{2}{9 n} \Sigma \bar{\varepsilon}_i \phi_i^3 + \frac{4B n^2}{3} N - \frac{4B}{9} \Sigma \phi_i^2 - \frac{32 B n^2}{27} N$$

$$+ \frac{8B}{27 n} \Sigma \phi_i^3 - \frac{B}{3 n} \Sigma \phi_i^3 + \frac{B}{9 n^3} \Sigma \phi_i^5 + \frac{8B}{27 n} \Sigma \phi_i^3 - \frac{2B}{27 n^4} \Sigma \phi_i^6$$

$$TERM2 = n^4 N - \frac{2n^2}{3} \Sigma \phi_i^2 - \frac{16n^4}{9} N + \frac{4n}{9} \Sigma \phi_i^3 + \frac{1}{9} \Sigma \phi_i^4 + \frac{16n^2}{27} \Sigma \phi_i^2 - \frac{32n}{81} \Sigma \phi_i^3$$

$$- \frac{4}{27n} \Sigma \phi_i^5 + \frac{64n^4}{81} N + \frac{4}{81n^2} \Sigma \phi_i^6.$$

(g) The results of the above steps yield relationships for the local and average enhancement of the form:

$$\varepsilon_\phi = a_0 + a_2 \phi^2 + a_3 \phi^3$$

$$\bar{\varepsilon}_\phi = b_0 + b_2 \phi^2 + b_3 \phi^3$$

where the values of the a coefficients were defined above and the values of the b coefficients are related to the a coefficients as follows:

$$b_0 = -\left(a_2 n^2 + a_3 n^3 \right)$$

$$b_2 = a_2$$

$$b_3 = a_3.$$

LIST OF REFERENCES

1. Yau, K. K., Cooper, J. R. and Rose, J. W., "Effects of Fin Spacing on the Performance of Horizontal Integral-Fin Condenser Tubes," _Journal of Heat Transfer_, Vol. 107, May 1985, pp. 377-383.

2. Wanniarachchi, A. S., Marto, P. J. and Rose, J. W., "Filmwise Condensation of Steam on Externally-Finned Horizontal Tubes," _Fundamentals of Phase Change: Boiling and Condensation_, HTD-Vol. 38, C. T. Avedisian and T. M. Rudy (Eds.), Dec 1984, pp. 133-141.

3. Wanniarachchi, A. S., Marto, P. J. and Rose, J. W., "Filmwise Condensation of Steam on Horizontal Finned Tubes: Effect of Fin Spacing, Thickness and Height," _Multiphase Flow and Heat Transfer_, HTD-Vol. 47, V. K. Dhir, J. C. Chen, and O. C. Jones (Eds.), pp. 93-99, 1985.

4. Rudy, T. M. and Webb, R. L., "Condensate Retention of Horizontal Integral-Fin Tubing," _Advances in Heat Transfer_, ASME Symp. Vol. HTD-18, 1981, pp. 35-41.

5. Honda, H., Nozu, S. and Mitsumori, K., "Augmentation of Condensation on Horizontal Finned Tubes by Attaching Porous Drainage Plate," Proc. ASME-JSME Thermal Engineering Joint Conference, Honolulu, Vol. 3, 1983, pp. 289-296.

6. Rudy, T. M. and Webb, R. L., "An Analytical Model to Predict Condensate Retention on Horizontal Integral-Fin Tubes," Proc. ASME-JSME Thermal Engineering Joint Conference, Honolulu, Vol. 1, 1983, pp. 373-378.

7. Rudy, T. M. and Webb, R. L., "Theoretical Model for Condensation on Horizontal Integral-Fin Tubes," _AIChE Symp. Ser._, No. 225, Vol. 79, 1983, pp. 11-18.

8. Owen, R. G., Sardesai, R. G., Smith, R. A. and Lee, W. C., "Gravity Controlled Condensation on Horizontal Low-Fin Tube," _Condensers: Theory and Practice_, Inst. Chem. Engrs. Symp. Ser. 75, 1983, pp. 415-428.

9. Honda, H., Nozu, S. and Uchima, B., "A Generalized Prediction Method for Heat Transfer during Film Condensation on a Horizontal Low Finned Tube," ASME/JSME Thermal Engineering Joint Conference, Vol. 4, 1987, pp. 385-392.

10. Mitrou, E. S., "Film Condensation of Steam on Externally Enhanced Horizontal Tubes," M. S. Thesis, Naval Postgraduate School, Monterey, California, March 1986.

11. Katz, D. L., Hope, R. E. and Dasko, S. C., " Liquid Retention on Finned Tubes," Dept, of Eng. Research, University of Michigan, Ann Arbor, Michigan, Project M592, 1946.

12. Rifert, V. G., " Steam Condensation on Profiled Surfaces," Heat and Mass-Transfer Processes in Porous Media with Phase Transformation, Academy of Science, BSSR, A. B. Lykov (Ed.), Minsk, 1982, pp. 149-170.

13. Rudy, T. M. and Webb, R. L., " An Analytical Model to Predict the Condensate Retention on Horizontal Integral-Fin Tubes," ASME Journal of Heat Transfe. Vol. 107, 1985, pp. 361-368.

14. Holman, J. P., Heat Transfer, 4th ed., McGraw-Hill Book Company, New York, 1976, p. 38.

15. Masuada, H., and Rose, J. W., "Static Configuration of Liquid Films on Horizontal Tubes With Low Radial Fins: Implications for Condensation Heat Transfer", paper to be published in Proceeings of the Royal Society, London.

16. Beatty, B. O. and Katz, D. L., "Condensation of Vapors on Outside of Finned Tubes," Chemical Engineering Process, Vol. 44, No. 1, January 1948, pp. 55-69.

17. Nusselt, W., "die Oberflachenkondensation des Wasserdampfes," VDI Z., Vol. 60, 1916, p. 541.

18. Wanniarachchi, A. S., Marto, P. J. and Rose, J. W., "Film Condensation of Steam on Horizontal Finned Tubes: Effect of Fin Spacing," Transactions of the ASME, Vol. 108, November 1986, pp. 960-966.

19. Karkhu, V. A. and Borovkov, V. P., "Film Condensation of Vapor at Finely-Finned Horizontal Tubes," Heat Transfer-Soviet Research, Vol. 3, No. 2, March-April 1971, pp. 183-191.

20. Carnavos, T. C., "An Experimental Study: Condensation R-11 on Augmented Tubes," ASME paper No. 80-HT-54, 19th National Heat Transfer Conference, Milwaukee, Wisconsin, August 1981.

21. Gregorig, R., "Filmwise Condensation on Finely Rippled Surfaces with Condensation of Surfaces Tension," _Zeitschrift fr Angewantde Mathematik und Physic,_ Vol. V, 1954 (Translation by D. K. Edwards), pp. 36-49.

22. Webb, R. L., Rudy, T. M. and Kedzierski, M. A., " Prediction of the Condensation Coefficient on Horizontal Integral-Fin Tubes," _ASME Journal of Heat Transfer,_ Vol. 107, 1985, pp. 369-376.

23. Adamek, T., "Bestimmung der Kondensationgrossen auf feingewellten Oberflachen zur Auslegung aptimaler Wandprofile," _Warme und Stoffubertranqung,_ Vol. 15, 1981, pp. 255-270.

24. Krohn, R. L., " An Experimental Apparatus to Study Enhanced Condensation Heat-Transfer of Steam on Horizontal Tubes," M. S. Thesis, Naval Postgraduate School, Monterey, California, June 1982.

25. Graber, K. A., " Condensation Heat Transfer of Steam on a Single Horizontal Tube," M. S. Thesis, Naval Postgraduate School, Monterey, California, June 1983.

26. Poole, W. M., "Filmwise Condensation of Steam on Externally-Finned Horizontal Tubes," M. S. Thesis, Naval Postgraduate School, Monterey, California, December 1983.

27. Georgiadis, I. V., "Filmwise Condensation of Steam on Low Integral-Finned Tubes," M. S. Thesis, Naval Postgraduate School, Monterey, California, September 1984.

28. Flook, F. V., " Filmwise Condensation of Steam on Low Integral-Finned Tubes," M. S. Thesis, Naval Postgraduate School, Monterey, California, March 1985.

29. Cakan, O., " Filmwise Condensation of Steam on Low Integral-Finned Tubes with Drainage Strips," M. S. Thesis, Naval Postgraduate School, Monterey, California, December 1986.

30. Kline, S. J. and McClintok, F. A., "Describing Uncertainties in in Single-Sample Experiments," _Mechanical Engineering,_ Vol. 74, January 1953, pp. 3-8.

INITIAL DISTRIBUTION LIST

		No. Copies
1.	Defense Technical Information Center Cameron Station Alexandria, Virginia 22304-6145	2
2.	Library, Code 0142 Naval Postgraduate School Monterey, California 93943-5002	2
3.	Chairman, Code 69He Mechanical Engineering Department Naval Postgraduate School Monterey, California 93943-5000	1
4.	Professor P. J. Marto, Code 69Mx Department of Mechanical Engineering Naval Postgraduate School Monterey, California 93943-5000	5
5.	Dr. A. S. Wanniarachchi, Code 69Wa Department of Mechanical Engineering Naval Postgraduate School Monterey, California 93943-5000	3
6.	Professor John W. Rose Department of Mechanical Engineering Queen Mary College London E1 4NS England	1
7.	Dr. E. M. Sparrow Program Director Thermal Systems and Engineering Program National Science Foundation Washington, D. C. 20550	1
8.	LT Donald J. Lester, Jr. Pearl Harbor Naval Shipyard Box 400 Code 215 Pearl Harbor, HI 96860	5
9.	Mr. R. Helmick, Code 2745 David W. Taylor Naval Ship Research and Development Center Annapolis, Maryland 21402	1